12-2007

A Generalized Hamiltonian-Based Algorithm for Rigorous Nonequilibrium Molecular Dynamics Simulation in the NVT Ensemble

Joseph Gerald Leo Rajkumar
University of Tennessee - Knoxville

To the Graduate Council:

I am submitting herewith a thesis written by Joseph Gerald Leo Rajkumar entitled "A Generalized Hamiltonian-Based Algorithm for Rigorous Nonequilibrium Molecular Dynamics Simulation in the NVT Ensemble." I have examined the final electronic copy of this thesis for form and content and recommend that it be accepted in partial fulfillment of the requirements for the degree of Master of Science, with a major in Chemical Engineering.

Brian J. Edwards, Major Professor

We have read this thesis and recommend its acceptance:

David J. Keffer, William V. Steele

Accepted for the Council:
Carolyn R. Hodges

Vice Provost and Dean of the Graduate School

(Original signatures are on file with official student records.)

To the Graduate Council:

I am submitting herewith a thesis written by Joseph Gerald Leo Rajkumar entitled "A Generalized Hamiltonian-Based Algorithm for Rigorous Nonequilibrium Molecular Dynamics Simulation in the NVT Ensemble." I have examined the final electronic copy of this thesis for form and content and recommend that it be accepted in partial fulfillment of the requirements for the degree of Master of Science, with a major in Chemical Engineering.

Brian J. Edwards, Major Professor

We have read this thesis

And recommend its acceptance:

David J. Keffer

William V. Steele

Accepted for the council:

Carolyn R. Hodges

Vice Provost and Dean of the

Graduate School

(Original signatures are on file with official student records.)

A GENERALIZED HAMILTONIAN-BASED ALGORITHM FOR RIGOROUS NONEQUILIBRIUM MOLECULAR DYNAMICS SIMULATION IN THE NVT ENSEMBLE

A Thesis

Presented for the

Master of Science

Degree

The University of Tennessee, Knoxville

Joseph Gerald Leo Rajkumar

December 2007

Acknowledgements

I wish to thank all those who helped me complete my Master of Science degree in Chemical Engineering. I would like to thank Dr. Brian J. Edwards for his ideas and valuable guidance through the research process. I would like to thank Dr. David J. Keffer for his guidance and his effort in making me familiar with Hamiltonian systems and Molecular Dynamics Simulations. I would also like to thank Dr William V. Steele for serving on my committee.

Lastly I would like to thank my family and friends, whose encouragement made this work possible.

Abstract

Using a recently developed, methodical, Hamiltonian-based procedure, we derive rigorous algorithms for nonequilibrium molecular dynamic (NEMD) simulation in the NVE and NVT ensembles. We demonstrate that the equivalence of the kinetic temperature and configurational temperatures that exists at equilibrium is maintained in nonequilibrium states, given the proper nonequilibrium expression (in the microcanonical ensemble). Specifically, we apply the procedure to the p-SLLOD algorithm, which allows for rigorous NEMD simulation in the presence of an arbitrary, externally imposed flow field. The resulting algorithms are general in that they apply in the presence or absence of external fields in addition to the imposed flow field. Of particular note is the resulting algorithm for the canonical ensemble. The use of the Nosé-Hoover thermostat in the SLLOD and p-SLLOD algorithms has not been rigorously correct to date. We follow a methodical procedure to obtain a rigorous Hamiltonian-based NEMD algorithm using a reformulated Nosé-Hoover and Nosé-Poincaré thermostat. Although the resulting algorithms were unstable, it provided proof that it is the boundary conditions that drive the flow, contrary to the conventional belief that an external flow field has to be introduced into the equations of motion to simulate nonequilbrium flows.

Preface

With the advances in computing, it has become increasingly popular to use simulations to study the behavior of complex fluids. Such complex fluids can be treated as a classical or a quantum mechanical many-bodied problem. At present, quantum mechanical calculations can be very time consuming whereas classical mechanics allows a very accurate and fast simulations. Hence, applying Newton's equations to simulations is a very reliable method to model complex fluids, even in nonequilibrium states. It has been commonly accepted that to model nonequilibrium conditions using Newtonian mechanics, one has to insert an external force into the Newton's equations of motion. Recently, Edwards et al. [1] have pointed out that to model nonequilibrium systems one has to have just Newton's equations of motion and the flow is in fact driven by the boundary conditions. In this work, we follow this philosophy to develop an NEMD algorithm that is theoretically sound and follows real experiments closely.

Table of Contents

List of Tables

List of Figures

List of Symbols

$\mathbf{p}_i$	Momentum of particle, i
$\mathbf{v}_i$	Velocity of particle, i
γ^*	Reduced shear rate
H	Hamiltonian
ΔH	Change in Hamiltonian
S	Entropy
E	Energy
ϕ	Functional
σ^2	Variance
σ	Particle exclusion diameter
ε	Well depth
$\rho'_{i,\alpha}$, $\pi'_{i,\alpha}$	Peculiar position and momentum of particle in the mathematical frame reference
$\rho_{i,\alpha}$, $\pi_{i,\alpha}$	Peculiar position and momentum of particle in the physical frame of reference
R'_α , P'_α	Center of mass position and momentum of particle in the mathematical frame of reference
R_α , P_α	Center of mass position and momentum of particle in the physical frame reference
η_T , ζ_T	Time dilation and thermostat momentum variable
$\sigma_{H,}$ $\sigma_{TsE,,}$ σ_{KE}	Standard deviation of Hamiltonian, thermostat energy and kinetic energy
iL	Liouville operator
P(t;Δt)	Time propagator

NOMENCLATURE

J	joules
aJ	atta joules
K	kelvin
gm/cm^3	grams per cubic centimeter

Abbreviations

EMD	Equilibrium molecular dynamics
NEMD	Nonequilibrium molecular dynamics
T_{kin}	Kinetic temperature
T_{eq}	Equilibrium temperature
T_{conf}	Configurational temperature
T_{set}	set temperature
T_{kin}^{EQ}	SLLOD definition of temperature
T_{kin}^{NE}	Nonequilibrium kinetic temperature
COM	Center of mass
LEBCs	Lees-Edwards boundary conditions

Chapter I

Introduction

Nonequilibrium Molecular Dynamics (NEMD) [2, 3] simulations play a vital role in the field of rheology and help us understand the structure and behavior of polymers under flow. NEMD simulations are of particular interest in situations where it is difficult to perform experiments. However, their applications are not limited to rheology alone, and they have a huge potential to be used in the field of proteomics and the study of bio-molecules. The use of NEMD simulations can be tremendously insightful, giving us a better understanding of molecules at the nanoscale level (performing experiments at this level can be difficult if not impossible).

NEMD algorithms have to be theoretically sound and should mimic the real experiments as closely as possible. There exist several algorithms that are capable for simulating nonequilibrium flows. Specifically for the case of shear flow, the DOLLS [4] and the SLLOD [3, 5] tensor algorithms are well known. The DOLLS algorithm [4] is rigorous for low shear rates but fails to make accurate predictions at high shear rates [3, 5]. SLLOD has been proven to be rigorous at high shear rates using nonlinear response theory [5]. It is commonly believed that the flow is introduced by including an external force into the equations of motions. The existing algorithms insert an external force field into the equations of motion to simulate nonequilibrium states, which is quite unrealistic and contradicts the behavior in real experiments. Also the SLLOD algorithm [3, 5] is

known to have some serious problems such as exponential growth of the linear momentum in the contracting direction) when used to simulate planar elongational flow [6].

In order to have an algorithm that closely follows the real experiments, one should only need boundary conditions and Newton's equations of motions. The problem arises because one cannot do the simulation the way that the experiment is performed. We run into well-known problems associated with the finite size of the simulation box, as well as the problems associated with the artificial production of heat (i.e. thermostat effects) [7].

The p-SLLOD algorithm [8, 9] is formulated in such a way that it mimics the equations of motion of the actual experiment as closely as possible. Boundary conditions are used to drive the flow, just as in actual experiments. All the effects of these boundary conditions are then felt on each particle through the interparticle force applied to it, just as in actual experiments [1]. This algorithm has been previously used to simulate homogeneous flows [9, 10]. However, these simulations use an ad-hoc Nosé-Hoover thermostat [11, 12] to maintain the system temperature. It is our goal to develop equations of motion based on the p-SLLOD algorithm [8] that rigorously thermostats only the nonequilibrium temperature. In other words, this new NEMD algorithm is 1) rigorous, 2) Hamiltonian-based, 3) identifies the correct temperature in nonequilibrium states and thermostats this temperature rigorously, and 4) remains valid in the presence or absence of an external field.

In the second chapter, we use the p-SLLOD transformation [8, 9] to identify the correct nonequilibrium temperature in the microcanonical ensemble (NVE). The existing

NEMD algorithms use the equilibrium definition of temperature. In the special case of planar couette flow (and the absence of external flow), the SLLOD [3, 5] and the p-SLLOD algorithm [8, 9] are equivalent. The time dependant boundary conditions and thermostat mask the inhomogeneous nature of the velocity distribution. To avoid the artifacts, we perform simulations in the microcanonical ensemble. We use conventional periodic boundary conditions in the x and z dimensions. In the y dimension, we impose a smooth, repulsive wall to maintain the system density. We see that the momentum has a non-constant profile along the y dimension and also that the velocity distribution does not fit to a Maxwell-Boltzmann distribution, neither locally nor globally. We propose a new definition of temperature based on the transformed momenta. The temperature measured using the new definition was found to be equal to temperature measured using the configurational information. This suggests the equivalence of the kinetic and configurational temperature in nonequilibrium states.

In the third chapter, the methodical procedure for deriving a generalized Hamiltonian-based algorithm for rigorous nonequilibrium molecular dynamics simulation in the NVT ensemble using a reformulated Nosé-Hoover thermostat [11, 12] is discussed and derived. The procedure begins with a Hamiltonian and involves a non-canonical transformation (p-SLLOD transformation [8, 9]) from laboratory coordinates in a mathematical frame of reference to peculiar coordinates in a physical frame of reference. We identify the nonequilibrium temperature and rigorously thermostat just the peculiar momenta. The algorithms generated by this procedure are valid in the absence or presence of external forces. The resulting algorithm conserves the Hamiltonian and is implemented in a simulation using the r-RESPA [13, 14] integration scheme. We show

that the Hamiltonian is a conserved quantity in the absence of the Lees-Edwards boundary conditions (LEBCs). However, in the presence of the Lees-Edwards boundary conditions (LEBCs), the Hamiltonian is no longer a conserved quantity. The algorithm was found to be unstable as the time dilation variable (i.e., one of the two Nosé-Hoover thermostat [11, 12] variables) did not reach a steady state. Thus, we looked at the possibility of using a thermostat apart from Nosé-Hoover thermostat [11, 12] that is Hamiltonian-based, and would yield an algorithm that is stable even under large fluctuations of temperature and thermostat variables.

The Nosé-Poincaré formulation [15] provided a thermostat that would result in a stable algorithm in equilibrium molecular dynamics simulation. The Nosé-Poincaré formulation has a canonical symplectic structure, unlike the Nosé-Hoover formulation, which provides a real-variable system through a noncanonical change of variables. In the fourth chapter, we use this formulation to derive a nonequilibrium molecular dynamics algorithm using a procedure very similar to the one discussed in the third chapter. The resulting algorithm conserves the Hamiltonian, and is implemented in simulations using the r-RESPA integration scheme [13, 14]. We show that the Hamiltonian is a conserved quantity in the absence of the Lees-Edwards boundary conditions (LEBCs). However, in the presence of the Lees-Edwards boundary conditions (LEBCs), the Hamiltonian is no longer a conserved quantity. Also the Hamiltonian tends to drift away from the initial value due to computational round-off errors introduced by the numerical integrators. The Nosé-Poincaré formulation [15] is such that the thermostat variables not only depend on the instantaneous temperature, but also depend on the instantaneous Hamiltonian. Hence we needed an integration scheme that would suppress deviations of the Hamiltonian in

order to have a stable thermostat. Nosé has derived a symplectic integration scheme [16] which ensures that the Hamiltonian of the system (a conserved quantity) does not drift away due to the computational round-off errors. We apply the same procedure to our equations of motion to integrate them. The time dilation variable did not reach a steady state and this led us to use several methods that would ensure that the Hamiltonian would be conserved across the periodic boundary conditions. This led us to investigate the effect of the thermostat and the periodic boundary condition on the stability of the algorithm.

We looked at the stress tensor of the particles in the canonical ensemble with and without the Lees-Edwards boundary conditions. Smooth repulsive boundaries are placed in the y dimension. In the absence of the Lees-Edwards boundary condition, the stress tensor is zero, which indicates that the p- SLLOD transformation [8, 9] does not introduce any flow into the system. In other words, the equations of motion do not drive the flow. Once we apply the Lees-Edwards boundary condition, the momenta are driven towards infinity, i.e., the boundary conditions drive the flow.

In the microcanonical ensemble, the shear stress does not correspond to the shear flow in the absence of the Lees-Edwards boundary conditions (smooth repulsive y boundaries). The shear stress corresponds to the shear flow in the presence of the Lees-Edwards boundary conditions. This proves that the periodic boundary conditions drive the flow in the microcanonical ensemble as well.

Chapter II

The Equivalence of Kinetic and Configurational Temperature in Nonequilibrium States

For equilibrium systems it has been shown that the temperature can be equivalently expressed in terms of a kinetic expression, which is a function of particle momenta, and a configurational expression, which is a function of particle positions. In this work, we provide a demonstration through the use of Nonequilibrium Molecular Dynamics (NEMD) simulation that the equivalence is maintained in nonequilibrium states. The nonequilibrium kinetic expression for the temperature is presented and is consistent with the noncanonical variable transformation associated with the p-SLLOD NEMD algorithm.

2.1. Introduction

In equilibrium molecular systems with a known Hamiltonian, one can evaluate the temperature by measuring the time average of the kinetic energy. However, Rugh [17] used a different approach to evaluate the temperature of Hamiltonian systems based on the geometric structure of the energy surface, in which the temperature was evaluated using the configuration (positions) and/or kinetic (momenta) information. The temperature is computed as the time average of the functional ϕ [17]

$$\phi = \nabla \cdot \left(\frac{\nabla H}{\left\| \nabla H \right\|^2} \right) \tag{2.1}$$

Where H is the Hamiltonian of the system (a function of momenta and positions). This expression for the temperature is based upon the equilibrium thermodynamic relation [17],

$$\frac{1}{T(E)} = \left. \frac{\partial S(E)}{\partial E} \right|_V \tag{2.2}$$

where S is the entropy and E is the energy of the microcanonical ensemble, and T is the thermodynamic temperature.

Following the same approach, an expression for temperature using either kinetic or the configurational information, or a combination of both kinetic, has been derived [18]. A more general expression for the temperature has been derived and proven to hold in the canonical and microcanonical molecular dynamics ensembles [19],

$$kT = \frac{\langle \nabla H \cdot B(\Gamma) \rangle}{\langle \nabla \cdot B(\Gamma) \rangle} \tag{2.3}$$

where $B(\Gamma)$ is any arbitrary vector field and $H(\Gamma)$ is the Hamiltonian of the system given by $H(\Gamma) = \sum \left((\mathbf{p}_i \cdot \mathbf{p}_i)/2m_i \right) + V\left(\{\mathbf{q}_j\} \right)$. Further, this general expression has provided proof for the equivalence of temperature expressions based on kinetic energy and on the configurations in equilibrium states [19].

To date, there has been no proof that any of the above methods of measuring the temperature is valid for nonequilibrium systems. However conventional NEMD

simulations of flowing systems have used one of the two expressions to identify the temperature in nonequilibrium systems. Since the presence of a flow field rather obviously changes the distribution of momentum within the system, there has been a tendency to identify the configurational temperature as the "more correct" temperature to use in NEMD simulations.

The goal of this work is to show that the equivalence of the kinetic temperature and configurational temperature that exists at equilibrium is maintained in nonequilibrium states, given the proper nonequilibrium expression. Moreover, our goal is to arrive at this expression via a methodical, Hamiltonian-based procedure. We shall continue to invoke the local equilibrium approximation, which is essential to apply either the kinetic or configurational definition of temperature.

Specifically, we shall persist in our adherence to the Maxwell-Boltzmann distribution (MBD) for velocities at each local point. The two key features of the MBD are (1) that the mean velocity is zero and (2) that the variance of the velocity is related to the temperature through $\sigma^2 = k_B T/m$, where k_B is Boltzmann's constant and m is the mass of the particle. The first feature ensures that the velocity described by the MBD is a peculiar velocity, in which center-of-mass (COM) components have been removed. The second feature is equivalent to the equipartition theorem relating the peculiar kinetic energy to the temperature. The velocity described by the MBD in an NEMD simulation provides the kinetic temperature. We can compare this temperature with the configurational temperature.

In the case of nonequilibrium states, the Hamiltonian defining the system (NVE ensemble) can be expressed as

$$H(\Gamma) = \sum \left((\mathbf{p}_i + m_i \mathbf{q}_i \cdot \nabla u) \cdot (\mathbf{p}_i + m_i \mathbf{q}_i \cdot \nabla u) / 2m_i \right) + V\left(\{ \mathbf{q}_j \} \right) \tag{2.4.a}$$

In this equation, m_i, $\mathbf{p}_i$ and $\mathbf{q}_i$ are the mass, momentum and position of particle i, respectively. Based on equation (2.3), we can expect to generate the temperature when we take the kinetic or the configurational information as vector $B(\Gamma)$ (i.e $B(\Gamma) = \nabla\left(\sum \left((\mathbf{p}_i + m_i \mathbf{q}_i \cdot \nabla u) \cdot (\mathbf{p}_i + m_i \mathbf{q}_i \cdot \nabla u) / 2m_i \right) \right)$ or $B(\Gamma) = \nabla\left(V\left(\{ \mathbf{q}_j \} \right) \right)$. When we use the kinetic information in equation (2.3), we get the equipartition theorem and this is equivalent to the temperature expression generated using the configurational information.

$$kT = \frac{\langle \nabla H \cdot \nabla K(\mathbf{p}_i) \rangle}{\langle \nabla \cdot \nabla K(\mathbf{p}_i) \rangle} = \frac{\sum \left((\mathbf{p}_i + m_i \mathbf{q}_i \cdot \nabla u) \cdot (\mathbf{p}_i + m_i \mathbf{q}_i \cdot \nabla u) / m_i \right)}{3N} \tag{2.4.b}$$

which is nothing but the equipartition theorem, and the kinetic energy is given by $K(\mathbf{p}_i) = \left(\sum \left((\mathbf{p}_i + m_i \mathbf{q}_i \cdot \nabla u) \cdot (\mathbf{p}_i + m_i \mathbf{q}_i \cdot \nabla u) / 2m_i \right) \right)$. We shall define this temperature to be T_{kin}^{NE}. If we substitute the configurational information in equation (2.3), we get a new definition of temperature,

$$kT = \frac{\langle \nabla H \cdot \nabla V\left(\{ \mathbf{q}_j \} \right) \rangle}{\langle \nabla \cdot \nabla V\left(\{ \mathbf{q}_j \} \right) \rangle} = \frac{\sum_i F_i^2 - (1 + m\dot{\gamma})\dot{\gamma} \sum_i q_i \cdot F_i}{-\sum_i \nabla \cdot F_i} \tag{2.4.c}$$

At shear rates less than unity, the value of the last term in the numerator of the equation (2.4.c) is negligible compared to the other two terms and can be neglected during

temperature evaluation. Although equations (2.4.b) and (2.4.c) are evaluated from different information, they are essentially equivalent as they generate temperature based on the same definition (i.e., equation (2.3)). Thus we see that the equilibrium definition of temperature can be extended to nonequilibrium states, and also that the kinetic and configurational temperatures are equivalent in nonequilibrium states

2.2. Simulation Methodology

When studying fluids in nonequilibrium states, one must choose an NEMD algorithm. In this work, we choose the p-SLLOD algorithm [8, 9], which is a Hamiltonian-based approach, consistent with nonlinear response theory [20]. A key component of this approach is the identification of a noncanonical transformation of the momenta from the laboratory to the flowing coordinate system,

$$\mathbf{p}_i' = \mathbf{p}_i + m_i \mathbf{q}_i \cdot \nabla \mathbf{u} \tag{2.5}$$

The $\nabla \mathbf{u}$ is the velocity gradient tensor. In this work, we will study planar Couette flow (PCF), in which the flow field in the x-direction is a function of the position in the y dimension, $\nabla_y u_x = \dot{\gamma}$, where $\dot{\gamma}$ is the shear rate. The p-SLLOD [8, 9] equations of motion are

$$\begin{aligned} \dot{\mathbf{q}}_i &= \frac{\mathbf{p}_i}{m_i} + \mathbf{q}_i \cdot \nabla \mathbf{u} \ , \\ \dot{\mathbf{p}}_i &= \mathbf{F}_i - \mathbf{p}_i \cdot \nabla \mathbf{u} - m_i \mathbf{q}_i \cdot \nabla \mathbf{u} \cdot \nabla \mathbf{u} \end{aligned} \tag{2.6}$$

In these equations, $\mathbf{F}_i$ is force vector of particle i. In planar Couette flow, the *p*-SLLOD equations of motion are identical to the SLLOD [3, 5] equations of motion because the term $m_i\mathbf{q}_i \cdot \nabla\mathbf{u} \cdot \nabla\mathbf{u}$ vanishes. For a recent discussion of the relative merits of the SLLOD and p-SLLOD algorithms, see Refs. [9, 20-22].

For PCF in the absence of time-dependent boundary conditions, the SLLOD dynamics predict a linear but nonuniform momentum profile [23], and the conventional methods identify this momentum to be related to the temperature T_{kin}^{EQ},

$$\frac{3}{2}Nk_BT_{kin}^{EQ} = \sum \frac{\mathbf{p}_i \cdot \mathbf{p}_i}{2m_i} \tag{2.7}$$

Consequently, the temperature will have a non-uniform profile in the sheared system. Here, we present the transformation which identifies the temperature based on the momentum that is homogeneous. We call this the nonequilibrium temperature T_{kin}^{NE},

$$\frac{3}{2}Nk_BT_{kin}^{NE} = \sum \frac{\mathbf{p}_i' \cdot \mathbf{p}_i'}{2m_i} = \sum \frac{\left(\mathbf{p}_i + \mathbf{q}_i \cdot \nabla\mathbf{u}\right) \cdot \left(\mathbf{p}_i + \mathbf{q}_i \cdot \nabla\mathbf{u}\right)}{2m_i} \tag{2.8}$$

The vast majority of the applications of NEMD simulations of fluid under flow couple the NEMD algorithm with Lees-Edwards Boundary Conditions (LEBCs) and with a thermostat, used to control the temperature. We should point out that the derivation [8] and proof that p-SLLOD [20] and SLLOD [5] satisfy nonlinear response theory were presented in the absence of both LEBCs and a thermostat. In this work, in order to avoid any artifacts due to LEBCs or a thermostat, we simulate a flowing system in the microcanonical (NVE) ensemble. We simulated a three dimensional system of 500

spherical particles interacting with a Lennard-Jones potential, shifted upwards by ε and truncated at the LJ potential minimum of $2^{1/6}\sigma$ at a reduced density of 0.844. The *p*-SLLOD equations of motion were integrated using the reversible Reference System Propagator Algorithm (*r*-RESPA), as developed by Tuckerman *et al*. [13] and applied by Cui. *et al* [24] . The time step was 2.57 fs and we simulated for 1.28 ns. We used conventional periodic boundary conditions in the x and z dimensions. In the y dimension, we imposed a smooth, repulsive wall to maintain the system density. This wall potential interacts with the fluids only in the y dimension (*i.e*., it is frictionless and there is no external force in the flow dimension), and is of the form $U_{wall} = 1/(L-y)^9$, where $L-y$ is the distance of a particle from the wall in the y dimension. We have used an equilibrated set of positions and momenta corresponding to an equilibrium reduced temperature of $T_{eq} = 0.722$ and reduced density of 0.844 to start the simulation.

2.3. Results and Discussions

In Figure 1, we show the profile of the momenta, $\mathbf{p}_i$, and transformed momenta, $\mathbf{p}'_i$, in the x-direction (the flow direction). We have divided the simulation volume into forty planar bins along the y axis. As has been reported before for PCF in the absence of time-dependent boundary conditions, SLLOD dynamics predicts a linear but nonuniform momentum profile [23]. The transformed momenta $\mathbf{p}'_i$ were found to be homogeneous throughout the system.

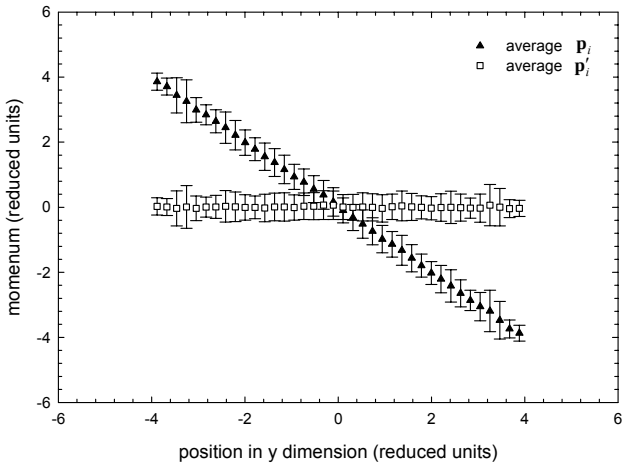

Figure. 1. Comparison of the average $\mathbf{p}_i$ and $\mathbf{p}'_i$ as functions of the y axis. The $\mathbf{p}_i$ (filled circles) have a non-constant profile along the y axis and $\mathbf{p}'_i$ (open circles) have constant profiles. All simulations were carried out at $\gamma^* = 1.0$ (reduced shear rate).

Clearly, if the $\mathbf{p}_i$ is used in the equipartition theory, the temperature evaluated will not be homogeneous throughout the system. In our simulations, we find that the application of a thermostat or the presence of LEBCs serve to mask the nonuniform distribution of $\mathbf{p}_i$. In Figure 2, we collect the forty bins into five groups of eight bins each. We provide a histogram of the probability distribution of $\mathbf{v}_i = \mathbf{p}_i / m_i$ in each group of bins. Rather obviously, the distributions are not all centered around zero, indicating that this momenta does not satisfy the first feature of the MBD, namely that the mean is zero.

More significantly, although less obvious, all five histograms are broader than a Gaussian distribution. This additional variance is due to the presence not only of thermal fluctuations in the velocity, but also fluctuations due to the flow field. In Figure 3, we average over all bins to present the probability distribution of the velocity for the entire simulation box. Here, the total distribution emphasizes the non-Gaussian shape of the

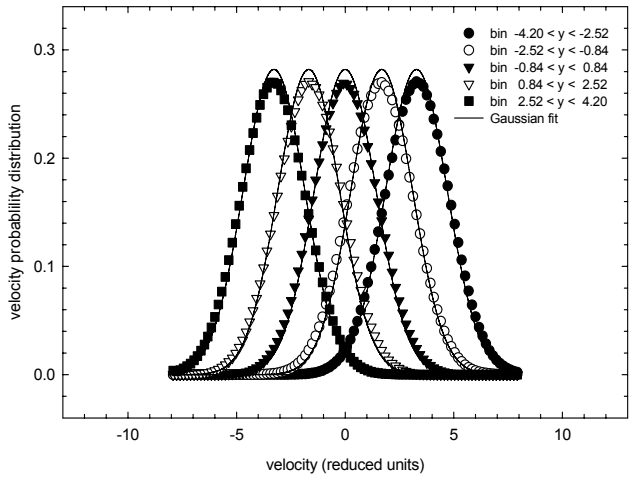

Figure 2. Distribution function for the *x* component of the velocity $\mathbf{v}_i$ for five bins along the y axis. Fits to Gaussian form are plotted as solid lines.

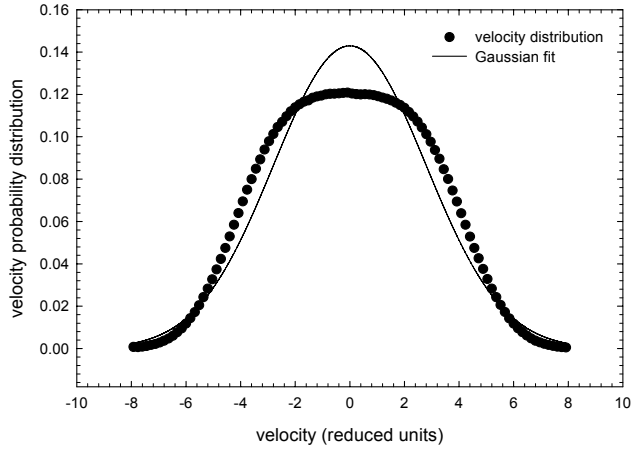

Figure 3. Distribution function for the x component of the velocity $\mathbf{v}_i$ for the entire simulation volume. Fit to a Gaussian form is plotted as a solid line.

distribution. The fact that the distribution is centered around zero is a coincidence due to our choice of defining the coordinate system of the simulation box to span from –L/2 to L/2. Had we defined it to run from 0 to L, the distribution would be centered elsewhere.

In Figure 4, we again collect the forty bins into five groups of eight bins each. We provide a histogram of the probability distribution of $\mathbf{v}_i' = \mathbf{p}_i'/m_i$ in each group of bins. The distributions (1) are identical, (2) have a mean at zero, and (3) fit a Gaussian curve with fluctuations of $\sqrt{k_B T_{kin}^{NE}/m} = \sqrt{2}$. In other words, if we proceed with the p-SLLOD transformation as the basis for the nonequilibrium kinetic temperature, we obtain distributions of the velocity that (i) are uniform through-out the simulation volume and (ii) satisfy the MBD.

This evidence provides a promising indication that the temperature should be evaluated using the transformed momentum. One way to understand these distributions is to consider the relationship between the variance (fluctuations) of $\mathbf{v}_i$ and $\mathbf{v}_i'$. Given the transformation, we have

$$\sigma_{\mathbf{v}_i'}^2 = \sigma_{\mathbf{v}_i}^2 - \sigma_{\mathbf{q}_i \cdot \nabla \mathbf{u}}^2 \tag{2.9}$$

We can see in equation (8) that only the fluctuations of $\mathbf{v}_i'$ correspond to thermal fluctuations. The additional terms in the variance correspond to fluctuations in $\mathbf{v}_i$ due to the external flow field.

Further evidence that the transformed momentum should be used to define a nonequilibrium kinetic temperature is provided in Fig. 5, where we compare block

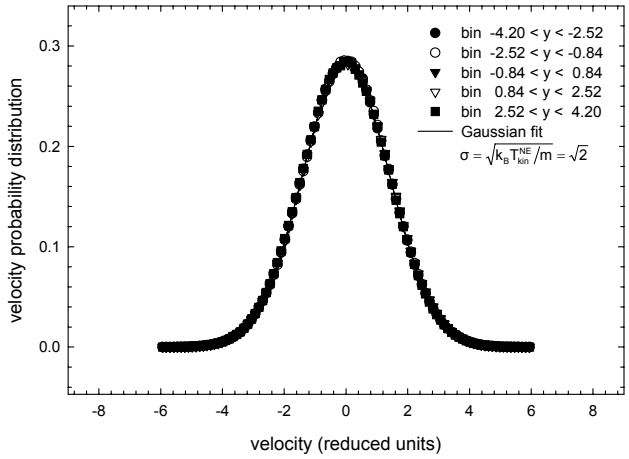

Figure 4. Distribution function for the x component of the transformed velocity $\mathbf{v}_i'$ for five bins along the y axis. Fit to a Gaussian form is plotted as a solid line.

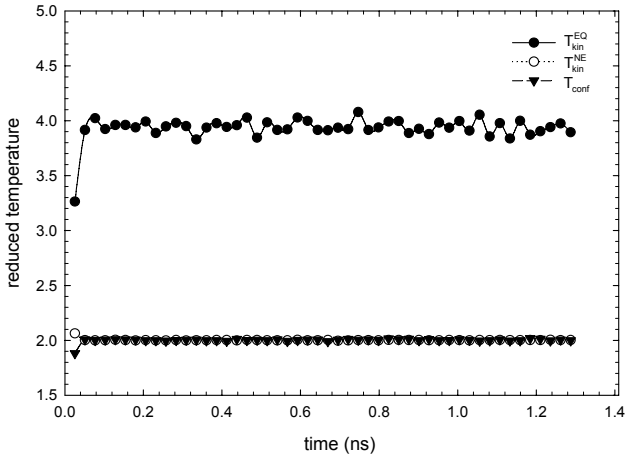

Figure 5. Temperature as a function of time. The conventional (filled circles), the configurational (open circles) and the nonequilibrium temperatures (closed triangles) are plotted as a function of time (in nanoseconds).

averages of the conventional kinetic temperature T_{kin}^{EQ}, the nonequilibrium kinetic temperature T_{kin}^{NE}, and the configurational temperature T_{conf}. The conventional kinetic temperature is completely different from the nonequilibrium kinetic temperature and the configurational temperature, which are the same within the uncertainty of the experiments.

We have examined the ratio of the nonequilibrium kinetic temperature to the configurational temperature as a function of density and shear rate. It is always near unity, for shear rates ranging from 0.1 to 10.0 and for densities (reduced) ranging from 0.1 to 1.0. The proximity of $T_{kin}^{NE} \big/ T_{config}$ to unity across a wide range of densities and shear rates indicates that there is equivalence between the kinetic and configurational temperature even in nonequilibrium states.

2.4. Conclusions:

In the absence of a time-dependant periodic condition, the SLLOD dynamics predicts a momentum with a linear profile. Using these momenta to identify the temperature will result in an inhomogeneous temperature. We have identified the nonequilibrium temperature by isolating the thermal fluctuations using the p-SLLOD transformation. The application of time-dependant boundary conditions in SLLOD dynamics removes the velocity profile, making it impossible to observe this behavior under NEMD simulations in which time dependant boundary conditions are applied. Hence we impose a smooth, repulsive wall along the y boundaries to observe this

behavior. The new definition of nonequilibrium temperature was found to be homogeneous in the entire system volume, and is consistent with the noncanonical transformation associated with the p-SLLOD NEMD algorithm. The velocity distribution of the momenta (according to the new definition) obeys the equipartition theorem and fits to a Maxwell-Boltzmann distribution both locally and globally. The temperature simulated using the new definition was found to be equal to the temperature measured using the configurational information (theoretically and through simulation). This suggests the equivalence of the kinetic and configurational temperature in nonequilibrium states.

Chapter III

A Generalized Hamiltonian-Based Algorithm for Rigorous Nonequilibrium Molecular Dynamics Simulation in the NVT Ensemble using the Nosé-Hoover Thermostat

A methodical, Hamiltonian-based procedure to generate rigorous algorithms for equilibrium molecular dynamics (EMD) simulation in the NVE, NVT, NpT, and NpH ensembles was developed by Keffer et al. [25-27]. The equations of motion, thus generated were proven to generate rigorous trajectories corresponding to the appropriate statistical mechanical ensemble. In this work, we apply the same procedure to generate rigorous nonequilibrium molecular dynamics (NEMD) algorithm in the extended ensemble (NVT). Specifically, we apply this procedure to the NVE p-SLLOD algorithm, which allows for rigorous NEMD simulation in the presence of an arbitrary, externally imposed flow field.

The procedure contains the following steps:

1. Define the Hamiltonian in terms of the laboratory coordinates in the mathematical (potentially aphysical) frame of reference.
2. Express the Hamiltonian in terms of the peculiar and center of mass (COM) coordinates in the mathematical frame of reference.
3. Identify a noncanonical (p-SLLOD) transformation from the peculiar and COM coordinates in the mathematical frame of reference to the peculiar and COM coordinates in the physical frame of reference.

4. Express the Hamiltonian in terms of the peculiar and COM coordinates in the physical frame of reference.
5. Identify the kinetic energy term that contributes to the nonequilibrium temperature and implement a Hamiltonian-based thermostat (Nosé-Hoover thermostat) rigorously.
6. Express the Hamiltonian in terms of the laboratory coordinates in the mathematical frame of reference where a canonical (symplectic) relationship exists between the Hamiltonian and the equations of motion.
7. Derive the equations of motion in terms of the laboratory coordinates in the mathematical frame of reference.
8. Express the equations of motions in the peculiar and COM coordinates in the physical frame of reference using the noncanonical transformation.

We begin with a brief review of the p-SLLOD algorithm. A variation of the p-SLLOD algorithm was first proposed by Tuckerman *et al.* [23]; however, it returned the philosophy of the SLLOD algorithm: that flow is driven by an externally imposed field. Edwards and Dressler derived the p-SLLOD algorithm from a Hamiltonian, using a noncanonical transformation, for the microcanonical ensemble [8]. Baig *et al.* have provided the simulation strategy to implement p-SLLOD [9] in NEMD simulations, and have generated numerical examples for simple fluids [9] and linear alkanes under shear and planar elongational flow fields [10]. Edwards *et al.* have demonstrated that the p-SLLOD algorithm is completely consistent with nonequilibrium statistical mechanics and nonlinear response theory [20].

The relationship of p-SLLOD to its predecessor, SLLOD [3, 5], is as follows. SLLOD is rigorous for a limited set of flows, including shear flow, which satisfy the constraint $\nabla \mathbf{u}^* \cdot \nabla \mathbf{u}^* = \sum_{\alpha=1}^{3}\sum_{\gamma=1}^{3} \boldsymbol{\delta}_\alpha \boldsymbol{\delta}_\gamma \sum_{\beta=1}^{3} \frac{\partial u_\beta^*}{\partial r_\alpha} \frac{\partial u_\gamma^*}{\partial r_\beta} = 0$, where $\mathbf{u}^*$ is the velocity of the imposed flow field, $\mathbf{r}$ is the position. In contrast, the p-SLLOD algorithm is rigorous for an arbitrary flow field, and reduces to the SLLOD algorithm in shear flow [9]. One of the accomplishments of the p-SLLOD algorithm is that it is able to simulate elongational flow correctly, without the generation of aphysical phase transitions observed when using SLLOD to model elongational flow [6].

In this work, we will implement a version of the Nosé-Hoover thermostat [11, 12] in a consistent and rigorous way. The resulting algorithm will not suffer from the limitations of the original formulation of the Nosé-Hoover thermostat, in which, one was limited to the absence of external forces and the total momentum was fixed at zero.

3.1. The Methodical Procedure

To begin with the derivation, we provide necessary definitions. The peculiar position, $\rho'_{i,\alpha}$, and peculiar momentum, $\pi'_{i,\alpha}$, are defined with respect to the COM position, R'_α, and COM momentum, P'_α, as

$$\rho'_{i,\alpha} \equiv r'_{i,\alpha} - R'_\alpha \tag{3.1.a}$$

$$\frac{\pi'_{i,\alpha}}{m'_i} \equiv \frac{p'_{i,\alpha}}{m'_i} - \frac{P'_\alpha}{M'} \tag{3.1.b}$$

where the COM momentum, P'_α, is

$$P'_\alpha \equiv \sum_{i=1}^{N} p'_{i,\alpha} \tag{3.2.a}$$

the COM position, R'_α, is

$$R'_\alpha \equiv \frac{\sum_{i=1}^{N} m'_i r'_{i,\alpha}}{M'} \tag{3.2.b}$$

and the total mass of the system, M', is

$$M' \equiv \sum_{i=1}^{N} m'_i \quad . \tag{3.2.c}$$

As a result of the definitions in equation (3.1.a) and equation (3.1.b), it is clear that the following constraints apply to the peculiar position and momentum,

$$\sum_{i=1}^{N} \pi'_{i,\alpha} = 0 \tag{3.3.a}$$

$$\sum_{i=1}^{N} m'_i \rho'_{i,\alpha} = 0 \tag{3.3.b}$$

In other words, only *N*-1 of the particles have independent peculiar coordinates.

Once the transformation from the laboratory coordinates to the peculiar coordinates have been defined, the next step is to follow the methodical procedure to generate a

rigorous NEMD algorithm. The first step of the procedure is to write the Hamiltonian in terms of the laboratory coordinates in the mathematical (potentially aphysical) frame of reference. As known, we can write the Hamiltonian for NVE in terms of laboratory coordinates in the mathematical frame of reference as

$$H'_{NVE} = \frac{1}{2}\sum_{i=1}^{N}\sum_{\alpha=1}^{3}\frac{1}{m'_i}p'^{2}_{i,\alpha} + U\left(r'_{i,\alpha} - r'_{j,\alpha}\right) \tag{3.4}$$

The second step of the procedure is to express the Hamiltonian in terms of the peculiar and center of mass (COM) coordinates in the mathematical frame of reference. We change the frame of reference using equations (3.1a) and (3.1b)

$$\begin{aligned} H'_{NVE} = {} & \frac{1}{2}\sum_{i=1}^{N}\sum_{\alpha=1}^{3}\frac{\pi'^{2}_{i,\alpha}}{m'_i} + \sum_{i=1}^{N}\sum_{\alpha=1}^{3}\pi'_{i,\alpha}\frac{P'_\alpha}{M'} + \frac{1}{2}\sum_{i=1}^{N}\sum_{\alpha=1}^{3}m'_i\left(\frac{P'_\alpha}{M'}\right)^2 \\ & + U_{int}\left(\rho'_{i,\alpha} - \rho'_{j,\alpha}\right) + U_{ext}\left(\rho'_{i,\alpha}, R'_\alpha\right) \end{aligned} \tag{3.5}$$

The third step of the procedure is to identify a noncanonical transformation from the mathematical frame of reference to the physical frame of reference

$$\rho_{i,\alpha} = \rho'_{i,\alpha} \tag{3.6.a}$$

$$\pi_{i,\alpha} = \pi'_{i,\alpha} - m'_i u_\alpha\left(r_i, t\right) + \frac{m'_i}{M'}\sum_{j=1}^{N}m'_j u_\alpha\left(r_j, t\right) \tag{3.6.b}$$

$$R_\alpha = R'_\alpha \tag{3.6.c}$$

$$\frac{P_\alpha}{M} = \frac{P'_\alpha}{M'} - \frac{1}{M'}\sum_{j=1}^{N}m'_j u_\alpha\left(\mathbf{r}_j, t\right) \tag{3.6.d}$$

$$dt = dt' \tag{3.6.e}$$

$$m_i = m_i' \tag{3.6.f}$$

The fourth step is to express the Hamiltonian in terms of the peculiar and COM coordinates in the physical frame of reference. To do this, we can substitute equation (3.6) into equation (3.5):

$$\begin{aligned} H_{NVE} = & \frac{1}{2}\sum_{i=1}^{N}\sum_{\alpha=1}^{3}\frac{{\pi_{i,\alpha}}^2}{m_i} + \sum_{\alpha=1}^{3}\sum_{i=1}^{N}\left(\pi_{i,\alpha}\right)\left(u_\alpha\left(r_i,t\right)\right)\frac{1}{2}\sum_{\alpha=1}^{3}\sum_{i=1}^{N}m_i\left(u_\alpha\left(r_i,t\right)\right)^2 \\ & + \frac{1}{2}\sum_{i=1}^{N}\sum_{\alpha=1}^{3}m_i\left(\frac{P_\alpha}{M}\right)^2 + \left(\sum_{j=1}^{N}\sum_{\alpha=1}^{3}m_j u_\alpha\left(\mathbf{r}_j,t\right)\right)\left(\frac{P_\alpha}{M}\right) \\ & + \sum_{i=1}^{N}\sum_{\alpha=1}^{3}\pi_{i,\alpha}\left(\frac{P_\alpha}{M}\right) + U_{\text{int}}\left(\rho_{i,\alpha}' - \rho_{j,\alpha}'\right) + U_{ext}\left(\rho_{i,\alpha}', R_\alpha'\right) \end{aligned} \tag{3.7}$$

The next step is to identify the kinetic energy term that contributes to the nonequilibrium temperature and implement a Hamiltonian-based thermostat (Nosé-Hoover thermostat) rigorously:

$$\begin{aligned} H_{NVT} = & \frac{1}{2}\sum_{i=1}^{N}\sum_{\alpha=1}^{3}\frac{{\pi_{i,\alpha}}^2}{m_i s^2} + \sum_{i=1}^{N}\sum_{\alpha=1}^{3}\left(\pi_{i,\alpha}\right)\left(u_\alpha\left(r_i,t\right)\right) + \frac{1}{2}\sum_{i=1}^{N}\sum_{\alpha=1}^{3}m_i\left(u_\alpha\left(r_i,t\right)\right)^2 \\ & + \frac{1}{2}\sum_{i=1}^{N}\sum_{\alpha=1}^{3}m_i\left(\frac{P_\alpha}{M}\right)^2 + \left(\sum_{j=1}^{N}\sum_{\alpha=1}^{3}m_j u_\alpha\left(\mathbf{r}_j,t\right)\right)\left(\frac{P_\alpha}{M}\right) \\ & + \sum_{i=1}^{N}\sum_{\alpha=1}^{3}\pi_{i,\alpha}\left(\frac{P_\alpha}{M}\right) + U_{\text{int}}\left(\rho_{i,\alpha}' - \rho_{j,\alpha}'\right) + U_{ext}\left(\rho_{i,\alpha}', R_\alpha'\right) \\ & + \frac{1}{2Q_s}p_s^2 + fk_B T_{set}\ln\left(s\right) \end{aligned} \tag{3.8}$$

The penultimate term on the RHS of (3.8) is the kinetic energy of the thermostat, and the last term is the potential energy of the thermostat. s is the thermostat metric (with a value of unity when there is no thermostat), p_s is the thermostat momentum (with a value of zero when there is no thermostat), Q_s is the inertial mass of the thermostat, f is the number of degrees of freedom associated with the momenta in the system, k_B is Boltzmann's constant, and T_{set} is the set temperature. We have only applied the thermostat to the first term.

The sixth step is to express the Hamiltonian in terms of the laboratory coordinates in the mathematical frame of reference. We substitute equations (3.6) and equations (3.1) and equations (3.2) in equation (3.8):

$$\begin{aligned} H'_{NVT} = & \frac{1}{2}\sum_{i=1}^{N}\sum_{\alpha=1}^{3}\frac{\left(p'_{i,\alpha}\right)^2}{m'_i s^2} + \frac{1}{2M'}\left(1-\frac{1}{s^2}\right)\sum_{\alpha=1}^{N}\left(\sum_{j=1}^{N}p'_{j,\alpha}\right)^2 + \left(1-\frac{1}{s^2}\right)\sum_{i=1}^{N}\sum_{\alpha=1}^{3}\left(p'_{i,\alpha}\right)u_\alpha\left(r_i,t\right) \\ & - \frac{1}{M'}\left(1-\frac{1}{s^2}\right)\sum_{i=1}^{N}\sum_{\alpha=1}^{3}\left(m'_i u_\alpha\left(r_i,t\right)\right)\sum_{j=1}^{N}p'_{j,\alpha} - \frac{1}{2}\left(1-\frac{1}{s^2}\right)\sum_{i=1}^{N}\sum_{\alpha=1}^{3}m'_i\left(u_\alpha\left(r_i,t\right)\right)^2 \\ & + \frac{1}{2M'}\left(1-\frac{1}{s^2}\right)\sum_{\alpha=1}^{3}\left(\sum_{j=1}^{N}m'_j u_\alpha\left(\mathbf{r}_j,t\right)\right)^2 + U_{\text{int}}\left(\rho'_{i,\alpha}-\rho'_{j,\alpha}\right) + U_{ext}\left(\rho'_{i,\alpha},R'_\alpha\right) \\ & + \frac{1}{2Q_s}p_s^2 + fk_B T_{set}\ln\left(s\right) \end{aligned} \tag{3.9}$$

The seventh step of the procedure is to derive the equations of motion in terms of the laboratory coordinates in the mathematical frame of reference. In this step, we rely on the canonical relationship between the Hamiltonian and the equations of motion:

$$\frac{dr'_{i,\alpha}}{dt'} = \frac{\partial H'_{NVT}}{\partial p'_{i,\alpha}} = \frac{p'_{i,\alpha}}{m'_i s^2} + \frac{1}{M'}\left(1-\frac{1}{s^2}\right)\left(\sum_{j=1}^{N} p'_{j,\alpha}\right) + \left(1-\frac{1}{s^2}\right)u_\alpha(r_i,t) - \frac{1}{M'}\left(1-\frac{1}{s^2}\right)\sum_{i=1}^{N}\left(m'_i u_\alpha(r_i,t)\right) \tag{3.10.a}$$

$$\frac{dp'_{i,\beta}}{dt'} = -\frac{\partial H'_{NVT}}{\partial r'_{i,\beta}} = -\left(1-\frac{1}{s^2}\right)\sum_{\gamma=1}^{3}\left(p'_{i,\gamma}\right)\frac{\partial u_\gamma(r_i,t)}{\partial r'_{i,\beta}} + \frac{1}{M'}\left(1-\frac{1}{s^2}\right)\sum_{\gamma=1}^{3}\left(m'_i\frac{\partial u_\gamma(r_i,t)}{\partial r'_{i,\beta}}\right)\sum_{j=1}^{N}p'_{j,\gamma} + \left(1-\frac{1}{s^2}\right)\sum_{\gamma=1}^{3}m'_i\left(u_\gamma(r_i,t)\right)\frac{\partial u_\gamma(r_i,t)}{\partial r'_{i,\beta}} - \frac{1}{M'}\left(1-\frac{1}{s^2}\right)\sum_{\gamma=1}^{3}m'_i\left(\sum_{j=1}^{N}m'_j u_\gamma(\mathbf{r}_j,t)\right)\frac{\partial u_\gamma(r_i,t)}{\partial r'_{i,\beta}} + F_{i,\beta}^{'\,\mathrm{int}} + F_{i,\beta}^{'ext,pec} - \frac{m_i^{'}}{M^{'}}\sum_{j=1}^{N}F_{j,\beta}^{'ext,pec} + F_{\beta}^{'ext,COM}\,\frac{m_i^{'}}{M^{'}} \tag{3.10.b}$$

$$\frac{ds}{dt'} = \frac{\partial H'_{NVT}}{\partial p_s} = \frac{p_s}{Q_s} \tag{3.10.c}$$

$$\frac{dp_s}{dt'} = -\frac{\partial H'_{NVT}}{\partial s} = \sum_{\alpha=1}^{N}\sum_{i=1}^{3}\frac{\left(\pi'_{i,\alpha} - m'_i u_\alpha(r_i,t) + \frac{m'_i}{M'}\sum_{j=1}^{N}m'_j u_\alpha(r_j,t)\right)^2}{m_i s^3} - \frac{f k_B T_{set}}{s} \tag{3.10.d}$$

The final step is to express the equations of motions in the peculiar and COM coordinates in the physical frame of reference using the following noncanonical transformations:

$$dt = \frac{1}{s}dt' \tag{3.11.a}$$

$$m_i = m_i' \tag{3.11.b}$$

$$\rho_{i,\alpha} = \rho_{i,\alpha}' \tag{3.11.c}$$

$$\pi_{i,\alpha} = \frac{\pi_{i,\alpha}' - m_i' u_\alpha\left(r_i,t\right) + \frac{m_i'}{M'}\sum_{j=1}^{N} m_j' u_\alpha\left(r_j,t\right)}{s} \tag{3.11.d}$$

$$R_\alpha = R_\alpha' \tag{3.11.e}$$

$$\frac{P_\alpha}{M} = \frac{P_\alpha'}{M'} - \frac{\sum_{j=1}^{N} m_j' u_\alpha\left(\mathbf{r}_j,t\right)}{M'} \tag{3.11.f}$$

$$\eta_T = s \tag{3.11.g}$$

$$\zeta_T = \frac{p_s}{Q_s} \tag{3.11.h}$$

We use equations (3.11) and (3.1) in equation (3.10). The following equations are derived in Appendix A:

$$\frac{d\rho_{i,\alpha}}{dt} = \frac{\pi_{i,\alpha}}{m_i} + \eta_T u_\alpha\left(r_i,t\right) - \frac{\eta_T}{M}\sum_{i=1}^{N}\left(m_i u_\alpha\left(r_i,t\right)\right) \tag{3.12.a}$$

$$\begin{aligned}\frac{d\pi_{i,\alpha}}{dt} &= -\left(1-\frac{1}{\eta_T{}^2}\right)\sum_{\gamma=1}^{3}\left(\eta_T\pi_{i,\gamma}\right)\frac{\partial u_\gamma(r_i,t)}{\partial r_{i,\alpha}} \\ &+ F_{i,\alpha}^{\text{int}} + F_{i,\alpha}^{ext,pec} - \frac{m_i}{M'}\sum_{j=1}^{N}F_{j,\alpha}^{ext,pec} \\ &+ \frac{m_i}{M}\left(1-\frac{1}{\eta_T{}^2}\right)\sum_{i=1}^{N}\sum_{\gamma=1}^{3}\left(\eta_T\pi_{i,\gamma}\right)\frac{\partial u_\gamma(r_i,t)}{\partial r_{i,\alpha}} \\ &- m_i\left(\frac{1}{\eta_T}\frac{\partial u_\alpha(\mathbf{r}_i,t)}{\partial t}+\sum_{\gamma=1}^{3}\frac{\partial u_\alpha(\mathbf{r}_i,t)}{\partial r_{i,\gamma}}\left(\frac{\pi_{i,\gamma}}{m_i\eta_T}+\frac{P_\gamma}{M}+u_\gamma(r_i,t)\right)\right) \\ &+ \frac{m_i}{M}\sum_{j=1}^{N}m_j\left(\frac{1}{\eta_T}\frac{\partial u_\alpha(\mathbf{r}_j,t)}{\partial t}+\sum_{\gamma=1}^{3}\frac{\partial u_\alpha(\mathbf{r}_j,t)}{\partial r_{i,\gamma}}\left(\frac{\pi_{j,\gamma}}{m_j\eta_T}+\frac{P_\gamma}{M}+u_\gamma(r_j,t)\right)\right) \\ &- \pi_{i,\alpha}\zeta_T\end{aligned} \tag{3.12.b}$$

$$\begin{aligned}\frac{dP_\alpha}{dt} &= -\eta_T{}^2\left(1-\frac{1}{\eta_T{}^2}\right)\sum_{i=1}^{N}\sum_{\gamma=1}^{3}\left(\pi_{i,\gamma}\right)\frac{\partial u_\gamma(r_i,t)}{\partial r_{i,\alpha}} + \eta_T F_\alpha^{ext,COM} \\ &- \eta_T\sum_{j=1}^{N}m_j\left(\frac{1}{\eta_T}\frac{\partial u_\alpha(\mathbf{r}_j,t)}{\partial t}+\sum_{\gamma=1}^{3}\frac{\partial u_\alpha(\mathbf{r}_j,t)}{\partial r_{i,\gamma}}\left(\frac{\pi_{j,\gamma}}{m_j\eta_T}+\frac{P_\gamma}{M}+u_\gamma(r_j,t)\right)\right)\end{aligned} \tag{3.12.c}$$

$$\frac{dR_\alpha}{dt} = \frac{dR'_\alpha}{dt} = \frac{sP'_\beta}{M'} = \frac{\eta_T}{M}\left(P_\alpha + \sum_{j=1}^{N}m_j u_\alpha(\mathbf{r}_j,t)\right) \tag{3.12.d}$$

$$\frac{d\eta_T}{dt} = \eta_T\zeta_T \tag{3.12.e}$$

$$\frac{d\zeta_T}{dt} = \vartheta^2\left(\frac{T(t)}{T_{set}}-1\right) \tag{3.12.f}$$

where we used the law of equipartition to define the temperature in terms of the peculiar momenta,

$$T(t) = \frac{1}{f\,k_B}\sum_{i=1}^{N}\sum_{\alpha=1}^{3}\frac{\pi_{i,\alpha}^2}{m_i} \tag{3.13}$$

and where we have dropped the inertial mass of the thermostat, Q_s, in favor of a thermostat response frequency, ν_T,

$$\nu_T \equiv \sqrt{\frac{f\, k_B T_{set}}{Q_s}} \tag{3.14}$$

because ν_T is independent of system size, whereas Q_s is not. In the absence of a thermostat (*i.e.*, $\eta_T = 1;\ \nu_T = 0$), equation (3.12) reduces to the NVE equations of motion.

3.2. Simplified Algorithm for Time Invariant Flows

Let us see how the equations of motion in (3.12) will simplify under the following constraints (i) time invariant flow and (ii) absence of external forces,

$$u_\alpha(\mathbf{r}_i, t) = u_\alpha(\mathbf{r}_i) \tag{3.15}$$

$$\begin{aligned} F_{i,\alpha}^{ext,pec} &= 0 \\ F_\alpha^{ext,COM} &= 0 \end{aligned} \tag{3.16}$$

The equations of motion are now

$$\frac{d\rho_{i,\alpha}}{dt} = \frac{\pi_{i,\alpha}}{m_i} + \eta_T u_\alpha(r_i) - \frac{\eta_T}{M}\sum_{i=1}^{N}\left(m_i u_\alpha(r_i)\right) \tag{3.17.a}$$

$$\begin{aligned}\frac{d\pi_{i,\alpha}}{dt} &= -\left(1-\frac{1}{{\eta_T}^2}\right)\sum_{\gamma=1}^{3}\left(\eta_T\pi_{i,\gamma}\right)\frac{\partial u_\gamma\left(r_i\right)}{\partial r_{i,\alpha}} \\ &+ F_{i,\alpha}^{\text{int}} + \frac{m_i}{M}\left(1-\frac{1}{{\eta_T}^2}\right)\sum_{i=1}^{N}\sum_{\gamma=1}^{3}\left(\eta_T\pi_{i,\gamma}\right)\frac{\partial u_\gamma\left(r_i\right)}{\partial r_{i,\alpha}} \\ &- m_i\left(\sum_{\gamma=1}^{3}\frac{\partial u_\alpha\left(\mathbf{r}_i\right)}{\partial r_{i,\gamma}}\left(\frac{\pi_{i,\gamma}}{m_i\eta_T}+\frac{P_\gamma}{M}+u_\gamma\left(r_i\right)\right)\right) \\ &+ \frac{m_i}{M}\sum_{j=1}^{N}m_j\left(\sum_{\gamma=1}^{3}\frac{\partial u_\alpha\left(\mathbf{r}_j\right)}{\partial r_{i,\gamma}}\left(\frac{\pi_{j,\gamma}}{m_j\eta_T}+\frac{P_\gamma}{M}+u_\gamma\left(r_j\right)\right)\right) \\ &- \pi_{i,\alpha}\zeta_T\end{aligned} \tag{3.17.b}$$

$$\begin{aligned}\frac{dP_\alpha}{dt} &= -{\eta_T}^2\left(1-\frac{1}{{\eta_T}^2}\right)\sum_{i=1}^{N}\sum_{\gamma=1}^{3}\left(\pi_{i,\gamma}\right)\frac{\partial u_\gamma\left(r_i\right)}{\partial r_{i,\alpha}} \\ &- \eta_T\sum_{j=1}^{N}m_j\left(\sum_{\gamma=1}^{3}\frac{\partial u_\alpha\left(\mathbf{r}_j\right)}{\partial r_{i,\gamma}}\left(\frac{\pi_{j,\gamma}}{m_j\eta_T}+\frac{P_\gamma}{M}+u_\gamma\left(r_j\right)\right)\right)\end{aligned} \tag{3.17.c}$$

$$\frac{dR_\alpha}{dt} = \frac{\eta_T}{M}\left(P_\alpha + \sum_{j=1}^{N}m_j u_\alpha\left(\mathbf{r}_j\right)\right) \tag{3.17.d}$$

Equations (3.12e) and (3.12f) do not change.

Next, consider a system with the following additional assumptions: (iii) the momentum is initialized to zero, $\sum_{i=1}^{N}p_{i,\alpha}=0$, (iv) the gradient of the velocity profile is independent of position, i.e., homogeneous flow as is the case for purely shear and purely elongational flow, $u_\alpha\left(\mathbf{r}_i\right)=\sum_{\beta=1}^{3}\frac{\partial u_\alpha}{\partial r_\beta}r_{i,\beta}$ and (v) Planar Couette flow. With these constraints, equation (3.17) becomes

$$\frac{d\rho_{i,\alpha}}{dt} = \frac{\pi_{i,\alpha}}{m_i} + \eta_T \sum_{\beta=1}^{3} \frac{\partial u_\alpha}{\partial r_\beta} r_{i,\beta} - \frac{\eta_T}{M} \sum_{i=1}^{N} \sum_{\beta=1}^{3} m_i r_{i,\beta} \frac{\partial u_\alpha}{\partial r_\beta} \tag{3.18.a}$$

$$\frac{d\pi_{i,\alpha}}{dt} = -\left(\eta_T - \frac{1}{\eta_T}\right) \sum_{\beta=1}^{3} \pi_{i,\beta} \frac{\partial u_\beta}{\partial r_\alpha} + F_{i,\alpha}^{\text{int}} - \frac{1}{\eta_T} \sum_{\beta=1}^{3} \pi_{i,\beta} \frac{\partial u_\alpha}{\partial r_\beta} - \pi_{i,\alpha} \zeta_T \tag{3.18.b}$$

$$\frac{dP_\alpha}{dt} = -\eta_T \sum_{j=1}^{N} m_j \left(\sum_{\gamma=1}^{3} \frac{\partial u_\alpha(\mathbf{r}_j)}{\partial r_{i,\gamma}} \left(\frac{P_\gamma}{M} \right) \right) \tag{3.18.c}$$

$$\frac{dR_\alpha}{dt} = \frac{\eta_T}{M} \left(P_\alpha + \sum_{j=1}^{N} m_j \sum_{\beta=1}^{3} \frac{\partial u_\alpha}{\partial r_\beta} r_{j,\beta} \right) \tag{3.18.d}$$

$$\frac{d\eta_T}{dt} = \eta_T \zeta_T \tag{3.18.e}$$

$$\frac{d\zeta_T}{dt} = \vartheta^2 \left(\frac{T(t)}{T_{set}} - 1 \right) \tag{3.18.f}$$

In the case of shear flow, equation (3.20.c) reduces to equations (3.21.a) and (3.21.b). If we initialize the simulation to have zero center of mass (COM) momentum, then the center of mass momentum will be zero throughout the simulation:

$$\frac{dP_y}{dt} = \frac{dP_z}{dt} = 0 \tag{3.19.a}$$

$$\frac{dP_x}{dt} = -\eta_T \sum_{j=1}^{N} m_j \frac{\partial u_x(\mathbf{r}_j)}{\partial r_{i,y}} \left(\frac{P_y}{M} \right) \tag{3.19.b}$$

The equation of motion for the laboratory positions in the physical frame of reference is given by

$$\frac{dr_{i,\alpha}}{dt} = \frac{\pi_{i,\alpha}}{m_i} + \eta_T \sum_{\beta=1}^{3} \frac{\partial u_\alpha}{\partial r_\beta} r_{i,\beta} \tag{3.20}$$

3.3. Conservation of Hamiltonian

In the section, we prove by direct evaluation that the Hamiltonian in the physical frame of reference in the NVT ensemble is a conserved quantity when expressed in terms of the peculiar and COM coordinates.

The Hamiltonian in terms of the peculiar coordinates in the physical frame of reference is given by

$$\begin{aligned} H_{NVT} = & \frac{1}{2}\sum_{i=1}^{N}\sum_{\alpha=1}^{3}\frac{\left(\pi_{i,\alpha}\right)^2}{m_i} + \frac{1}{2}\sum_{i=1}^{N}\sum_{\alpha=1}^{3} m_i u_\alpha^2\left(r_i,t\right) + \frac{1}{2}\sum_{i=1}^{N}\sum_{\alpha=1}^{3} m_i \frac{\left(P_\alpha\right)^2}{M^2} \\ & + \sum_{i=1}^{N}\sum_{\alpha=1}^{3}\left(\eta_T \pi_{i,\alpha}\right) u_\alpha\left(r_i,t\right) + \sum_{i=1}^{N}\sum_{\alpha=1}^{3} m_i u_\alpha\left(r_i,t\right)\frac{\left(P_\alpha\right)}{M} \\ & + U_{int}\left(\rho_{i,\alpha} - \rho_{j,\alpha}\right) + U_{ext}\left(\rho_{i,\alpha}, R_\alpha\right) \\ & + \frac{1}{2}\frac{f\,k_B T_{set}}{\nu_T^2}\zeta_T^2 + f\,k_B T_{set}\ln\left(\eta_T\right) \end{aligned} \tag{3.21}$$

The evolution of the Hamiltonian is given by

$$\begin{aligned} \frac{dH_{NVT}}{dt} = & \sum_{i=1}^{N}\sum_{\alpha=1}^{3}\frac{\partial H_{NVT}}{\partial \pi_{i,\alpha}}\frac{d\pi_{i,\alpha}}{dt} + \sum_{i=1}^{N}\sum_{\alpha=1}^{3}\frac{\partial H_{NVT}}{\partial \rho_{i,\alpha}}\frac{d\rho_{i,\alpha}}{dt} + \sum_{i=1}^{N}\sum_{\alpha=1}^{3}\frac{\partial H_{NVT}}{\partial P_\alpha}\frac{dP_\alpha}{dt} \\ & + \sum_{i=1}^{N}\sum_{\alpha=1}^{3}\frac{\partial H_{NVT}}{\partial R_\alpha}\frac{dR_\alpha}{dt} + \frac{\partial H_{NVT}}{\partial \zeta_T}\frac{d\zeta_T}{dt} + \frac{\partial H_{NVT}}{\partial \eta_T}\frac{d\eta_T}{dt} + \frac{\partial H_{NVT}}{\partial t} \end{aligned} \tag{3.22}$$

Let us first evaluate the partial derivatives of the Hamiltonian. The Hamiltonian in equation (3.21) is differentiated partially with respect to the variable $\pi_{i,\alpha}$:

$$\frac{\partial H_{NVT}}{\partial \pi_{i,\alpha}} = \frac{\pi_{i,\alpha}}{m_i} + \eta_T u_\alpha(r_i,t) \tag{3.23.a}$$

The Hamiltonian in equation (3.21) is differentiated partially with respect to the variable $\rho_{i,\alpha}$:

$$\begin{aligned}\frac{\partial H_{NVT}}{\partial \rho_{i,\alpha}} &= \sum_{\beta=1}^{3} m_i u_\beta(r_i,t) \sum_{\gamma=1}^{3} \frac{\partial u_\beta(r_i,t)}{\partial r_{i,\gamma}} \frac{\partial r_{i,\gamma}}{\partial \rho_{i,\alpha}} + \sum_{\beta=1}^{3} (\eta_T \pi_{i,\beta}) \sum_{\gamma=1}^{3} \frac{\partial u_\beta(r_i,t)}{\partial r_{i,\gamma}} \frac{\partial r_{i,\gamma}}{\partial \rho_{i,\alpha}} + \\ &+ \sum_{\beta=1}^{3} m_i \frac{(P_\beta)}{M} \sum_{\gamma=1}^{3} \frac{\partial u_\beta(r_i,t)}{\partial r_{i,\gamma}} \frac{\partial r_{i,\gamma}}{\partial \rho_{i,\alpha}} + \frac{\partial U_{int}(\rho_{i,\alpha} - \rho_{j,\alpha})}{\partial \rho_{i,\alpha}} + \frac{\partial U_{ext}(\rho_{i,\alpha}, R_\alpha)}{\partial \rho_{i,\alpha}} \\ &= \sum_{\beta=1}^{3} m_i u_\beta(r_i,t) \sum_{\gamma=1}^{3} \frac{\partial u_\beta(r_i,t)}{\partial r_{i,\gamma}} \frac{\partial r_{i,\gamma}}{\partial \rho_{i,\alpha}} + \sum_{\beta=1}^{3} (\eta_T \pi_{i,\beta}) \sum_{\gamma=1}^{3} \frac{\partial u_\beta(r_i,t)}{\partial r_{i,\gamma}} \frac{\partial r_{i,\gamma}}{\partial \rho_{i,\alpha}} + \\ &+ \sum_{\beta=1}^{3} m_i \frac{(P_\beta)}{M} \sum_{\gamma=1}^{3} \frac{\partial u_\beta(r_i,t)}{\partial r_{i,\gamma}} \frac{\partial r_{i,\gamma}}{\partial \rho_{i,\alpha}} - F_{i,\alpha}^{\text{int}} - F_{i,\alpha}^{ex,pec}\end{aligned} \tag{3.23.b}$$

where the external force and the internal force is defined as

$$\begin{aligned}&\frac{\partial U_{int}(\rho_{i,\alpha} - \rho_{j,\alpha})}{\partial \rho_{i,\alpha}} = \sum_{\substack{j=1 \\ j \neq i}}^{N} \frac{\partial U_{int}(\rho_{i,\alpha} - \rho_{j,\alpha})}{\partial(\rho_{i,\alpha} - \rho_{j,\alpha})} \frac{\partial(\rho_{i,\alpha} - \rho_{j,\alpha})}{\partial \rho_{i,\alpha}} = -F_{i,\alpha}^{\text{int}} \\ &\frac{\partial U_{ext}(\rho_{i,\alpha}, R_{i,\alpha})}{\partial \rho_{i,\alpha}} = -F_{i,\alpha}^{ext,pec}\end{aligned} \tag{3.23.c}$$

The Hamiltonian in equation (3.21) is differentiated partially with respect to the variable P_α:

$$\frac{\partial H_{NVT}}{\partial P_\alpha} = \sum_{i=1}^{N} m_i \frac{(P_\alpha)}{M^2} + \frac{1}{M} \sum_{i=1}^{N} m_i u_\alpha(r_i,t) \tag{3.23.d}$$

The Hamiltonian in equation (3.21) is differentiated partially with respect to the variable R_α:

$$\frac{\partial H_{NVT}}{\partial R_\alpha} = \sum_{i=1}^{N}\sum_{\beta=1}^{3} m_i u_\beta(r_i,t)\sum_{\gamma=1}^{3}\frac{\partial u_\beta(r_i,t)}{\partial r_{i,\gamma}}\frac{\partial r_{i,\gamma}}{\partial R_\alpha} + \sum_{i=1}^{N}\sum_{\beta=1}^{3}\left(\eta_T \pi_{i,\beta}\right)\sum_{\gamma=1}^{3}\frac{\partial u_\beta(r_i,t)}{\partial r_{i,\gamma}}\frac{\partial r_{i,\gamma}}{\partial R_\alpha} + \sum_{i=1}^{N}\sum_{\beta=1}^{3} m_i \frac{\left(P_\beta\right)}{M}\sum_{\gamma=1}^{3}\frac{\partial u_\beta(r_i,t)}{\partial r_{i,\gamma}}\frac{\partial r_{i,\gamma}}{\partial R_\alpha} - F_\alpha^{ext,COM} \tag{3.23.e}$$

where the external force in terms of the center of mass coordinates is defined as

$$\frac{\partial U_{ext}\left(\rho_{i,\alpha}, R_{i,\alpha}\right)}{\partial R_\alpha} = -F_\alpha^{ext,COM} \tag{3.23.f}$$

The Hamiltonian in equation (3.21) is differentiated partially with respect to the variable ζ_T:

$$\frac{\partial H_{NVT}}{\partial \zeta_T} = \frac{f\, k_B T_{set}}{\nu_T^2}\zeta_T \tag{3.23.g}$$

The Hamiltonian in equation (3.21) is differentiated with respect to the time dilation variable ν_T:

$$\frac{\partial H_{NVT}}{\partial \eta_T} = +\sum_{\alpha=1}^{3}\sum_{i=1}^{N}\left(\pi_{i,\alpha}\right)u_\alpha(r_i,t) + \frac{f\, k_B T_{set}}{\eta_T} \tag{3.23.h}$$

The Hamiltonian in equation (3.21) is differentiated partially with respect to the variable t:

$$\frac{\partial H_{NVT}}{\partial t} = +\sum_{\alpha=1}^{3}\sum_{i=1}^{N} m_i u_\alpha(r_i,t)\frac{\partial u_\alpha(r_i,t)}{\partial t} + \sum_{\alpha=1}^{3}\sum_{i=1}^{N}(\eta_T \pi_{i,\alpha})\frac{\partial u_\alpha(r_i,t)}{\partial t} + \sum_{\alpha=1}^{3}\sum_{i=1}^{N} m_i \frac{(P_\alpha)}{M}\frac{\partial u_\alpha(r_i,t)}{\partial t} \tag{3.23.i}$$

Now we substitute equations (3.12) and equations (3.23) in equation (3.22) and simplify:

$$\frac{dH_{NVT}}{dt} = \left(\eta_T - \frac{1}{\eta_T}\right)\sum_{i=1}^{N}\sum_{\alpha=1}^{3}\pi_{i,\alpha}\frac{\partial u_\alpha(\mathbf{r}_i,t)}{\partial t} \tag{3.24}$$

If we consider time invariant flow, then the evolution of the Hamiltonian would be zero; i.e., the Hamiltonian would be a conserved quantity,

$$\frac{dH_{NVT}}{dt} = 0 \tag{3.25}$$

3.4. Reversible Reference System Propagator Algorithm

We derive the r-RESPA [13, 24] integration algorithm for integrating the equations of motion using the p-SLLOD equations in the NVT ensemble. We assume one time step. In other words, the thermostat and the forces act on the same time scale. This will work for simple fluids without intramolecular degrees of freedom. In the absence of any imposed field beyond that of the imposed flow field, equations (3.18) can be represented as

$$\frac{dr_{i,\alpha}}{dt} = \frac{\pi_{i,\alpha}}{m_i} + \eta_T \sum_{\beta=1}^{3} \frac{\partial u_\alpha}{\partial r_\beta} r_{i,\beta} \tag{3.26.a}$$

$$\frac{d\pi_{i,\alpha}}{dt} = -\left(\eta_T - \frac{1}{\eta_T}\right)\sum_{\beta=1}^{3} \pi_{i,\beta} \frac{\partial u_\beta}{\partial r_\alpha} + F_{i,\alpha}^{\text{int}} - \frac{1}{\eta_T}\sum_{\beta=1}^{3} \pi_{i,\beta} \frac{\partial u_\alpha}{\partial r_\beta} - \pi_{i,\alpha}\zeta_T \tag{3.26.b}$$

$$\frac{d\eta_T}{dt} = \eta_T \zeta_T \tag{3.26.c}$$

$$\frac{d\zeta_T}{dt} = \vartheta^2 \left(\frac{T(t)}{T_{set}} - 1\right) \tag{3.26.d}$$

For this system, the Liouville operator is

$$iL = \frac{dr_{i,\alpha}}{dt}\frac{\partial}{\partial r_{i,\alpha}} + \frac{d\pi_{i,\alpha}}{dt}\frac{\partial}{\partial \pi_{i,\alpha}} + \frac{d\eta_T}{dt}\frac{\partial}{\partial \eta_T} + \frac{d\zeta_T}{dt}\frac{\partial}{\partial \zeta_T} \tag{3.27.a}$$

Equations (3.26) are substituted into equation (3.27.a):

$$\begin{aligned} iL = & \left(\frac{\pi_{i,\alpha}}{m_i} + \eta_T \sum_{\beta=1}^{3} \frac{\partial u_\alpha}{\partial r_\beta} r_{i,\beta}\right)\frac{\partial}{\partial r_{i,\alpha}} \\ & + \left(-\left(\eta_T - \frac{1}{\eta_T}\right)\sum_{\beta=1}^{3} \pi_{i,\beta} \frac{\partial u_\beta}{\partial r_\alpha} + F_{i,\alpha}^{\text{int}} - \frac{1}{\eta_T}\sum_{\beta=1}^{3} \pi_{i,\beta} \frac{\partial u_\alpha}{\partial r_\beta} - \pi_{i,\alpha}\zeta_T\right)\frac{\partial}{\partial \pi_{i,\alpha}} \\ & + \eta_T \zeta_T \frac{\partial}{\partial \eta_T} + \vartheta^2 \left(\frac{T(t)}{T_{set}} - 1\right)\frac{\partial}{\partial \zeta_T} \end{aligned} \tag{3.27.b}$$

The operators are split in a symmetric manner. The Liouville operator is then applied on the variables:

$$
\begin{aligned}
iL = & \frac{1}{2}\vartheta^2\left(\frac{T(t)}{T_{set}}-1\right)\frac{\partial}{\partial\zeta_T}+\frac{F_{i,\alpha}^{\text{int}}}{4}\frac{\partial}{\partial\pi_{i,\alpha}}-\frac{\pi_{i,\alpha}\zeta_T}{2}\frac{\partial}{\partial\pi_{i,\alpha}}+\frac{F_{i,\alpha}^{\text{int}}}{4}\frac{\partial}{\partial\pi_{i,\alpha}} \\
& +\frac{\eta_T\zeta_T}{2}\frac{\partial}{\partial\eta_T}-\frac{1}{2}\left(\left(\eta_T-\frac{1}{\eta_T}\right)\sum_{\beta=1}^{3}\pi_{i,\beta}\frac{\partial u_\beta}{\partial r_\alpha}\right)\frac{\partial}{\partial\pi_{i,\alpha}} \\
& -\frac{1}{2}\left(\frac{1}{\eta_T}\sum_{\beta=1}^{3}\pi_{i,\beta}\frac{\partial u_\alpha}{\partial r_\beta}\right)\frac{\partial}{\partial\pi_{i,\alpha}}+\frac{\eta_T}{2}\left(\sum_{\beta=1}^{3}\frac{\partial u_\alpha}{\partial r_\beta}r_{i,\beta}\right)\frac{\partial}{\partial r_{i,\alpha}} \\
& +\frac{\pi_{i,\alpha}}{m_i}\frac{\partial}{\partial r_{i,\alpha}}+\frac{\eta_T}{2}\left(\sum_{\beta=1}^{3}\frac{\partial u_\alpha}{\partial r_\beta}r_{i,\beta}\right)\frac{\partial}{\partial r_{i,\alpha}}-\frac{1}{2}\left(\frac{1}{\eta_T}\sum_{\beta=1}^{3}\pi_{i,\beta}\frac{\partial u_\alpha}{\partial r_\beta}\right)\frac{\partial}{\partial\pi_{i,\alpha}} \\
& -\frac{1}{2}\left(\left(\eta_T-\frac{1}{\eta_T}\right)\sum_{\beta=1}^{3}\pi_{i,\beta}\frac{\partial u_\beta}{\partial r_\alpha}\right)\frac{\partial}{\partial\pi_{i,\alpha}}+\frac{\eta_T\zeta_T}{2}\frac{\partial}{\partial\eta_T}+\frac{F_{i,\alpha}^{\text{int}}}{4}\frac{\partial}{\partial\pi_{i,\alpha}}-\frac{\pi_{i,\alpha}\zeta_T}{2}\frac{\partial}{\partial\pi_{i,\alpha}} \\
& +\frac{F_{i,\alpha}^{\text{int}}}{4}\frac{\partial}{\partial\pi_{i,\alpha}}+\frac{1}{2}\vartheta^2\left(\frac{T(t)}{T_{set}}-1\right)\frac{\partial}{\partial\zeta_T}
\end{aligned}
\tag{3.27.c}
$$

The first operator changes the thermostat momentum variable,

$$
\zeta_T{}^{(1)} = \exp\left\{i\frac{\Delta t}{2}F_n\left(\pi_{i,\alpha}\right)\frac{\partial}{\partial\zeta_T}\right\}\zeta_T{}^{(0)} = \zeta_T{}^{(0)}+\frac{\Delta t}{2}\vartheta^2\left(\frac{T^{(0)}}{T_{set}}-1\right) \tag{3.28}
$$

The second operator changes the momentum of the particle,

$$
\pi_{i,\alpha}{}^{(2)} = \exp\left\{i\frac{\Delta t}{4}F_{i,\alpha}^{\text{int}}\frac{\partial}{\partial\pi_{i,\alpha}}\right\}\pi_{i,\alpha}{}^{(1)} = \pi_{i,\alpha}{}^{(1)}+\frac{\Delta t}{4}F_{i,\alpha}^{\text{int}}\left(r_{i,\alpha}{}^{(1)}\right) \tag{3.29}
$$

The third operator changes the momentum of the particle,

$$
\pi_{i,\alpha}{}^{(3)} = \exp\left\{-i\frac{\Delta t}{2}\pi_{i,\alpha}\zeta_T\frac{\partial}{\partial\pi_{i,\alpha}}\right\}\pi_{i,\alpha}{}^{(2)} = \pi_{i,\alpha}{}^{(2)}\exp\left\{-\frac{\Delta t}{2}\zeta_T{}^{(2)}\right\} \tag{3.30}
$$

The fourth operator changes the momentum of the particle,

$$\pi_{i,\alpha}{}^{(4)} = \exp\left\{ i\frac{\Delta t}{4} F_{i,\alpha}^{\text{int}} \frac{\partial}{\partial \pi_{i,\alpha}} \right\} \pi_{i,\alpha}{}^{(3)} = \pi_{i,\alpha}{}^{(3)} + \frac{\Delta t}{4} F_{i,\alpha}^{\text{int}}(r_{i,\alpha}{}^{(3)}) \tag{3.31}$$

The fifth operator changes the time dilation variable,

$$\eta_T{}^{(5)} = \exp\left\{ i\frac{\Delta t}{2} \eta_T \zeta_T \frac{\partial}{\partial \eta_T} \right\} \eta_T{}^{(4)} = \eta_T{}^{(4)} \exp\left\{ \frac{\Delta t}{2} \zeta_T{}^{(4)} \right\} \tag{3.32}$$

The sixth operator changes the momentum of the particle,

$$\pi_{i,\alpha}{}^{(6)} = \exp\left\{ -i\frac{\Delta t}{2} \left(\left(\eta_T - \frac{1}{\eta_T} \right) \sum_{\beta=1}^{3} \pi_{i,\beta} \frac{\partial u_\beta}{\partial r_\alpha} \right) \frac{\partial}{\partial \pi_{i,\alpha}} \right\} \pi_{i,\alpha}{}^{(5)} \tag{3.33.a}$$

This equation changes the y momentum to

$$\pi_{i,y}{}^{(6)} = \pi_{i,y}{}^{(5)} - \frac{\Delta t}{2} \left(\eta_T{}^{(5)} - \frac{1}{\eta_T{}^{(5)}} \right) \frac{\partial u_x}{\partial r_y} \pi_{i,x}{}^{(5)} \tag{3.33.b}$$

The seventh operator changes the momentum of the particle,

$$\pi_{i,\alpha}{}^{(7)} = \exp\left\{ -i\frac{\Delta t}{2} \left(\frac{1}{\eta_T} \sum_{\beta=1}^{3} \pi_{i,\beta} \frac{\partial u_\alpha}{\partial r_\beta} \right) \frac{\partial}{\partial \pi_{i,\alpha}} \right\} \pi_{i,\alpha}{}^{(6)} \tag{3.34.a}$$

This equation changes the x momentum:

$$\pi_{i,x}{}^{(7)} = \pi_{i,x}{}^{(6)} - \frac{\Delta t}{2} \left(\frac{1}{\eta_T{}^{(6)}} \right) \frac{\partial u_x}{\partial r_y} \pi_{i,y}{}^{(6)} \tag{3.34.b}$$

The eighth operator changes the particle position,

$$r_{i,\alpha}{}^{(8)} = \exp\left\{ i\frac{\Delta t}{2}\eta_T \left(\sum_{\beta=1}^{3} \frac{\partial u_\alpha}{\partial r_\beta} r_{i,\beta} \right) \frac{\partial}{\partial r_{i,\alpha}} \right\} r_{i,\alpha}{}^{(7)} \tag{3.35.a}$$

This equation changes the x position:

$$r_{i,x}{}^{(8)} = r_{i,x}{}^{(7)} + \frac{\Delta t}{2}\eta_T{}^{(7)} \frac{\partial u_x}{\partial r_y} r_{i,y}^{(7)} \tag{3.35.b}$$

The ninth operator changes the particle position,

$$r_{i,\alpha}{}^{(9)} = \exp\left\{ i\Delta t \frac{\pi_{i,\alpha}}{m_i} \frac{\partial}{\partial r_{i,\alpha}} \right\} r_{i,\alpha}{}^{(8)} = r_{i,\alpha}{}^{(8)} + \Delta t \frac{\pi_{i,\alpha}{}^{(8)}}{m_i} \tag{3.36}$$

The tenth operator changes the particle position,

$$r_{i,\alpha}{}^{(10)} = \exp\left\{ i\frac{\Delta t}{2}\eta_T \left(\sum_{\beta=1}^{3} \frac{\partial u_\alpha}{\partial r_\beta} r_{i,\beta} \right) \frac{\partial}{\partial r_{i,\alpha}} \right\} r_{i,\alpha}{}^{(9)} \tag{3.37.a}$$

This equation changes the x position:

$$r_{i,x}{}^{(10)} = r_{i,x}{}^{(9)} + \frac{\Delta t}{2}\eta_T{}^{(9)} \frac{\partial u_x}{\partial r_y} r_{i,y}^{(9)} \tag{3.37.b}$$

The eleventh operator changes the momentum of the particle. This equation changes the x momentum to

$$\pi_{i,\alpha}{}^{(11)} = \exp\left\{ -i\frac{\Delta t}{2} \left(\frac{1}{\eta_T} \sum_{\beta=1}^{3} \pi_{i,\beta} \frac{\partial u_\alpha}{\partial r_\beta} \right) \frac{\partial}{\partial \pi_{i,\alpha}} \right\} \pi_{i,\alpha}{}^{(10)} \tag{3.38.a}$$

$$\pi_{i,x}^{(11)} = \pi_{i,x}^{(10)} - \frac{\Delta t}{2}\frac{1}{\eta_T^{(10)}}\frac{\partial u_x}{\partial r_y}\pi_{i,y}^{(10)} \tag{3.38.b}$$

The twelfth operator changes the momentum of the particle,

$$\pi_{i,\alpha}^{(12)} = \exp\left\{-i\frac{\Delta t}{2}\left(\left(\eta_T - \frac{1}{\eta_T}\right)\sum_{\beta=1}^{3}\pi_{i,\beta}\frac{\partial u_\beta}{\partial r_\alpha}\right)\frac{\partial}{\partial \pi_{i,\alpha}}\right\}\pi_{i,\alpha}^{(11)} \tag{3.39.a}$$

This equation changes the y momentum:

$$\pi_{i,y}^{(12)} = \pi_{i,y}^{(11)} - \frac{\Delta t}{2}\left(\eta_T^{(11)} - \frac{1}{\eta_T^{(11)}}\right)\frac{\partial u_x}{\partial r_y}\pi_{i,x}^{(11)} \tag{3.39.b}$$

The thirteenth operator changes the time dilation variable,

$$\eta_T^{(13)} = \exp\left\{i\frac{\Delta t}{2}\eta_T\zeta_T\frac{\partial}{\partial \eta_T}\right\}\eta_T^{(12)} = \eta_T^{(12)}\exp\left\{\frac{\Delta t}{2}\zeta_T^{(12)}\right\} \tag{3.40}$$

The fourteenth operator changes the momentum of the particle,

$$\pi_{i,\alpha}^{(14)} = \exp\left\{i\frac{\Delta t}{4}F_{i,\alpha}^{\text{int}}\frac{\partial}{\partial \pi_{i,\alpha}}\right\}\pi_{i,\alpha}^{(13)} = \pi_{i,\alpha}^{(13)} + \frac{\Delta t}{4}F_{i,\alpha}^{\text{int}}(r_{i,\alpha}^{(13)}) \tag{3.41}$$

The fifteenth operator changes the momentum of the particle,

$$\pi_{i,\alpha}^{(15)} = \exp\left\{-i\frac{\Delta t}{2}\pi_{i,\alpha}\zeta_T\frac{\partial}{\partial \pi_{i,\alpha}}\right\}\pi_{i,\alpha}^{(14)} = \pi_{i,\alpha}^{(14)}\exp\left\{-\frac{\Delta t}{2}\zeta_T^{(14)}\right\} \tag{3.42}$$

The sixteenth operator changes the moment of the particle,

$$\pi_{i,\alpha}^{(16)} = \exp\left\{ i\frac{\Delta t}{4} F_{i,\alpha}^{\text{int}} \frac{\partial}{\partial \pi_{i,\alpha}} \right\} \pi_{i,\alpha}^{(15)} = \pi_{i,\alpha}^{(15)} + \frac{\Delta t}{4} F_{i,\alpha}^{\text{int}}\left(r_{i,\alpha}^{(15)}\right) \tag{3.43}$$

The seventeenth operator changes the thermostat momentum. This operator requires the calculation of temperature:

$$\zeta_T^{(17)} = \exp\left\{ i\frac{\Delta t}{2} F_n\left(\pi_{i,\alpha}\right) \frac{\partial}{\partial \zeta_T} \right\} \zeta_T^{(16)} = \zeta_T^{(16)} + \frac{\Delta t}{2} \vartheta^2 \left(\frac{T^{(16)}}{T_{set}} - 1 \right) \tag{3.44}$$

3.5. Results and Discussion

In this section, we present the results obtained by simulating a system of N=500 particles at a reduced temperature of 0.722 and at a reduced number density of $n=N/V$=0.844. We use the equipartition theorem to identify the temperature from the simulation. We use the Weeks-Chandler-Andersen (WCA)[28] fluid, modeled with an interaction potential

$$\phi(r) = \begin{cases} 4\varepsilon\left(\left(\frac{\sigma}{r}\right)^{12} - \left(\frac{\sigma}{r}\right)^{6} \right) + \varepsilon, & r \le 2^{1/6}\sigma \\ 0, & r > 2^{1/6}\sigma \end{cases} \tag{3.45}$$

Here, ε is the well depth of the pair potential and σ is the particle exclusion diameter. This is the Lennard-Jones potential, shifted upwards by ε and truncated at the LJ potential minimum of $2^{1/6}\sigma$.

The initial configurations were obtained from an equilibrated EMD simulation performed at the same reduced temperature and number density. The equations of motion are integrated using the r-RESPA [13, 24] integration scheme. The controller frequency was set at $\tau = 0.05$ (reduced units). All simulations were performed in the absence of any external field, although the equations of motion are capable of simulating systems with external fields.

The conservation of the Hamiltonian is a proper diagnostic check to determine if simple coding errors exist in the program. Due to the fact that we use a numerical algorithm to solve for the equations of motion, we get approximate solutions. Hence, we do not conserve the Hamiltonian exactly. However, there are ways to check for conservation of the Hamiltonian. The Hamiltonian is said to be conserved if the standard deviation of the Hamiltonian is at least two orders of magnitude lesser than the standard deviation of kinetic, potential or the thermostat energy of the system, whichever is the least:

$$\frac{\sigma_{KE}}{\sigma_H} \text{ or } \frac{\sigma_{PE}}{\sigma_H} \text{ or } \frac{\sigma_{TsE}}{\sigma_H} \geq 100 \tag{3.46}$$

where σ_H is the standard deviation of the Hamiltonian, σ_{KE} standard deviation of kinetic energy, σ_{KE} standard deviation of potential energy, and σ_{TsE} standard deviation of thermostat energy. Table 1 shows the average and standard deviations of all the energies in the system.

Since we use a second-order integrator, the errors are of the order Δt^2. Consequently, the standard deviation of the Hamiltonian evaluated at a particular time

Table 1. The average and standard deviation values for the Hamiltonian, kinetic energy, potential energy and the thermostat energy of the system (using Nosé-Hoover formulation).

Energy	Time average	Standard deviation
H	9.0835E+02	7.7286E-05
$\frac{1}{2}\sum_{i=1}^{N}\sum_{\alpha=1}^{3}\frac{(\pi_{i,\alpha})^2}{m_i}$	5.4302E+02	1.5628E+01
$\sum_{i=1}^{N}\sum_{\alpha=1}^{3}(\eta_T\pi_{i,\alpha})u_\alpha(r_i,t)$	-2.2809E+03	2.0881E+03
$\frac{1}{2}\sum_{i=1}^{N}\sum_{\alpha=1}^{3}m_i u_\alpha^2(r_i,t)$	1.1343E+03	9.7139E+02
Potential energy	8.5338E+00	3.5161E+01
Thermostat energy	1.5034E+03	1.1294E+03

step should be two orders of magnitude greater that the standard deviation of the Hamiltonian evaluated at one-tenth of that time step. Table 2 shows the standard deviation of the Hamiltonian evaluated at two different time steps (2.5 ns and 0.25 ns). In Figure 6, the time evolutions of the various energies of the system are shown. The simulation was performed at a reduced shear rate of 0.1 and a time step of 2.5 ns. The Lees-Edwards Boundary Conditions (LEBCs) are not applied in the y dimension. In other words, we allow the particles to float away in the y dimension. Once we apply the LEBCs, the Hamiltonian is no longer a conserved quantity since some of the kinetic energy terms are dependent on the y position, and application of LEBCs will introduce a sudden change in them. Figure 7 shows the time evolutions of the various energies of the system under the application of the LEBCs.

Table 2. The average and standard deviation values of the Hamiltonian (Nosé-Hoover) evaluated at two different times.

Time (ns)	$<H>$	σ_H
2.5	9.0836E+02	2.1069E-02
0.25	9.0835E+02	7.7286E-05

In Figure 7, the potential energy decreases as the particles move farther away from each other. Obviously, since the particles float away the potential energy decreases. Also, the kinetic energies $\frac{1}{2}\sum_{i=1}^{N}\sum_{\alpha=1}^{3} m_i u_\alpha^2(r_i,t)$ and $\sum_{i=1}^{N}\sum_{\alpha=1}^{3}(\eta_T \pi_{i,\alpha}) u_\alpha(r_i,t)$ continue to increase in magnitude due to this removal of the y periodic conditions (i.e., LEBCs). However, as one energy term increases, another decreases, compensating for this increase and thus conserving the Hamiltonian. For example, the decrease in potential energy is compensated by the increase in the thermostat energy.

This simulation could be performed for a very short period of time since the kinetic energies that are dependent on the y positions would increase to values that will disturb the simulation. Once we apply the LEBCs, the Hamiltonian is no longer a conserved quantity since some of the kinetic energy terms are dependent on the y position, and the LEBCs tend to change their values. The algorithm was found to be unstable under the application of the LEBCs. The time dilation variable increases exponentially, resulting in an unstable algorithm. Figure 8 shows the time dilation and the thermostat momentum variables as functions of time.

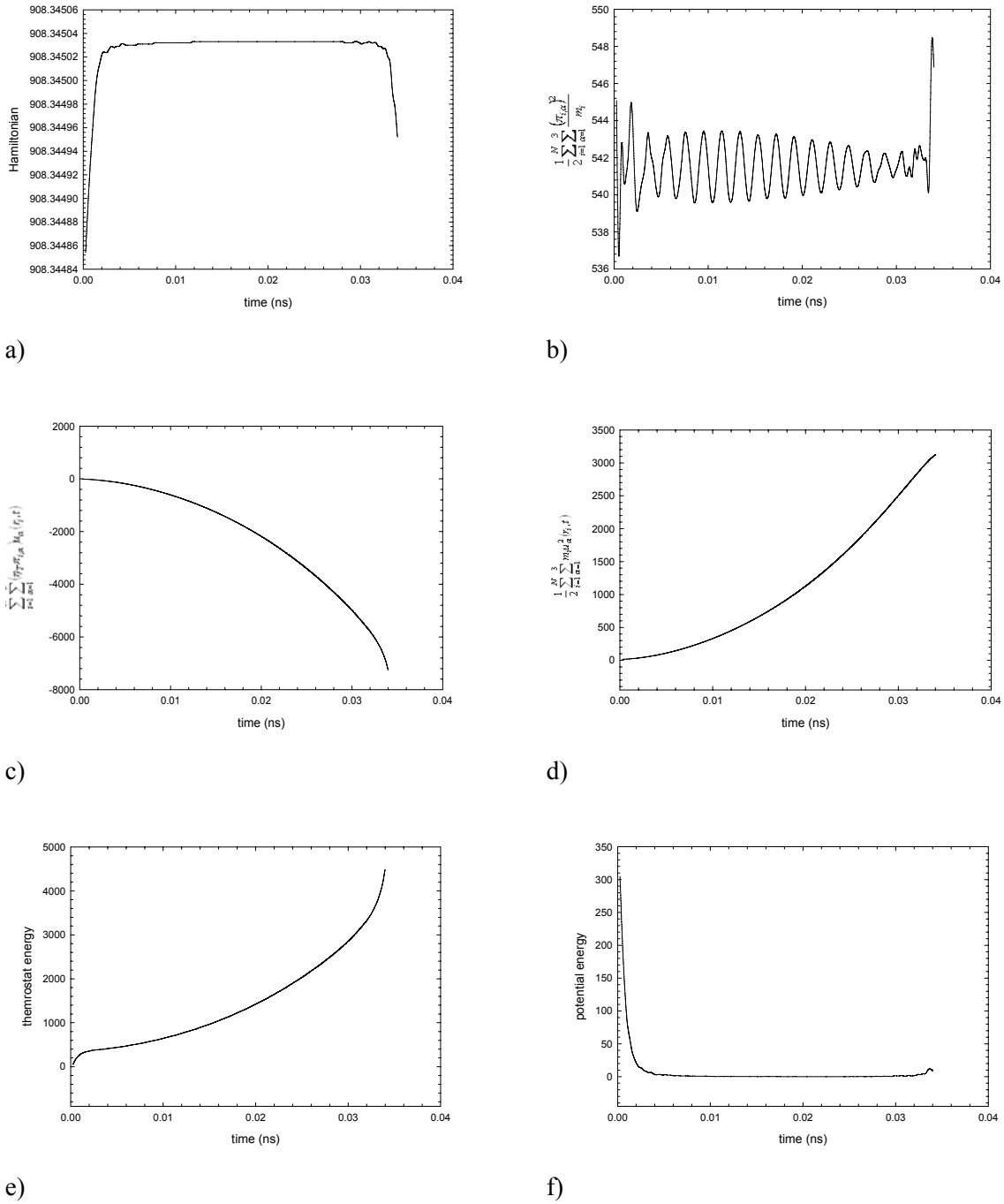

Figure 6. The time evolution of Hamiltonian (using Nosé-Hoover thermostat conserved) a) Hamiltonian as a function of time, b) $\sum_{i=1}^{N}\sum_{\alpha=1}^{3}\frac{\pi_{i,\alpha}{}^{2}}{2m_i}$ as a function of time, c) $\frac{1}{2}\sum_{i=1}^{N}\sum_{\alpha=1}^{3} m_i u_\alpha^2(r_i,t)$ as a function of time, d) $\sum_{i=1}^{N}\sum_{\alpha=1}^{3}(\eta_T \pi_{i,\alpha})u_\alpha(r_i,t)$ as a function of time, e) thermostat energy as a function of time, and f) potential energy as a function of time. This simulation was carried out without the application of LEBCs (no periodic boundaries in the y dimension). All energies are in reduced units.

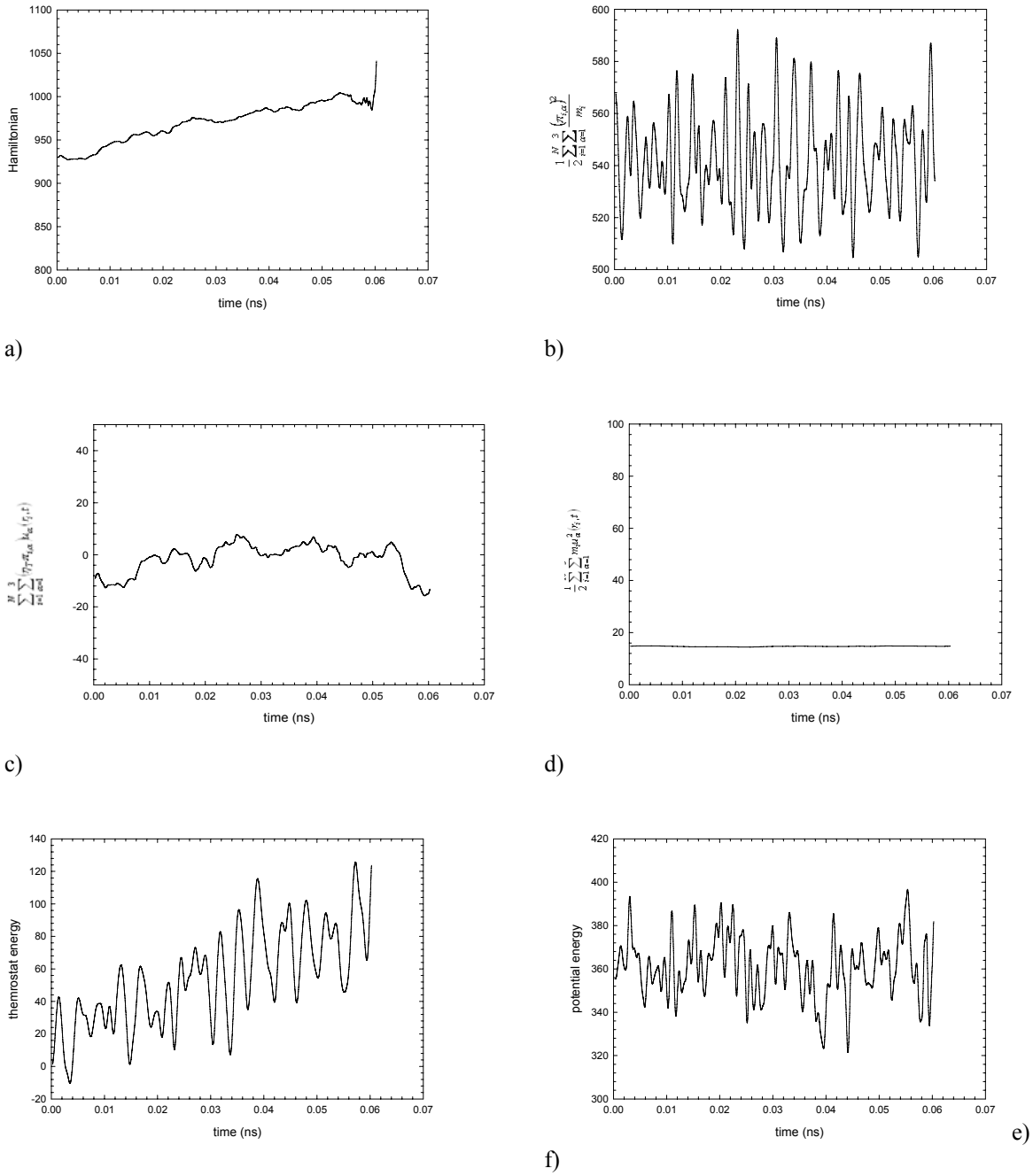

Figure 7. The time evolution of Hamiltonian (using Nosé-Hoover thermostat with LEBCs) a) Hamiltonian as a function of time, b) $\sum_{i=1}^{N}\sum_{\alpha=1}^{3}\frac{{\pi_{i,\alpha}}^2}{2m_i}$ as a function of time, c) $\frac{1}{2}\sum_{i=1}^{N}\sum_{\alpha=1}^{3} m_i u_\alpha^2\left(r_i,t\right)$ as a function of time, d) $\sum_{i=1}^{N}\sum_{\alpha=1}^{3}\left(\eta_T\pi_{i,\alpha}\right)u_\alpha\left(r_i,t\right)$ as a function of time, e) thermostat energy as a function of time, and f) potential energy as a function of time.

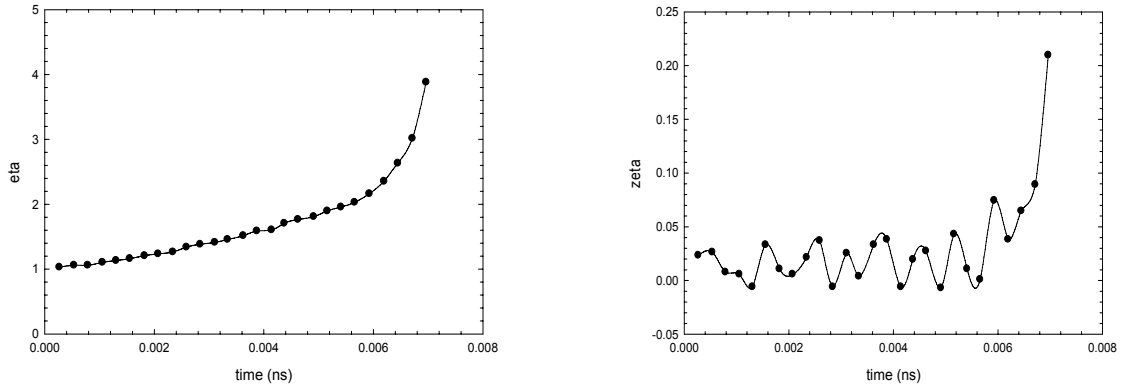

a) b)

Figure 8. The time evolution of the thermostat variables (unstable algorithm with LEBCs) a) time dilation variable (eta) as a function of time , and b) thermostat momentum variable (zeta) as a function of time .

As known, it is the LEBCs that drive the shear flow and the equations of motion merely follow the Newton's law. Due to the fact that the LEBCs drive the flow, once we switch on the LEBCs, the kinetic energy is driven by the flow towards infinity.

Clearly, this increase is absorbed by the thermostat and the time dilation variable tends to increase and never attains a steady-state. In order to force η_T to a steady-state value, we resorted to a new formulation,

$$\begin{aligned} H'_{NVT} = & \frac{1}{2}\sum_{i=1}^{N}\sum_{\alpha=1}^{3}\frac{\left(p'_{i,\alpha}\right)^2}{m'_i s^2} + \frac{1}{2M'}\left(1-\frac{1}{s^2}\right)\sum_{\alpha=1}^{N}\left(\sum_{j=1}^{N}p'_{j,\alpha}\right)^2 + \left(1-\frac{1}{s^2}\right)\sum_{i=1}^{N}\sum_{\alpha=1}^{3}\left(p'_{i,\alpha}\right)u_\alpha\left(r_i,t\right) \\ & -\frac{1}{M'}\left(1-\frac{1}{s^2}\right)\sum_{i=1}^{N}\sum_{\alpha=1}^{3}\left(m'_i u_\alpha\left(r_i,t\right)\right)\sum_{j=1}^{N}p'_{j,\alpha} - \frac{1}{2}\left(1-\frac{1}{s^2}\right)\sum_{i=1}^{N}\sum_{\alpha=1}^{3}m'_i\left(u_\alpha\left(r_i,t\right)\right)^2 \\ & +\frac{1}{2M'}\left(1-\frac{1}{s^2}\right)\sum_{\alpha=1}^{3}\left(\sum_{j=1}^{N}m'_j u_\alpha\left(\mathbf{r}_j,t\right)\right)^2 + U_{\text{int}}\left(\rho'_{i,\alpha}-\rho'_{j,\alpha}\right) + U_{ext}\left(\rho'_{i,\alpha},R'_\alpha\right) \\ & +\frac{1}{2Q_s}\left(p_s - p_s^{steadystate}\right)^2 + fk_B T_{set}\ln\left(s\right) \end{aligned} \tag{3.45}$$

This new formulation would affect the equation of motion for the time dilation variable alone,

$$\frac{d\eta_T}{dt} = \eta_T\left(\zeta_T - \zeta_T^{steady\,state}\right) \tag{3.46}$$

The steady-state value of ζ_T was iteratively evaluated such that η_T reaches a steady-state. Contrary to the convention, the value of η_T reached a steady-state value less than unity. However, the algorithm was not able to find a steady-state for shear rates higher than 3. In Figure 9, the steady-state values of η_T and ζ_T are plotted as functions of shear rate.

We realized that by merely trying to control the time dilation variable, using this formulation would not be a rigorous method for NEMD simulations. Hence, we resorted to the use of an entirely new formulation, i.e., the Nosé-Poincaré formulation, to obtain a stable algorithm.

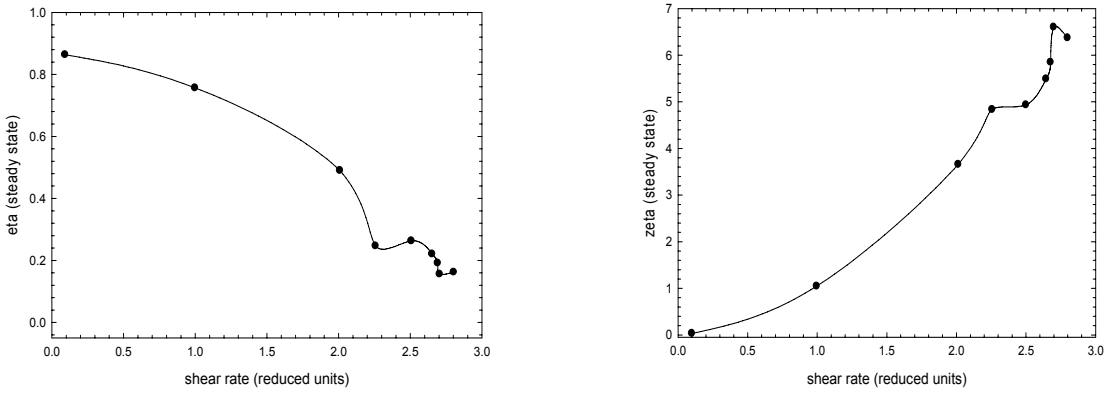

a) b)

Figure 9. Steady-state values for the thermostat variables (using the steady-state formulation) a) η_T (steady-state) as function shear rate, and b) ζ_T (steady-state) as a function of shear rate.

3.6. Conclusions

A Hamiltonian-based rigorous algorithm for NEMD simulations in the NVT ensemble using a reformulated Nosé-Hoover Thermostat was derived. The p-SLLOD transformation was used to identify the variable transformation from the mathematical frame of reference to the physical frame of reference. An eight step methodical procedure was followed to obtain the equations of motion in terms of the peculiar coordinates in the physical frame of reference. The equations of motion, thus derived 1) follow Hamiltonian dynamics, 2) are valid in the presence of an external field, and 3) rigorously thermostat the nonequilibrium temperature. The resulting equations of motion were found to conserve the Hamiltonian in the absence of the LEBCs in the y dimension. In the presence of the LEBCs, the equations of motion did not conserve the Hamiltonian, as some of the kinetic energy terms were dependent on the y position of the particle, and the application of the LEBCs was found to alter the values of these energy terms. The underlying fact is that the LEBCs drive the flow, causing the kinetic energy to increase, and this increase is absorbed by the thermostat. Consequently, the time dilation variable was found to increase exponentially, causing instability in the algorithm. A new formulation for the thermostat momentum variable (using the steady-state value of ζ_T) was used to develop a stable algorithm by forcing η_T to a steady-state. However, this formulation was not able to yield a stable algorithm at shear rates higher than 3.0.

Chapter IV

A Generalized Hamiltonian-Based Algorithm for Rigorous Nonequilibrium Molecular Dynamics Simulation in the NVT Ensemble using Nosé-Poincaré Thermostat

The Nosé-Poincaré formulation [15] provides improved stability in simulations with large fluctuations in the thermostat variable. The Nosé-Poincaré formulation [15] has a canonical symplectic structure, unlike the Nosé-Hoover formulation which provides a real-variable system through a noncanonical change of variables. However, this formulation has been used for equilibrium systems, and we will extend it here to include NEMD systems as well. The procedure to derive a Hamiltonian-based algorithm using the Nosé-Poincaré formulation [15] is similar to the eight step procedure described in the previous chapter.

1. Define the Hamiltonian in terms of the laboratory coordinates in the mathematical (potentially aphysical) frame of reference.
2. Express the Hamiltonian in terms of the peculiar and center of mass (COM) coordinates in the mathematical frame of reference.
3. Identify a noncanonical transformation from the peculiar and COM coordinates in the mathematical frame of reference to the peculiar and COM coordinates in the physical frame of reference.
4. Express the Hamiltonian in terms of the peculiar and COM coordinates in the physical frame of reference.

5. Identify the kinetic energy term that contributes to the nonequilibrium temperature and implement a Hamiltonian-based thermostat (Nosé-Poincaré thermostat) rigorously.
6. Express the Hamiltonian in terms of the laboratory coordinates in the mathematical frame of reference where a canonical (symplectic) relationship exists between the Hamiltonian and the equations of motion.
7. Derive the equations of motion in terms of the laboratory coordinates in the mathematical frame of reference.
8. Express the equations of motions in the peculiar and COM coordinates in the physical frame of reference using the noncanonical transformation.

4.1. The Methodical Procedure

We begin our derivation from equation (3.7) as the first four steps will be identical to both formulations. The Hamiltonian expressed in terms of the peculiar coordinates in the mathematical frame of reference is given by

$$\begin{aligned} H_{NVE} = & \frac{1}{2}\sum_{i=1}^{N}\sum_{\alpha=1}^{3}\frac{\pi_{i,\alpha}{}^{2}}{m_i} + \sum_{\alpha=1}^{3}\sum_{i=1}^{N}\left(\pi_{i,\alpha}\right)\left(u_\alpha\left(r_i,t\right)\right)\frac{1}{2}\sum_{\alpha=1}^{3}\sum_{i=1}^{N}m_i\left(u_\alpha\left(r_i,t\right)\right)^2 \\ & + \frac{1}{2}\sum_{i=1}^{N}\sum_{\alpha=1}^{3}m_i\left(\frac{P_\alpha}{M}\right)^2 + \left(\sum_{j=1}^{N}\sum_{\alpha=1}^{3}m_j u_\alpha\left(\mathbf{r}_j,t\right)\right)\left(\frac{P_\alpha}{M}\right) \\ & + \sum_{i=1}^{N}\sum_{\alpha=1}^{3}\pi_{i,\alpha}\left(\frac{P_\alpha}{M}\right) + U_{\text{int}}\left(\rho'_{i,\alpha}-\rho'_{j,\alpha}\right) + U_{ext}\left(\rho'_{i,\alpha},R'_\alpha\right) \end{aligned} \tag{4.1}$$

The fifth step is to identify the correct kinetic energy that contributes to the nonequilibrium temperature, and to use the Nosé-Poincaré formulation to rigorously thermostat the nonequilibrium temperature. The Hamiltonian is

$$\tilde{H} = s\left(\begin{array}{l} \frac{1}{2}\sum_{i=1}^{N}\sum_{\alpha=1}^{3}\frac{\pi_{i,\alpha}{}^{2}}{m_i s^{2}} + \sum_{i=1}^{N}\sum_{\alpha=1}^{3}\left(\pi_{i,\alpha}\right)\left(u_\alpha\left(r_i,t\right)\right) + \frac{1}{2}\sum_{i=1}^{N}\sum_{\alpha=1}^{3} m_i\left(u_\alpha\left(r_i,t\right)\right)^2 \\ + \frac{1}{2}\sum_{i=1}^{N}\sum_{\alpha=1}^{3} m_i\left(\frac{P_\alpha}{M}\right)^2 + \left(\sum_{j=1}^{N}\sum_{\alpha=1}^{3} m_j u_\alpha\left(\mathbf{r}_j,t\right)\right)\left(\frac{P_\alpha}{M}\right) \\ + \sum_{i=1}^{N}\sum_{\alpha=1}^{3}\pi_{i,\alpha}\left(\frac{P_\alpha}{M}\right) + U_{\text{int}}\left(\rho'_{i,\alpha} - \rho'_{j,\alpha}\right) + U_{ext}\left(\rho'_{i,\alpha}, R'_\alpha\right) \\ + \frac{1}{2Q_s}p_s^2 + fk_B T_{set}\ln(s) - H_0 \end{array}\right) \qquad (4.2.a)$$

where $\frac{1}{2Q_s}p_s^2$ is the kinetic energy of the thermostat, and the last term in the equation is the potential energy of the thermostat. s is the thermostat metric (with a value of unity when there is no thermostat), p_s is the thermostat momentum (with a value of zero when there is no thermostat), Q_s is the inertial mass of the thermostat, f is the number of degrees of freedom associated with the momenta in the system, k_B is Boltzmann's constant, and T_{set} is the set temperature. We have only applied the thermostat to the first term.

The next step in the procedure is to express the Hamiltonian in terms of the laboratory coordinates in the mathematical frame of reference because the symplectic relationship between the Hamiltonian and the equations of motion exists in this frame. We substitute equations (3.6) and equations (3.1) and (3.2) in equation (4.2):

$$\tilde{H}' = \begin{pmatrix} \frac{1}{2}\sum_{i=1}^{N}\sum_{\alpha=1}^{3}\frac{\left(p'_{i,\alpha}\right)^2}{m'_i s^2} + \frac{1}{2M'}\left(1-\frac{1}{s^2}\right)\sum_{\alpha=1}^{3}\left(\sum_{j=1}^{N} p'_{j,\alpha}\right)^2 \\ +\left(1-\frac{1}{s^2}\right)\sum_{i=1}^{N}\sum_{\alpha=1}^{3}\left(p'_{i,\alpha}\right)u_\alpha\left(r_i,t\right) - \frac{1}{2}\left(1-\frac{1}{s^2}\right)\sum_{i=1}^{N}\sum_{\alpha=1}^{3} m'_i\left(u_\alpha\left(r_i,t\right)\right)^2 \\ -\frac{1}{M'}\left(1-\frac{1}{s^2}\right)\sum_{i=1}^{N}\sum_{\alpha=1}^{3}\left(m'_i u_\alpha\left(r_i,t\right)\right)\sum_{j=1}^{N} p'_{j,\alpha} \\ +\frac{1}{2M'}\left(1-\frac{1}{s^2}\right)\sum_{\alpha=1}^{3}\left(\sum_{j=1}^{N} m'_j u_\alpha\left(\mathbf{r}_j,t\right)\right)^2 + U_{\text{int}}\left(\rho'_{i,\alpha}-\rho'_{j,\alpha}\right) \\ +U_{ext}\left(\rho'_{i,\alpha},R'_\alpha\right)+\frac{1}{2Q_s}p_s^2 + fk_B T_{set}\ln\left(s\right) - H_0 \end{pmatrix} s \qquad (4.2.b)$$

which can also be written as

$$\tilde{H}' = \left(H(t) - H_0\right)s \qquad (4.2.c)$$

The seventh step of the procedure is to derive the equations of motion in terms of the laboratory coordinates in the mathematical frame of reference. In this step, we rely on the canonical relationship existing between the Hamiltonian and the equations of motion:

$$\frac{dr'_{i,\alpha}}{dt'} = \frac{\partial\tilde{H}'}{\partial p'_{i,\alpha}} = s\begin{pmatrix} \frac{p'_{i,\alpha}}{m'_i s^2} + \frac{1}{M'}\left(1-\frac{1}{s^2}\right)\sum_{j=1}^{N} p'_{j,\alpha} + \left(1-\frac{1}{s^2}\right)u_\alpha\left(r_i,t\right) \\ -\frac{1}{M'}\left(1-\frac{1}{s^2}\right)\sum_{i=1}^{N}\left(m'_i u_\alpha\left(r_i,t\right)\right) \end{pmatrix} \qquad (4.3.a)$$

$$\frac{dp'_{i,\alpha}}{dt'} = -\frac{\partial \tilde{H}'}{\partial r'_{i,\alpha}}$$

$$= -s\left(\begin{array}{l} \left(1-\frac{1}{s^2}\right)\sum_{\beta=1}^{3}\left(p'_{i,\beta}\right)\frac{\partial u_\beta\left(r_i,t\right)}{\partial r'_{i,\alpha}} - \frac{1}{M'}\left(1-\frac{1}{s^2}\right)\sum_{\beta=1}^{3}\left(m'_i\frac{\partial u_\beta\left(r_i,t\right)}{\partial r'_{i,\alpha}}\right)\sum_{j=1}^{N}p'_{j,\beta} \\ -\left(1-\frac{1}{s^2}\right)\sum_{\beta=1}^{3}m'_i u_\beta\left(r_i,t\right)\frac{\partial u_\beta\left(r_i,t\right)}{\partial r'_{i,\alpha}} \\ +\frac{1}{M'}\left(1-\frac{1}{s^2}\right)\sum_{\beta=1}^{3}\left(\sum_{j=1}^{N}m'_j u_\beta\left(\mathbf{r}_j,t\right)\right)m'_j\frac{\partial u_\beta\left(r_j,t\right)}{\partial r'_{i,\alpha}} \\ +\frac{\partial U_{\text{int}}\left(\rho'_{i,\alpha}-\rho'_{j,\alpha}\right)}{\partial r'_{i,\alpha}} + \frac{\partial U_{ext}\left(\rho'_{i,\alpha},R'_\alpha\right)}{\partial r'_{i,\alpha}} \end{array}\right) \tag{4.3.b}$$

$$\frac{ds}{dt'} = \frac{\partial \tilde{H}'}{\partial p_s} = s\frac{p_s}{Q_s} \tag{4.3.c}$$

$$\frac{dp_s}{dt'} = -\frac{\partial \tilde{H}'}{\partial s} = -\left(H(t)-H_0\right)$$

$$-s\left(\begin{array}{l} -\sum_{i=1}^{N}\sum_{\alpha=1}^{3}\frac{\left(p'_{i,\alpha}\right)^2}{m'_i s^3} + \frac{1}{M'}\left(\frac{1}{s^3}\right)\sum_{\alpha=1}^{3}\left(\sum_{j=1}^{N}p'_{j,\alpha}\right)^2 \\ +\left(\frac{2}{s^3}\right)\sum_{i=1}^{N}\sum_{\alpha=1}^{3}\left(p'_{i,\alpha}\right)u_\alpha\left(r_i,t\right) - \frac{1}{M'}\left(\frac{2}{s^3}\right)\sum_{i=1}^{N}\sum_{\alpha=1}^{3}\left(m'_i u_\alpha\left(r_i,t\right)\right)\sum_{j=1}^{N}p'_{j,\alpha} \\ -\left(\frac{1}{s^3}\right)\sum_{i=1}^{N}\sum_{\alpha=1}^{3}m'_i\left(u_\alpha\left(r_i,t\right)\right)^2 + \frac{1}{M'}\left(\frac{1}{s^3}\right)\sum_{\alpha=1}^{3}\left(\sum_{j=1}^{N}m'_j u_\alpha\left(\mathbf{r}_j,t\right)\right)^2 \\ +\frac{fk_B T_{set}}{s} \end{array}\right)$$

$$= +\sum_{i=1}^{N}\sum_{\alpha=1}^{3}\frac{\left(p'_{i,\alpha}\right)^2}{m'_i s^2} - \frac{1}{M'}\left(\frac{1}{s^2}\right)\sum_{\alpha=1}^{3}\left(\sum_{j=1}^{N}p'_{j,\alpha}\right)^2 - \left(\frac{2}{s^2}\right)\sum_{i=1}^{N}\sum_{\alpha=1}^{3}\left(p'_{i,\alpha}\right)u_\alpha\left(r_i,t\right) \tag{4.3.d}$$

$$+\frac{1}{M'}\left(\frac{2}{s^2}\right)\sum_{i=1}^{N}\sum_{\alpha=1}^{3}\left(m'_i u_\alpha\left(r_i,t\right)\right)\sum_{j=1}^{N}p'_{j,\alpha} + \left(\frac{1}{s^2}\right)\sum_{i=1}^{N}\sum_{\alpha=1}^{3}m'_i\left(u_\alpha\left(r_i,t\right)\right)^2$$

$$-\frac{1}{M'}\left(\frac{1}{s^2}\right)\sum_{\alpha=1}^{3}\left(\sum_{j=1}^{N}m'_j u_\alpha\left(\mathbf{r}_j,t\right)\right)^2 - fk_B T_{set} - \Delta H_f$$

From here onwards, we shall refer to $\left(H(t)-H_0\right)$ as ΔH_f.

The final step is to express the equations of motions in the peculiar and COM coordinates in the physical frame of reference using equations (3.1) and the noncanonical (p-SLLOD) transformation equations (3.11). These equations are derived in Appendix C:

$$\frac{d\rho_{i,\alpha}}{dt}=\eta_T\left(\frac{\pi_{i,\alpha}}{m_i}+\eta_T u_\alpha(r_i,t)-\frac{\eta_T}{M}\sum_{i=1}^{N}\left(m_i u_\alpha(r_i,t)\right)\right) \tag{4.4.a}$$

$$\frac{d\pi_{i,\alpha}}{dt}=\eta_T\left(\begin{array}{l}-\left(1-\frac{1}{\eta_T{}^2}\right)\sum_{\gamma=1}^{3}\left(\eta_T\pi_{i,\gamma}\right)\frac{\partial u_\gamma(r_i,t)}{\partial r_{i,\alpha}}+F_{i,\alpha}^{\text{int}}+F_{i,\alpha}^{ext,pec}-\frac{m_i}{M'}\sum_{j=1}^{N}F_{j,\alpha}^{ext,pec}\\ +\frac{m_i}{M}\left(1-\frac{1}{\eta_T{}^2}\right)\sum_{i=1}^{N}\sum_{\gamma=1}^{3}\left(\eta_T\pi_{i,\gamma}\right)\frac{\partial u_\gamma(r_i,t)}{\partial r_{i,\alpha}}\\ -m_i\left(\frac{1}{\eta_T}\frac{\partial u_\alpha(\mathbf{r}_i,t)}{\partial t}+\sum_{\gamma=1}^{3}\frac{\partial u_\alpha(\mathbf{r}_i,t)}{\partial r_{i,\gamma}}\left(\frac{\pi_{i,\gamma}}{m_i\eta_T}+\frac{P_\gamma}{M}+u_\gamma(r_i,t)\right)\right)\\ +\frac{m_i}{M}\sum_{j=1}^{N}m_j\left(\frac{1}{\eta_T}\frac{\partial u_\alpha(\mathbf{r}_j,t)}{\partial t}+\sum_{\gamma=1}^{3}\frac{\partial u_\alpha(\mathbf{r}_j,t)}{\partial r_{i,\gamma}}\left(\frac{\pi_{j,\gamma}}{m_j\eta_T}+\frac{P_\gamma}{M}+u_\gamma(r_j,t)\right)\right)\\ -\pi_{i,\alpha}\zeta_T\end{array}\right) \tag{4.4.b}$$

$$\frac{dP_\alpha}{dt}=\eta_T\left(\begin{array}{l}-\eta_T{}^2\left(1-\frac{1}{\eta_T{}^2}\right)\sum_{i=1}^{N}\sum_{\gamma=1}^{3}\left(\pi_{i,\gamma}\right)\frac{\partial u_\gamma(r_i,t)}{\partial r_{i,\alpha}}+\eta_T F_\alpha^{ext,COM}\\ -\eta_T\sum_{j=1}^{N}m_j\left(\frac{1}{\eta_T}\frac{\partial u_\alpha(\mathbf{r}_j,t)}{\partial t}+\sum_{\gamma=1}^{3}\frac{\partial u_\alpha(\mathbf{r}_j,t)}{\partial r_{i,\gamma}}\left(\frac{\pi_{j,\gamma}}{m_j\eta_T}+\frac{P_\gamma}{M}+u_\gamma(r_j,t)\right)\right)\end{array}\right) \tag{4.4.c}$$

$$\frac{dR_\alpha}{dt} = \frac{\eta_T^{\,2}}{M}\left(P_\alpha + \sum_{j=1}^{N} m_j u_\alpha\left(\mathbf{r}_j, t\right)\right) \tag{4.4.d}$$

$$\frac{d\eta_T}{dt} = \eta_T^{\,2}\zeta_T \tag{4.4.e}$$

$$\frac{d\zeta_T}{dt} = \eta_T \vartheta^2\left(\frac{T(t)}{T_{set}} - 1 - \frac{\Delta H_f}{f k_B T_{set}}\right) \tag{4.4.f}$$

where we used the law of equipartition to define the temperature in terms of the peculiar momenta,

$$T(t) = \frac{1}{f\, k_B}\sum_{i=1}^{N}\sum_{\alpha=1}^{3}\frac{\pi_{i,\alpha}^2}{m_i} \tag{4.5.a}$$

and we have dropped the inertial mass of the thermostat, Q_s, in favor of a thermostat response frequency, ν_T,

$$\nu_T \equiv \sqrt{\frac{f\, k_B T_{set}}{Q_s}} \tag{4.5.b}$$

because ν_T is independent of system size, whereas Q_s is not. In the absence of a thermostat (*i.e.*, $\eta_T = 1$ and $\nu_T = 0$), equation (3.12) reduces to the NVE equations of motion.

4.2. Simplified Algorithm for Time Invariant Flows

We now consider how the equations of motion will simplify under the constraints of (i) time invariant flow and (ii) absence of external forces:

$$u_\alpha(\mathbf{r}_i, t) = u_\alpha(\mathbf{r}_i) \tag{4.6.a}$$

$$\begin{aligned} F_{i,\alpha}^{ext\,,\,pec} &= 0 \\ F_{\alpha}^{ext\,,\,COM} &= 0 \end{aligned} \tag{4.6.b}$$

The equations of motion become

$$\frac{d\rho_{i,\alpha}}{dt} = \eta_T\left(\frac{\pi_{i,\alpha}}{m_i} + \eta_T u_\alpha(r_i) - \frac{\eta_T}{M}\sum_{i=1}^{N}\left(m_i u_\alpha(r_i)\right)\right) \tag{4.7.a}$$

$$\frac{d\pi_{i,\alpha}}{dt} = \eta_T\left(\begin{array}{l} -\left(1-\frac{1}{{\eta_T}^2}\right)\sum_{\gamma=1}^{3}\left(\eta_T\pi_{i,\gamma}\right)\frac{\partial u_\gamma(r_i)}{\partial r_{i,\alpha}} + F_{i,\alpha}^{\text{int}} \\ +\frac{m_i}{M}\left(1-\frac{1}{{\eta_T}^2}\right)\sum_{i=1}^{N}\sum_{\gamma=1}^{3}\left(\eta_T\pi_{i,\gamma}\right)\frac{\partial u_\gamma(r_i)}{\partial r_{i,\alpha}} \\ -m_i\left(\frac{1}{\eta_T}\frac{\partial u_\alpha(\mathbf{r}_i)}{\partial t} + \sum_{\gamma=1}^{3}\frac{\partial u_\alpha(\mathbf{r}_i,t)}{\partial r_{i,\gamma}}\left(\frac{\pi_{i,\gamma}}{m_i\eta_T} + \frac{P_\gamma}{M} + u_\gamma(r_i)\right)\right) \\ +\frac{m_i}{M}\sum_{j=1}^{N}m_j\left(\frac{1}{\eta_T}\frac{\partial u_\alpha(\mathbf{r}_j)}{\partial t} + \sum_{\gamma=1}^{3}\frac{\partial u_\alpha(\mathbf{r}_j)}{\partial r_{i,\gamma}}\left(\frac{\pi_{j,\gamma}}{m_j\eta_T} + \frac{P_\gamma}{M} + u_\gamma(r_j)\right)\right) \\ -\pi_{i,\alpha}\zeta_T \end{array}\right) \tag{4.7.b}$$

$$\frac{dP_\alpha}{dt} = \eta_T\left(\begin{array}{l} -{\eta_T}^2\left(1-\frac{1}{{\eta_T}^2}\right)\sum_{i=1}^{N}\sum_{\gamma=1}^{3}\left(\pi_{i,\gamma}\right)\frac{\partial u_\gamma(r_i)}{\partial r_{i,\alpha}} \\ -\eta_T\sum_{j=1}^{N}m_j\left(\frac{1}{\eta_T}\frac{\partial u_\alpha(\mathbf{r}_j)}{\partial t} + \sum_{\gamma=1}^{3}\frac{\partial u_\alpha(\mathbf{r}_j)}{\partial r_{i,\gamma}}\left(\frac{\pi_{j,\gamma}}{m_j\eta_T} + \frac{P_\gamma}{M} + u_\gamma(r_j)\right)\right) \end{array}\right) \tag{4.7.c}$$

$$\frac{dR_\alpha}{dt} = \frac{\eta_T{}^2}{M}\left(P_\alpha + \sum_{j=1}^{N} m_j u_\alpha(\mathbf{r}_j) \right) \tag{4.7.d}$$

Equations (4.4.e) and (4.4.f) will not change. Next, consider a system with the additional assumptions that (iii) the momentum is initialized to zero, $\sum_{i=1}^{N} p_{i,\alpha} = 0$, (iv) the gradient of the velocity profile is independent of position, i.e., homogeneous flow, as is the case for purely shear and purely elongational flow, $u_\alpha(\mathbf{r}_i) = \sum_{\beta=1}^{3} \frac{\partial u_\alpha}{\partial r_\beta} r_{i,\beta}$, and (v) Planar Couette flow. With these constraints, equations (4.7) becomes

$$\frac{d\rho_{i,\alpha}}{dt} = \eta_T\left(\frac{\pi_{i,\alpha}}{m_i} + \eta_T u_\alpha(r_i) - \frac{\eta_T}{M}\sum_{i=1}^{N}\sum_{\beta=1}^{3} m_i r_{i,\beta}\frac{\partial u_\alpha}{\partial r_\beta} \right) \tag{4.8.a}$$

$$\frac{d\pi_{i,\alpha}}{dt} = \eta_T\left(-\left(\eta_T - \frac{1}{\eta_T} \right)\sum_{\beta=1}^{3} \pi_{i,\beta}\frac{\partial u_\beta}{\partial r_\alpha} + F_{i,\alpha}^{\text{int}} - \frac{1}{\eta_T}\sum_{\beta=1}^{3} \pi_{i,\beta}\frac{\partial u_\alpha}{\partial r_\beta} - \pi_{i,\alpha}\zeta_T \right) \tag{4.8.b}$$

$$\frac{dP_\alpha}{dt} = -\eta_T{}^2 \sum_{j=1}^{N} m_j \left(\sum_{\gamma=1}^{3} \frac{\partial u_\alpha(\mathbf{r}_j)}{\partial r_{i,\gamma}} \left(\frac{P_\gamma}{M} \right) \right) \tag{4.8.c}$$

$$\frac{dR_\alpha}{dt} = \frac{\eta_T{}^2}{M}\left(P_\alpha + \sum_{j=1}^{N} m_j \sum_{\beta=1}^{3} \frac{\partial u_\alpha}{\partial r_\beta} r_{j,\beta} \right) \tag{4.8.d}$$

$$\frac{d\eta_T}{dt} = \eta_T{}^2 \zeta_T \tag{4.8.e}$$

$$\frac{d\zeta_T}{dt} = \eta_T \frac{f k_B T_{set}}{Q_s}\left(\sum_{i=1}^{N}\sum_{\alpha=1}^{3} \frac{(\pi_{i,\alpha})^2}{m_i f k_B T_{set}} - 1 - \frac{\Delta H_f}{f k_B T_{set}} \right) \tag{4.8.f}$$

4.3. Conservation of Hamiltonian

In this section, we will prove by direct evaluation that the Hamiltonian in the physical frame of reference in the NVT ensemble is a conserved quantity when expressed in terms of the peculiar and COM coordinates.

The Hamiltonian in terms of the peculiar coordinates in the physical frame of reference is given by

$$\tilde{H}' = \begin{pmatrix} \frac{1}{2}\sum_{i=1}^{N}\sum_{\alpha=1}^{3}\frac{(\pi_{i,\alpha})^2}{m_i'} + \eta_T\sum_{i=1}^{N}\sum_{\alpha=1}^{3}\pi_{i,\alpha}(u_\alpha(r_i,t)) + \frac{1}{2}\sum_{i=1}^{N}\sum_{\alpha=1}^{3}m_i'(u_\alpha(r_i,t))^2 \\ +\frac{1}{2}\sum_{i=1}^{N}\sum_{\alpha=1}^{3}m_i'\left(\frac{P_\alpha}{M}\right)^2 + \left(\sum_{j=1}^{N}\sum_{\alpha=1}^{3}m_j' u_\alpha(\mathbf{r}_j,t)\right)\left(\frac{P_\alpha}{M}\right) + \eta_T\sum_{i=1}^{N}\sum_{\alpha=1}^{3}\pi_{i,\alpha}\frac{P_\alpha}{M} \\ +U_{\text{int}}(\rho_{i,\alpha}'-\rho_{j,\alpha}') + U_{ext}(\rho_{i,\alpha}',R_\alpha') + \frac{Q_s}{2}\zeta_T{}^2 + fk_BT_{set}\ln(\eta_T) - H_0 \end{pmatrix}\eta_T \quad (4.9)$$

The evolution of the Hamiltonian is given by

$$\begin{aligned} \frac{dH_{NVT}}{dt} = &\sum_{i=1}^{N}\sum_{\alpha=1}^{3}\frac{\partial H_{NVT}}{\partial \pi_{i,\alpha}}\frac{d\pi_{i,\alpha}}{dt} + \sum_{i=1}^{N}\sum_{\alpha=1}^{3}\frac{\partial H_{NVT}}{\partial \rho_{i,\alpha}}\frac{d\rho_{i,\alpha}}{dt} + \sum_{i=1}^{N}\sum_{\alpha=1}^{3}\frac{\partial H_{NVT}}{\partial P_\alpha}\frac{dP_\alpha}{dt} \\ &+\sum_{i=1}^{N}\sum_{\alpha=1}^{3}\frac{\partial H_{NVT}}{\partial R_\alpha}\frac{dR_\alpha}{dt} + \frac{\partial H_{NVT}}{\partial \zeta_T}\frac{d\zeta_T}{dt} + \frac{\partial H_{NVT}}{\partial \eta_T}\frac{d\eta_T}{dt} + \frac{\partial H_{NVT}}{\partial t} \end{aligned} \quad (4.10)$$

The Hamiltonian in equation (4.9) is differentiated partially with respect to the variable $\pi_{i,\alpha}$:

$$\frac{\partial H_{NVT}}{\partial \pi_{i,\alpha}} = \left(\frac{\pi_{i,\alpha}}{m_i'} + \eta_T u_\alpha(r_i,t)\right)\eta_T \quad (4.11.a)$$

The Hamiltonian in equation (4.9) is differentiated partially with respect to the variable $\rho_{i,\alpha}$:

$$\frac{\partial H_{NVT}}{\partial \rho_{i,\alpha}} = \left(\begin{array}{l} \eta_T \sum_{\beta=1}^{3} \pi_{i,\beta} \sum_{\gamma=1}^{3} \frac{\partial u_\beta(r_i,t)}{\partial r_{i,\gamma}} \frac{\partial r_{i,\gamma}}{\partial \rho_{i,\alpha}} + \sum_{\alpha=1}^{3} m_i u_\beta(r_i,t) \sum_{\gamma=1}^{3} \frac{\partial u_\beta(r_i,t)}{\partial r_{i,\gamma}} \frac{\partial r_{i,\gamma}}{\partial \rho_{i,\alpha}} \\ + \sum_{\alpha=1}^{3} m_i \frac{P_\beta}{M} \sum_{\gamma=1}^{3} \frac{\partial u_\beta(r_i,t)}{\partial r_{i,\gamma}} \frac{\partial r_{i,\gamma}}{\partial \rho_{i,\alpha}} - F_{i,\alpha}^{\text{int}} - F_{i,\alpha}^{ex,pec} \end{array} \right) \eta_T \tag{4.11.b}$$

where the external force and the internal force are defined as

$$\begin{aligned} \frac{\partial U_{int}(\rho_{i,\alpha} - \rho_{j,\alpha})}{\partial \rho_{i,\alpha}} &= \sum_{\substack{j=1 \\ j \neq i}}^{N} \frac{\partial U_{int}(\rho_{i,\alpha} - \rho_{j,\alpha})}{\partial(\rho_{i,\alpha} - \rho_{j,\alpha})} \frac{\partial(\rho_{i,\alpha} - \rho_{j,\alpha})}{\partial \rho_{i,\alpha}} = -F_{i,\alpha}^{\text{int}} \\ \frac{\partial U_{ext}(\rho_{i,\alpha}, R_{i,\alpha})}{\partial \rho_{i,\alpha}} &= -F_{i,\alpha}^{ext,pec} \end{aligned} \tag{4.11.c}$$

The Hamiltonian in equation (4.9) is differentiated partially with respect to the variable P_α:

$$\frac{\partial H_{NVT}}{\partial P_\alpha} = \left(\sum_{i=1}^{N} m_i \frac{P_\alpha}{M^2} + \frac{1}{M} \sum_{j=1}^{N} m_i u_\alpha(\mathbf{r}_j, t) \right) \eta_T \tag{4.11.d}$$

The Hamiltonian in equation (4.9) is differentiated partially with respect to the variable R_α:

$$\frac{\partial H_{NVT}}{\partial R_\alpha} = \left(\begin{array}{l} \eta_T \sum_{i=1}^{N} \sum_{\beta=1}^{3} \pi_{i,\beta} \sum_{\gamma=1}^{3} \frac{\partial u_\beta(r_i,t)}{\partial r_{i,\gamma}} \frac{\partial r_{i,\gamma}}{\partial R_\alpha} + \sum_{i=1}^{N} \sum_{\beta=1}^{3} m_i u_\beta(r_i,t) \sum_{\gamma=1}^{3} \frac{\partial u_\beta(r_i,t)}{\partial r_{i,\gamma}} \frac{\partial r_{i,\gamma}}{\partial R_\alpha} \\ + \left(\sum_{j=1}^{N} \sum_{\beta=1}^{3} m_i \frac{P_\beta}{M} \sum_{\gamma=1}^{3} \frac{\partial u_\beta(r_i,t)}{\partial r_{i,\gamma}} \frac{\partial r_{i,\gamma}}{\partial R_\alpha} \right) - F_\alpha^{ext,COM} \end{array} \right) \eta_T \tag{4.11.e}$$

where the external force in terms of the center of mass coordinates is defined as

$$\frac{\partial U_{ext}(\rho_{i,\alpha}, R_{i,\alpha})}{\partial R_\alpha} = -F_\alpha^{ext,COM} \tag{4.11.f}$$

The Hamiltonian in equation (4.9) is differentiated partially with respect to the variable ζ_T:

$$\frac{\partial H_{NVT}}{\partial \zeta_T} = \frac{f\, k_B T_{set}}{\nu_T^2} \eta_T \zeta_T \tag{4.11.g}$$

The Hamiltonian in equation (4.9) is differentiated with respect to the time dilation variable η_T:

$$\frac{\partial H_{NVT}}{\partial \eta_T} = \Delta H_f + \left(\eta_T \sum_{i=1}^{N} \sum_{\alpha=1}^{3} \pi_{i,\alpha}(u_\alpha(r_i,t)) + f k_B T_{set} \right) \tag{4.11.h}$$

The Hamiltonian in equation (4.9) is differentiated partially with respect to the variable t:

$$\frac{\partial H_{NVT}}{\partial t} = \eta_T \left(\begin{array}{l} + \sum_{\alpha=1}^{3} \sum_{i=1}^{N} m_i u_\alpha (r_i, t) \frac{\partial u_\alpha (r_i, t)}{\partial t} + \sum_{\alpha=1}^{3} \sum_{i=1}^{N} (\eta_T \pi_{i,\alpha}) \frac{\partial u_\alpha (r_i, t)}{\partial t} \\ + \sum_{\alpha=1}^{3} \sum_{i=1}^{N} m_i \frac{(P_\alpha)}{M} \frac{\partial u_\alpha (r_i, t)}{\partial t} \end{array} \right) \tag{4.11.i}$$

Now we substitute equations (4.4) and equations (4.11) in equation (4.10). If we consider time invariant flow, then the evolution of the Hamiltonian would be zero, i.e., the Hamiltonian would be a conserved quantity.

$$\frac{dH_{NVT}}{dt} = 0 \tag{4.12}$$

4.4. Reversible Reference System Propagator Algorithm

We derive the r-RESPA [13, 24] integration algorithm for integrating the equations of motion using the proper-SLLOD equations in the NVT ensemble. We assume one time scale. In other words, the thermostat and the forces act on the same time scale. This will work for simple fluids without intramolecular degrees of freedom. In the absence of any external field beyond that of the imposed flow field, equations (4.8) can be represented as

$$\frac{dr_{i,\alpha}}{dt} = \eta_T^2 \left(\frac{\pi_{i,\alpha}}{m_i \eta_T} + \sum_{\beta=1}^{3} \frac{\partial u_\alpha}{\partial r_\beta} r_{i,\beta} \right) \tag{4.13.a}$$

$$\frac{d\pi_{i,\alpha}}{dt} = \eta_T \left(-\pi_{i,\alpha}\zeta_T - \left(\eta_T - \frac{1}{\eta_T} \right) \sum_{\beta=1}^{3} \left(\pi_{i,\beta} \right) \frac{\partial u_\beta}{\partial r_\alpha} + F_{i,\alpha}^{'\ \text{int}} - \frac{1}{\eta_T} \sum_{\beta=1}^{3} \pi_{i,\beta} \frac{\partial u_\alpha}{\partial r_\beta} \right)$$

(4.13.b)

$$\frac{d\eta_T}{dt} = {\eta_T}^2 \zeta_T \tag{4.13.c}$$

$$\frac{d\zeta_T}{dt} = \eta_T \vartheta^2 \left(\frac{T(t)}{T_{set}} - 1 - \frac{\Delta H_f}{f k_B T_{set}} \right) \tag{4.13.d}$$

Equation (4.13.d) can be expressed as

$$\frac{d\zeta_T}{dt} = \eta_T \vartheta^2 \left(\frac{T(t)}{T_{set}} - 1 - \frac{\Delta H'_f}{f k_B T_{set}} \right) - \frac{\eta_T}{2} {\zeta_T}^2 \tag{4.13.e}$$

where

$$\Delta H_f = \Delta H'_f + \frac{Q_s}{2} {\zeta_T}^2 \tag{4.13.f}$$

ΔH_f has to be split into two terms. $\Delta H'_f$ as a constant can be evaluated in one operator, while the $\frac{Q_s}{2} {\zeta_T}^2$ is not a constant and hence has to be evaluated separately.

For this system, the Liouville operator is given by

$$iL = \frac{dr_{i,\alpha}}{dt} \frac{\partial}{\partial r_{i,\alpha}} + \frac{d\pi_{i,\alpha}}{dt} \frac{\partial}{\partial \pi_{i,\alpha}} + \frac{d\eta_T}{dt} \frac{\partial}{\partial \eta_T} + \frac{d\zeta_T}{dt} \frac{\partial}{\partial \zeta_T} \tag{4.14.a}$$

Equations (4.13) are substituted in equation (4.14), yielding

$$
\begin{aligned}
iL = {} & \eta_T^2\left(\frac{\pi_{i,\alpha}}{m_i\eta_T}+\sum_{\beta=1}^{3}\frac{\partial u_\alpha}{\partial r_\beta}r_{i,\beta}\right)\frac{\partial}{\partial r_{i,\alpha}} \\
& +\eta_T\left(-\pi_{i,\alpha}\zeta_T-\left(\eta_T-\frac{1}{\eta_T}\right)\sum_{\beta=1}^{3}\left(\pi_{i,\beta}\right)\frac{\partial u_\beta}{\partial r_\alpha}+F_{i,\alpha}^{'\ \mathrm{int}}-\frac{1}{\eta_T}\sum_{\beta=1}^{3}\pi_{i,\beta}\frac{\partial u_\alpha}{\partial r_\beta}\right)\frac{\partial}{\partial \pi_{i,\alpha}} \\
& +{\eta_T}^2\zeta_T\frac{\partial}{\partial \eta_T}+\eta_T\vartheta^2\left(\frac{T(t)}{T_{set}}-1-\frac{\Delta H_f}{fk_BT_{set}}\right)\frac{\partial}{\partial \zeta_T}
\end{aligned}
\tag{4.14.b}
$$

The operators are split in a symmetric manner.

The Liouville operator is then applied to the variables:

$$
\begin{aligned}
iL = {} & \frac{1}{2}\left(\eta_T\vartheta^2\left(\frac{T(t)}{T_{set}}-1-\frac{\Delta H'_f}{fk_BT_{set}}\right)-\frac{\eta_T}{2}{\zeta_T}^2\right)\frac{\partial}{\partial \zeta_T}+\frac{\eta_T F_{i,\alpha}^{\mathrm{int}}}{4}\frac{\partial}{\partial \pi_{i,\alpha}} \\
& -\frac{\pi_{i,\alpha}\eta_T\zeta_T}{2}\frac{\partial}{\partial \pi_{i,\alpha}}+\frac{\eta_T F_{i,\alpha}^{\mathrm{int}}}{4}\frac{\partial}{\partial \pi_{i,\alpha}}+\frac{{\eta_T}^2\zeta_T}{2}\frac{\partial}{\partial \eta_T} \\
& -\frac{\eta_T}{2}\left(\left(\eta_T-\frac{1}{\eta_T}\right)\sum_{\beta=1}^{3}\pi_{i,\beta}\frac{\partial u_\beta}{\partial r_\alpha}\right)\frac{\partial}{\partial \pi_{i,\alpha}}-\frac{\eta_T}{2}\left(\frac{1}{\eta_T}\sum_{\beta=1}^{3}\pi_{i,\beta}\frac{\partial u_\alpha}{\partial r_\beta}\right)\frac{\partial}{\partial \pi_{i,\alpha}} \\
& +\frac{{\eta_T}^2}{2}\left(\sum_{\beta=1}^{3}\frac{\partial u_\alpha}{\partial r_\beta}r_{i,\beta}\right)\frac{\partial}{\partial r_{i,\alpha}}+\frac{\eta_T\pi_{i,\alpha}}{m_i}\frac{\partial}{\partial r_{i,\alpha}} \\
& +\frac{\eta_T}{2}\left(\sum_{\beta=1}^{3}\frac{\partial u_\alpha}{\partial r_\beta}r_{i,\beta}\right)\frac{\partial}{\partial r_{i,\alpha}}-\frac{\eta_T}{2}\left(\frac{1}{\eta_T}\sum_{\beta=1}^{3}\pi_{i,\beta}\frac{\partial u_\alpha}{\partial r_\beta}\right)\frac{\partial}{\partial \pi_{i,\alpha}} \\
& -\frac{\eta_T}{2}\left(\left(\eta_T-\frac{1}{\eta_T}\right)\sum_{\beta=1}^{3}\pi_{i,\beta}\frac{\partial u_\beta}{\partial r_\alpha}\right)\frac{\partial}{\partial \pi_{i,\alpha}}+\frac{{\eta_T}^2\zeta_T}{2}\frac{\partial}{\partial \eta_T} \\
& +\eta_T\frac{F_{i,\alpha}^{\mathrm{int}}}{4}\frac{\partial}{\partial \pi_{i,\alpha}}-\frac{\pi_{i,\alpha}\eta_T\zeta_T}{2}\frac{\partial}{\partial \pi_{i,\alpha}}+\frac{\eta_T F_{i,\alpha}^{\mathrm{int}}}{4}\frac{\partial}{\partial \pi_{i,\alpha}} \\
& +\frac{1}{2}\left(\eta_T\vartheta^2\left(\frac{T(t)}{T_{set}}-1-\frac{\Delta H'_f}{fk_BT_{set}}\right)-\frac{\eta_T}{2}{\zeta_T}^2\right)\frac{\partial}{\partial \zeta_T}
\end{aligned}
\tag{4.15}
$$

The first operator changes the thermostat momentum variable,

$$\zeta_T^{(1)} = \exp\left\{ i\frac{\Delta t}{2} F_n(\pi_{i,\alpha}) \frac{\partial}{\partial \zeta_T} \right\} \zeta_T^{(0)} = \zeta_T^{(0)} + \frac{\eta_T^{(0)} \vartheta^2}{2} \left(\frac{T^{(0)}}{T_{set}} - 1 - \frac{\Delta H_f'^{(0)}}{f k_B T_{set}} \right) \quad (4.16)$$

The second operator acts on the thermostat momentum,

$$\zeta_T^{(2)} = \exp\left\{ \frac{i\Delta t}{4} \left(-\eta_T \zeta_T^{\,2} \right) \frac{\partial}{\partial \zeta_T} \right\} \zeta_T^{(1)} = \frac{\zeta_T^{(1)}}{1 + \frac{\Delta t}{4} \eta_T^{(1)} \zeta_T^{(1)}} \quad (4.17)$$

The third operator changes the momentum of the system,

$$\pi_{i,\alpha}^{(3)} = \exp\left\{ \frac{i\Delta t}{4} \eta_T F_{i,\alpha}^{\text{int}} \frac{\partial}{\partial \pi_{i,\alpha}} \right\} \pi_{i,\alpha}^{(0)} = \pi_{i,\alpha}^{(0)} + \eta_T^{(2)} \frac{\Delta t}{4} F_{i,\alpha}^{\text{int}}(r_i^{(0)}) \quad (4.18)$$

The fourth operator changes the momentum,

$$\pi_{i,\alpha}^{(4)} = \exp\left\{ -i\frac{\Delta t}{2} \eta_T (\pi_{i,\alpha} \zeta_T) \frac{\partial}{\partial \pi_{i,\alpha}} \right\} \pi_{i,\alpha}^{(3)} = \pi_{i,\alpha}^{(3)} \exp\left\{ -\frac{\Delta t}{2} \eta_T^{(3)} \zeta_T^{(3)} \right\}$$

(4.19)

The fifth operator changes the momentum,

$$\pi_{i,\alpha}^{(5)} = \exp\left\{ \frac{i\Delta t}{4} \eta_T F_{i,\alpha}^{\text{int}} \frac{\partial}{\partial \pi_{i,\alpha}} \right\} \pi_{i,\alpha}^{(4)} = \pi_{i,\alpha}^{(4)} + \eta_T^{(4)} \Delta t \frac{F_{i,\alpha}^{\text{int}}(r_i^{(0)})}{4} \quad (4.20)$$

The sixth operator changes the time dilation variable,

$$\eta_T{}^{(6)} = \exp\left\{ i\frac{\Delta t}{2}\eta_T{}^2\zeta_T\frac{\partial}{\partial\eta_T}\right\}\eta_T{}^{(5)} = \frac{\eta_T{}^{(5)}}{1-\frac{\Delta t}{2}\zeta_T{}^{(5)}\eta_T{}^{(5)}} \tag{4.21}$$

The seventh operator changes the momentum,

$$\pi_{i,\alpha}{}^{(7)} = \exp\left\{ -\frac{i\Delta t}{2}\left(\eta_T\left(\eta_T - \frac{1}{\eta_T}\right)\sum_{\beta=1}^{3}\left(\pi_{i,\beta}\right)\frac{\partial u_\beta}{\partial r_\alpha}\right)\frac{\partial}{\partial\pi_{i,\alpha}}\right\}\pi_{i,\alpha}{}^{(6)} \tag{4.22.a}$$

This equation changes the y momenta:

$$\pi_{i,y}{}^{(7)} = \pi_{i,y}{}^{(6)} - \frac{\Delta t}{2}\left(\left(\eta_T^2\right)^{(6)} - 1\right)\frac{\partial u_x}{\partial r_y}\pi_{i,x}{}^{(6)} \tag{4.22.b}$$

The eighth operator changes the momenta,

$$\pi_{i,\alpha}{}^{(8)} = \exp\left\{ -\frac{i\Delta t}{2}\left(\sum_{\beta=1}^{3}\pi_{i,\beta}\frac{\partial u_\alpha}{\partial r_\beta}\right)\frac{\partial}{\partial\pi_{i,\alpha}}\right\}\pi_{i,\alpha}{}^{(7)} \tag{4.23.a}$$

This equation changes the x momenta:

$$\pi_{i,x}{}^{(8)} = \pi_{i,x}{}^{(7)} - \frac{\Delta t}{2}\frac{\partial u_x}{\partial r_y}\pi_{i,y}{}^{(7)} \tag{4.23.b}$$

The ninth operator changes the position,

$$r_{i,\alpha}{}^{(9)} = \left\{ i\frac{\Delta t}{2}\eta_T{}^2\sum_{\beta=1}^{3}\frac{\partial u_\alpha}{\partial r_\beta}r_{i,\beta}\frac{\partial}{\partial r_{i,\alpha}}\right\}r_{i,\alpha}{}^{(8)} \tag{4.24.a}$$

This equation changes the x positions:

$$r_{i,x}^{(9)} = r_{i,x}^{(8)} + \frac{\Delta t}{2}\left(\eta_T^{\,2}\right)^{(8)} \frac{\partial u_x}{\partial r_y} r_{i,y}^{(8)} \tag{4.24.b}$$

The tenth operator changes the position,

$$r_{i,\alpha}^{(9)} = \exp\left\{ i\Delta t \frac{\eta_T \pi_{i,\alpha}}{m_i} \frac{\partial}{\partial r_{i,\alpha}} \right\} r_{i,\alpha}^{(8)} = r_{i,\alpha}^{(8)} + \Delta t \frac{\eta_T^{(8)} \pi_{i,\alpha}^{(8)}}{m_i} \tag{4.25}$$

The eleventh operator changes the position,

$$r_{i,\alpha}^{(11)} = \left\{ i \frac{\Delta t}{2} \eta_T^{\,2} \sum_{\beta=1}^{3} \frac{\partial u_\alpha}{\partial r_\beta} r_{i,\beta} \frac{\partial}{\partial r_{i,\alpha}} \right\} r_{i,\alpha}^{(10)} \tag{4.26.a}$$

This equation changes the x positions:

$$r_{i,x}^{(11)} = r_{i,x}^{(10)} + \frac{\Delta t}{2}\left(\eta_T^{\,2}\right)^{(10)} \frac{\partial u_x}{\partial r_y} r_{i,y}^{(10)} \tag{4.26.b}$$

The twelfth operator changes the momenta,

$$\pi_{i,\alpha}^{(12)} = \exp\left\{ -i \frac{\Delta t}{2} \left(\sum_{\beta=1}^{3} \pi_{i,\beta} \frac{\partial u_\alpha}{\partial r_\beta} \right) \frac{\partial}{\partial \pi_{i,\alpha}} \right\} \pi_{i,\alpha}^{(11)} \tag{4.27.a}$$

This equation changes the x momenta:

$$\pi_{i,x}^{(12)} = \pi_{i,x}^{(11)} - \frac{\Delta t}{2} \frac{\partial u_x}{\partial r_y} \pi_{i,y}^{(11)} \tag{4.27.b}$$

The thirteenth operator changes the momenta,

$$\pi_{i,\alpha}{}^{(13)} = \exp\left\{-i\frac{\Delta t}{2}\left(\eta_T\left(\eta_T - \frac{1}{\eta_T}\right)\sum_{\beta=1}^{3}\left(\pi_{i,\beta}\right)\frac{\partial u_\beta}{\partial r_\alpha}\right)\frac{\partial}{\partial \pi_{i,\alpha}}\right\}\pi_{i,\alpha}{}^{(12)} \tag{4.28.a}$$

This equation changes the y momenta:

$$\pi_{i,y}{}^{(13)} = \pi_{i,y}{}^{(12)} - \frac{\Delta t}{2}\left(\left(\eta_T{}^2\right)^{(12)} - 1\right)\frac{\partial u_x}{\partial r_y}\pi_{i,x}{}^{(12)} \tag{4.28.b}$$

The fourteenth operator changes the time dilation variable,

$$\eta_T{}^{(14)} = \exp\left\{i\frac{\Delta t}{2}\eta_T{}^2\zeta_T\frac{\partial}{\partial \eta_T}\right\}\eta_T{}^{(13)} = \frac{\eta_T{}^{(13)}}{1-\frac{\Delta t}{2}\zeta_T{}^{(13)}\eta_T{}^{(13)}} \tag{4.29}$$

The fifteenth operator changes the momenta,

$$\pi_{i,\alpha}{}^{(15)} = \exp\left\{\frac{i\Delta t}{4}\eta_T F_{i,\alpha}^{\text{int}}\frac{\partial}{\partial \pi_{i,\alpha}}\right\}\pi_{i,\alpha}{}^{(14)} = \pi_{i,\alpha}{}^{(14)} + \frac{\Delta t}{4}\eta_T{}^{(14)}F_{i,\alpha}^{\text{int}}(r_i{}^{(14)}) \tag{4.30}$$

The sixteenth operator changes the momenta,

$$\pi_{i,\alpha}{}^{(16)} = \exp\left\{-i\frac{\Delta t}{2}\eta_T\left(\pi_{i,\alpha}\zeta_T\right)\frac{\partial}{\partial \pi_{i,\alpha}}\right\}\pi_{i,\alpha}{}^{(15)} = \pi_{i,\alpha}{}^{(15)}\exp\left\{-\frac{\Delta t}{2}\eta_T{}^{(15)}\zeta_T{}^{(15)}\right\}$$

(4.31)

The seventeenth operator changes the momenta,

$$\pi_{i,\alpha}{}^{(17)} = \exp\left\{\frac{i\Delta t}{4}\eta_T F_{i,\alpha}^{\text{int}}\frac{\partial}{\partial\pi_{i,\alpha}}\right\}\pi_{i,\alpha}{}^{(16)} = \pi_{i,\alpha}{}^{(16)} + \frac{\Delta t}{4}\eta_T{}^{(16)}F_{i,\alpha}^{\text{int}}(r_i{}^{(16)}) \quad (4.32)$$

The eighteenth operator acts on the thermostat momentum,

$$\zeta_T{}^{(18)} = \exp\left\{\frac{i\Delta t}{4}\left(-\eta_T\zeta_T{}^2\right)\frac{\partial}{\partial\zeta_T}\right\}\zeta_T{}^{(17)} = \frac{\zeta_T{}^{(17)}}{1+\frac{\Delta t}{4}\eta_T{}^{(17)}\zeta_T{}^{(17)}} \quad (4.33)$$

The nineteenth operator changes the thermostat momentum. This operator requires the calculation of temperature:

$$\zeta_T{}^{(19)} = \exp\left\{i\frac{\Delta t}{2}F_n(\pi_{i,\alpha})\frac{\partial}{\partial\zeta_T}\right\}\zeta_T{}^{(18)} = \zeta_T{}^{(18)} + \frac{\eta_T{}^{(18)}\vartheta^2}{2}\left(\frac{T^{(18)}}{T_{set}} - 1 - \frac{\Delta H_f'{}^{(18)}}{fk_BT_{set}}\right) \quad (4.34)$$

4.5. Symplectic Integrator

Symplectic integrators are a class of geometric integrators that are designed for the numerical solution of Hamilton's canonical equations. They solve the equations of motion for the Hamiltonian system while keeping the symplectic structure of the system intact. Although the Hamiltonian of the system may not be exactly conserved, the energy fluctuations are bounded. We will integrate the phase space variable in the laboratory coordinates in the mathematical frame of reference for ease of calculation. Nosé has derived a symplectic integration scheme [16] for equilibrium systems that use the Nosé-

Poincaré thermostat [15]. We will follow this integration scheme closely for solving the equations of motion of NEMD systems.

The Hamiltonian expressed in terms of the laboratory coordinates in the mathematical frame of reference is given by

$$\tilde{H}' = \left(\begin{array}{l} \frac{1}{2}\sum_{i=1}^{N}\sum_{\alpha=1}^{3}\frac{(p'_{i,\alpha})^2}{m'_i s^2} + \frac{1}{2M'}\left(1-\frac{1}{s^2}\right)\sum_{\alpha=1}^{3}\left(\sum_{j=1}^{N} p'_{j,\alpha}\right)^2 + \\ -\frac{1}{M'}\left(1-\frac{1}{s^2}\right)\sum_{i=1}^{N}\sum_{\alpha=1}^{3}\left(m'_i u_\alpha(r_i,t)\right)\sum_{j=1}^{N} p'_{j,\alpha} - \frac{1}{2}\left(1-\frac{1}{s^2}\right)\sum_{j=1}^{N}\sum_{\alpha=1}^{3} m'_j\left(u_\alpha(r_j,t)\right)^2 \\ \left(1-\frac{1}{s^2}\right)\sum_{i=1}^{N}\sum_{\alpha=1}^{3}\left(p'_{i,\alpha}\right)u_\alpha(r_i,t) + \frac{1}{2M'}\left(1-\frac{1}{s^2}\right)\sum_{\alpha=1}^{3}\left(\sum_{j=1}^{N} m'_j u_\alpha(\mathbf{r}_j,t)\right)^2 \\ + U\left(r_{i,\alpha}-r_{j,\alpha}\right) + \frac{1}{2Q_s}p_s^2 + fk_B T_{set}\ln(s) - H_0 \end{array} \right) s \tag{4.35}$$

Here we have just redefined the potential energy in terms of the laboratory coordinates.

The time evolution of a property A(t) can be expressed as

$$A(t+\Delta t) = P(t;\Delta t)A(t) \tag{4.36.a}$$

where P(t;Δt) is the time propagator.

When we use symplectic integrators the time propagator can be decomposed into a product of easily obtainable smaller propagators [16], such as

$$P(t;\Delta t)=\exp(D_H\Delta t)=\exp\left(D_{H3}\frac{\Delta t}{2}\right)\exp\left(D_{H2}\frac{\Delta t}{2}\right)\exp(D_{H1}\Delta t)\exp\left(D_{H2}\frac{\Delta t}{2}\right)$$
$$\exp\left(D_{H3}\frac{\Delta t}{2}\right)$$

(4.36.b)

The Hamiltonian can be separated into five terms,

$$\tilde{H}' = H_1 + H_2 + H_3 + H_4 + H_5 \tag{4.37}$$

where

$$H_1 = \left[\frac{1}{2}\sum_{i=1}^{N}\sum_{\alpha=1}^{3}\frac{p'^{\,2}_{i,\alpha}}{m_i s^2} + gk_B T_{set}\ln(s) - H_o\right]s \tag{4.38}$$

$$H_2 = s\begin{bmatrix}\dfrac{1}{2M'}\left(1-\dfrac{1}{s^2}\right)\displaystyle\sum_{\alpha=1}^{3}\left(\sum_{j=1}^{N}p'_{j,\alpha}\right)^2 + \left(1-\dfrac{1}{s^2}\right)\sum_{i=1}^{N}\sum_{\alpha=1}^{3}\left(p'_{i,\alpha}\right)u_\alpha(r_i,t)\\ -\dfrac{1}{M'}\left(1-\dfrac{1}{s^2}\right)\displaystyle\sum_{i=1}^{N}\sum_{\alpha=1}^{3}\left(m'_i u_\alpha(r_i,t)\right)\sum_{j=1}^{N}p'_{j,\alpha}\end{bmatrix} \tag{4.39}$$

$$H_3 = s\left[-\frac{1}{2}\left(1-\frac{1}{s^2}\right)\sum_{j=1}^{N}\sum_{\alpha=1}^{3}m'_j\left(u_\alpha(r_j,t)\right)^2 + \frac{1}{2M'}\left(1-\frac{1}{s^2}\right)\sum_{\alpha=1}^{3}\left(\sum_{j=1}^{N}m'_j u_\alpha(\mathbf{r}_j,t)\right)^2\right]$$

(4.40)

$$H_4 = sU\left(r_{i,\alpha}-r_{j,\alpha}\right) \tag{4.41}$$

$$H_5 = s\left[\frac{(p_s)^2}{2Q_s}\right] \tag{4.42}$$

Now the time propagator algorithm is arranged symmetrically to evaluate the time evolution of the quantities [29],

$$\begin{aligned} P(t;\Delta t) = \exp\left[D_{H5} \frac{\Delta t}{2} \right] \exp\left[D_{H4} \frac{\Delta t}{2} \right] \exp\left[D_{H3} \frac{\Delta t}{2} \right] \\ \exp\left[D_{H2} \frac{\Delta t}{2} \right] \exp[D_{H1} \Delta t] \exp\left[D_{H2} \frac{\Delta t}{2} \right] \\ \exp\left[D_{H3} \frac{\Delta t}{2} \right] \exp\left[D_{H4} \frac{\Delta t}{2} \right] \exp\left[D_{H5} \frac{\Delta t}{2} \right] \end{aligned} \tag{4.43}$$

where

$$D_H = \sum_{i=1}^{N} \sum_{\alpha=1}^{3} \dot{\Gamma}_{i,\alpha} \frac{\partial}{\partial \Gamma} = \sum_i \sum_\alpha \frac{dp'_{i,\alpha}}{dt'} \frac{\partial}{\partial p_{i,\alpha}} + \sum_i \sum_\alpha \frac{dr_{i,\alpha}}{dt'} \frac{\partial}{\partial r_{i,\alpha}} + \frac{ds}{dt'} \frac{\partial}{\partial s} + \frac{dp_s}{dt'} \frac{\partial}{\partial p_s}$$

(4.44)

These operators can be expressed as

$$\begin{aligned} D_{H1} &= \sum_{i=1}^{N} \sum_{\alpha=1}^{3} \dot{\Gamma}_{i,\alpha} \frac{\partial}{\partial \Gamma} = \sum_i \sum_\alpha \frac{dp'_{i,\alpha}}{dt'} \frac{\partial}{\partial p_{i,\alpha}} + \sum_i \sum_\alpha \frac{dr_{i,\alpha}}{dt'} \frac{\partial}{\partial r_{i,\alpha}} + \frac{ds}{dt'} \frac{\partial}{\partial s} + \frac{dp_s}{dt'} \frac{\partial}{\partial p_s} \\ &= \sum_i \sum_\alpha \frac{\partial H_1}{\partial p'_{i,\alpha}} \frac{\partial}{\partial r_{i,\alpha}} - \sum_i \sum_\alpha \frac{\partial H_1}{\partial r_{i,\alpha}} \frac{\partial}{\partial p'_{i,\alpha}} + \frac{\partial H_1}{\partial p_s} \frac{\partial}{\partial s} - \frac{\partial H_1}{\partial s} \frac{\partial}{\partial p_s} \\ &= \sum_{i=1}^{N} \sum_{\alpha=1}^{3} \frac{p'_{i,\alpha}}{m_i s} \frac{\partial}{\partial r_{i,\alpha}} - \left(- \sum_{i=1}^{N} \sum_{\alpha=1}^{3} \frac{\left(p'_{i,\alpha}\right)^2}{2 m_i s^2} + g k_B T_{set} \ln(s) - H_o + g k_B T_{set} \right) \frac{\partial}{\partial p_s} \end{aligned}$$

(4.45)

$$
\begin{aligned}
D_{H2} &= \sum_i \sum_\alpha \frac{\partial H_2}{\partial p'_{i,\alpha}} \frac{\partial}{\partial r_{i,\alpha}} - \sum_i \sum_\alpha \frac{\partial H_2}{\partial r_{i,\alpha}} \frac{\partial}{\partial p'_{i,\alpha}} + \frac{\partial H_2}{\partial p_s} \frac{\partial}{\partial s} - \frac{\partial H_2}{\partial s} \frac{\partial}{\partial p_s} \\
&= \sum_{i=1}^{N} \sum_{\alpha=1}^{3} s \left(\frac{1}{M'} \left(1 - \frac{1}{s^2} \right) \sum_{j=1}^{N} p'_{j,\alpha} + \left(1 - \frac{1}{s^2} \right) u_\alpha (r_i, t) - \frac{1}{M'} \left(1 - \frac{1}{s^2} \right) \sum_{i=1}^{N} \left(m'_i u_\alpha (r_i, t) \right) \right) \frac{\partial}{\partial r_{i,\alpha}} \\
&+ \sum_{i=1}^{N} \sum_{\alpha=1}^{3} s \left(- \left(1 - \frac{1}{s^2} \right) \sum_{\beta=1}^{3} \left(p'_{i,\beta} \right) \frac{\partial u_\beta (r_i, t)}{\partial r'_{i,\alpha}} + \frac{1}{M'} \left(1 - \frac{1}{s^2} \right) \sum_{\beta=1}^{3} \left(m'_i \frac{\partial u_\beta (r_i, t)}{\partial r'_{i,\alpha}} \right) \sum_{j=1}^{N} p'_{j,\beta} \right) \frac{\partial}{\partial p'_{i,\alpha}} \\
&- \left(\begin{array}{l} \frac{1}{2M'} \left(1 + \frac{1}{s^2} \right) \sum_{\alpha=1}^{3} \left(\sum_{j=1}^{N} p'_{j,\alpha} \right)^2 + \left(1 + \frac{1}{s^2} \right) \sum_{i=1}^{N} \sum_{\alpha=1}^{3} \left(p'_{i,\alpha} \right) u_\alpha (r_i, t) \\ - \frac{1}{M'} \left(1 + \frac{1}{s^2} \right) \sum_{\alpha=1}^{3} \left(\sum_{j=1}^{N} m'_j u_\alpha (\mathbf{r}_j, t) \right)^2 \end{array} \right) \frac{\partial}{\partial p_s}
\end{aligned}
\tag{4.46}
$$

$$
\begin{aligned}
D_{H3} &= \sum_i \sum_\alpha \frac{\partial H_3}{\partial p'_{i,\alpha}} \frac{\partial}{\partial r_{i,\alpha}} - \sum_i \sum_\alpha \frac{\partial H_3}{\partial r_{i,\alpha}} \frac{\partial}{\partial p'_{i,\alpha}} + \frac{\partial H_3}{\partial p_s} \frac{\partial}{\partial s} - \frac{\partial H_3}{\partial s} \frac{\partial}{\partial p_s} \\
&= \sum_{i=1}^{N} \sum_{\alpha=1}^{3} s \left(\begin{array}{l} \left(1 - \frac{1}{s^2} \right) \sum_{\beta=1}^{3} m'_i u_\beta (r_i, t) \frac{\partial u_\beta (r_i, t)}{\partial r'_{i,\alpha}} \\ - \frac{1}{M'} \left(1 - \frac{1}{s^2} \right) \sum_{\beta=1}^{3} \left(\sum_{j=1}^{N} m'_j u_\beta (\mathbf{r}_j, t) \right) m'_i \frac{\partial u_\beta (r_i, t)}{\partial r'_{i,\alpha}} \end{array} \right) \frac{\partial}{\partial p'_{i,\alpha}} \\
&+ \left(\frac{1}{2} \left(1 + \frac{1}{s^2} \right) \sum_{j=1}^{N} \sum_{\alpha=1}^{3} m'_j \left(u_\alpha (r_j, t) \right)^2 - \frac{1}{2M} \left(1 + \frac{1}{s^2} \right) \sum_{\alpha=1}^{3} \left(\sum_{j=1}^{N} m'_j u_\alpha (\mathbf{r}_j, t) \right)^2 \right) \frac{\partial}{\partial p_s}
\end{aligned}
\tag{4.47}
$$

$$
\begin{aligned}
D_{H4} &= \sum_i \sum_\alpha \frac{\partial H_4}{\partial p'_{i,\alpha}} \frac{\partial}{\partial r_{i,\alpha}} - \sum_i \sum_\alpha \frac{\partial H_4}{\partial r_{i,\alpha}} \frac{\partial}{\partial p'_{i,\alpha}} + \frac{\partial H_4}{\partial p_s} \frac{\partial}{\partial s} - \frac{\partial H_4}{\partial s} \frac{\partial}{\partial p_s} \\
&= -s \sum_{i=1}^{N} \sum_{\alpha=1}^{3} \left(\frac{\partial U(r_j)}{\partial r_{i,\alpha}} \right) \frac{\partial}{\partial p'_{i,\alpha}} \\
&- \left(U(r_j) \right) \frac{\partial}{\partial p_s}
\end{aligned}
\tag{4.48}
$$

$$
\begin{aligned}
D_{H5} &= \sum_i \sum_\alpha \frac{\partial H_5}{\partial p'_{i,\alpha}} \frac{\partial}{\partial r_{i,\alpha}} - \sum_i \sum_\alpha \frac{\partial H_5}{\partial r_{i,\alpha}} \frac{\partial}{\partial p'_{i,\alpha}} + \frac{\partial H_5}{\partial p_s} \frac{\partial}{\partial s} - \frac{\partial H_5}{\partial s} \frac{\partial}{\partial p_s} \\
&= \frac{\partial \left(s \left[\frac{(p_s)^2}{2Q_s} \right] \right)}{\partial p_s} \frac{\partial}{\partial s} - \frac{\partial \left(s \left[\frac{(p_s)^2}{2Q_s} \right] \right)}{\partial s} \frac{\partial}{\partial p_s} \\
&= s \frac{p_s}{Q_s} \frac{\partial}{\partial s} - \frac{(p_s)^2}{2Q_s} \frac{\partial}{\partial p_s}
\end{aligned}
\tag{4.49}
$$

We now use equation (4.43) to solve for the variables. The first operator acts on the thermostat variables,

$$
\begin{aligned}
\left\{ r_{i,\alpha}{}^{(1)}, p'_{i,\alpha}{}^{(1)}, s^{(1)}, p_s{}^{(1)} \right\} &= \exp\left(D_{H5} \frac{\Delta t}{2} \right) \left\{ r_{i,\alpha}{}^{(0)}, p'_{i,\alpha}{}^{(0)}, s^{(0)}, p_s{}^{(0)} \right\} \\
&= \left\{ r_{i,\alpha}{}^{(0)}, p'_{i,\alpha}{}^{(0)}, s^{(0)} \left(1 + \frac{\Delta t}{2} \frac{p_s{}^{(0)}}{2Q_s} \right)^2, \frac{p_s{}^{(0)}}{1 + \frac{\Delta t}{2} \frac{p_s{}^{(0)}}{2Q_s}} \right\}
\end{aligned}
\tag{4.50}
$$

The second operator acts on the positions and the thermostat momentum,

$$
\begin{aligned}
\left\{ r_{i,\alpha}{}^{(2)}, p'_{i,\alpha}{}^{(2)}, s^{(2)}, p_s{}^{(2)} \right\} &= \exp\left(D_{H4} \frac{\Delta t}{2} \right) \left\{ r_{i,\alpha}{}^{(1)}, p'_{i,\alpha}{}^{(1)}, s^{(1)}, p_s{}^{(1)} \right\} \\
&= \left\{ r_{i,\alpha}{}^{(1)} + \frac{\Delta t}{2} \left(\left(F'_{i,\alpha}(r_j{}^{(1)}) \right) \right) s^{(1)}, p'_{i,\alpha}{}^{(1)}, s^{(1)}, p_s{}^{(1)} - \frac{\Delta t}{2} U\left(r_j \right) \right\}
\end{aligned}
\tag{4.51}
$$

The third operator acts on the momenta and the thermostat momentum,

$$\left\{r_{i,\alpha}^{(3)}, p'^{(3)}_{i,\alpha}, s^{(3)}, p_s^{(3)}\right\} = \exp\left(D_{H3}\frac{\Delta t}{2}\right)\left\{r_{i,\alpha}^{(2)}, p'^{(2)}_{i,\alpha}, s^{(2)}, p_s^{(2)}\right\}$$

$$\begin{Bmatrix} r_{i,\alpha}^{(3)} \\ p'^{(3)}_{i,\alpha} \\ s^{(3)} \\ p_s^{(3)} \end{Bmatrix} = \begin{Bmatrix} r_{i,\alpha}^{(2)} \\ p'^{(2)}_{i,\alpha} + \frac{\Delta t}{2} s^{(2)} \left(\left(1 - \frac{1}{s^{(2)2}}\right) \sum_{\beta=1}^{3} m'_i u_\beta\left(r_i^{(2)}, t\right) \frac{\partial u_\beta\left(r_i^{(2)}, t\right)}{\partial r'_{i,\alpha}} - \frac{1}{M'}\left(1 - \frac{1}{s^{(2)2}}\right) \sum_{\beta=1}^{3} \left(\sum_{j=1}^{N} m'_j u_\beta\left(r_j^{(2)}, t\right) \right) m'_i \frac{\partial u_\beta\left(r_i^{(2)}, t\right)}{\partial r'_{i,\alpha}} \right) \\ s^{(2)} \\ p_s^{(2)} + \frac{\Delta t}{2} \left(\frac{1}{2}\left(1 + \frac{1}{s^{(2)2}}\right) \sum_{j=1}^{N} \sum_{\alpha=1}^{3} m'_j \left(u_\alpha\left(r_j^{(2)}, t\right)\right)^2 - \frac{1}{2M}\left(1 + \frac{1}{s^{(2)2}}\right) \sum_{\alpha=1}^{3} \left(\sum_{j=1}^{N} m'_j u_\alpha\left(r_j^{(2)}, t\right) \right)^2 \right) \end{Bmatrix}$$

(4.52)

The fourth operator acts on the positions, momenta and the thermostat momentum,

$$\left\{r_{i,\alpha}^{(4)}, p'^{(4)}_{i,\alpha}, s^{(4)}, p_s^{(4)}\right\} = \exp\left(D_{H2}\frac{\Delta t}{2}\right)\left\{r_{i,\alpha}^{(3)}, p'^{(3)}_{i,\alpha}, s^{(3)}, p_s^{(3)}\right\}$$

$$\begin{Bmatrix} r_{i,\alpha}^{(4)} \\ p'^{(4)}_{i,\alpha} \\ s^{(4)} \\ p_s^{(4)} \end{Bmatrix} = \begin{Bmatrix} q_{i,\alpha}^{(3)} + \frac{\Delta t}{2} s^{(3)} \left(\frac{1}{M'}\left(1 - \frac{1}{s^{(3)2}}\right) \sum_{j=1}^{N} p'^{(3)}_{j,\alpha} + \left(1 - \frac{1}{s^{(3)2}}\right) u_\alpha\left(r_i^{(3)}, t\right) - \frac{1}{M'}\left(1 - \frac{1}{s^{(3)2}}\right) \sum_{i=1}^{N} \left(m'_i u_\alpha\left(r_i^{(3)}, t\right) \right) \right) \\ p'^{(3)}_{i,\alpha} + \frac{\Delta t}{2} s^{(3)} \left(-\left(1 - \frac{1}{s^{(3)2}}\right) \sum_{\beta=1}^{3} \left(p'^{(3)}_{i,\beta}\right) \frac{\partial u_\beta\left(r_i^{(3)}, t\right)}{\partial r'_{i,\alpha}} + \frac{1}{M'}\left(1 - \frac{1}{s^{(3)2}}\right) \sum_{\beta=1}^{3} \left(m'_i \frac{\partial u_\beta\left(r_i^{(3)}, t\right)}{\partial r'_{i,\alpha}} \right) \sum_{j=1}^{N} p'^{(3)}_{j,\beta} \right) \\ s^{(3)} \\ p_s^{(3)} - \frac{\Delta t}{2} \left(\frac{1}{2M'}\left(1 + \frac{1}{s^{(3)2}}\right) \sum_{\alpha=1}^{3} \left(\sum_{j=1}^{N} p'^{(3)}_{j,\alpha} \right)^2 + \left(1 + \frac{1}{s^{(3)2}}\right) \sum_{i=1}^{N} \sum_{\alpha=1}^{3} \left(p'^{(3)}_{i,\alpha}\right) u_\alpha\left(r_i^{(3)}, t\right) - \frac{1}{M'}\left(1 + \frac{1}{s^{(3)2}}\right) \sum_{\alpha=1}^{3} \left(\sum_{j=1}^{N} m'_j u_\alpha\left(r_j^{(3)}, t\right) \right)^2 \right) \end{Bmatrix}$$

(4.53)

The fifth operator acts on the positions and the thermostat momentum,

$$\left\{q_{i,\alpha}{}^{(5)},\, p'_{i,\alpha}{}^{(5)},\, s^{(5)},\, p_s{}^{(5)}\right\} = \exp\left(D_{H1}\Delta t\right)\left\{q_{i,\alpha}{}^{(4)},\, p'_{i,\alpha}{}^{(4)},\, s^{(4)},\, p_s{}^{(4)}\right\}$$

$$\begin{Bmatrix} r_{i,\alpha}{}^{(5)} \\ p'_{i,\alpha}{}^{(5)} \\ s^{(5)} \\ p_s{}^{(5)} \end{Bmatrix} = \begin{Bmatrix} q_{i,\alpha}{}^{(4)} + \Delta t\left(\dfrac{p'_{i,\alpha}{}^{(4)}}{m_i s^{(4)}}\right) \\ p'_{i,\alpha}{}^{(4)} \\ s^{(4)} \\ p_s{}^{(4)} - \Delta t\left(-\displaystyle\sum_{i=1}^{N}\sum_{\alpha=1}^{3}\frac{\left(p'_{i,\alpha}{}^{(4)}\right)^2}{2m'_i s^{(4)2}} + gk_B T_{set}\,\ln\left(s^{(4)}\right) - H_o + gk_B T_{set}\right) \end{Bmatrix}$$

(4.54)

The sixth operator acts on the positions, momenta and the thermostat momentum,

$$\left\{r_{i,\alpha}{}^{(6)}, p'_{i,\alpha}{}^{(6)}, s^{(6)}, p_s{}^{(6)}\right\} = \exp\left(D_{H2}\frac{\Delta t}{2}\right)\left\{r_{i,\alpha}{}^{(5)}, p'_{i,\alpha}{}^{(5)}, s^{(5)}, p_s{}^{(5)}\right\}$$

$$\begin{Bmatrix} r_{i,\alpha}{}^{(6)} \\ p'_{i,\alpha}{}^{(6)} \\ s^{(6)} \\ p_s{}^{(6)} \end{Bmatrix} = \begin{Bmatrix} q_{i,\alpha}{}^{(5)} + \dfrac{\Delta t}{2}s^{(5)}\left(\dfrac{1}{M'}\left(1-\dfrac{1}{s^{(5)2}}\right)\displaystyle\sum_{j=1}^{N}p'_{j,\alpha}{}^{(5)} + \left(1-\dfrac{1}{s^{(5)2}}\right)u_\alpha\left(r_i^{(5)},t\right) - \dfrac{1}{M'}\left(1-\dfrac{1}{s^{(5)2}}\right)\displaystyle\sum_{i=1}^{N}\left(m'_i u_\alpha\left(r_i^{(5)},t\right)\right)\right) \\ p'_{i,\alpha}{}^{(5)} + \dfrac{\Delta t}{2}s^{(5)}\left(-\left(1-\dfrac{1}{s^{(5)2}}\right)\displaystyle\sum_{\beta=1}^{3}\left(p'_{i,\beta}{}^{(5)}\right)\dfrac{\partial u_\beta\left(r_i^{(5)},t\right)}{\partial r'_{i,\alpha}} + \dfrac{1}{M'}\left(1-\dfrac{1}{s^{(5)2}}\right)\displaystyle\sum_{\beta=1}^{3}\left(m'_i\dfrac{\partial u_\beta\left(r_i^{(5)},t\right)}{\partial r'_{i,\alpha}}\right)\sum_{j=1}^{N}p'_{j,\beta}{}^{(5)}\right) \\ s^{(5)} \\ p_s{}^{(5)} - \dfrac{\Delta t}{2}\left(\dfrac{1}{2M'}\left(1+\dfrac{1}{s^{(5)2}}\right)\displaystyle\sum_{\alpha=1}^{3}\left(\sum_{j=1}^{N}p'_{j,\alpha}{}^{(5)}\right)^2 + \left(1+\dfrac{1}{s^{(5)2}}\right)\sum_{i=1}^{N}\sum_{\alpha=1}^{3}\left(p'_{i,\alpha}{}^{(5)}\right)u_\alpha\left(r_i^{(5)},t\right) - \dfrac{1}{M'}\left(1+\dfrac{1}{s^{(5)2}}\right)\displaystyle\sum_{\alpha=1}^{3}\left(\sum_{j=1}^{N}m'_j u_\alpha\left(r_j^{(5)},t\right)\right)^2\right) \end{Bmatrix}$$

(4.55)

The seventh operator acts on the momenta and the thermostat momentum variable,

$$\left\{r_{i,\alpha}^{(7)}, p_{i,\alpha}'^{(7)}, s^{(7)}, p_s^{(7)}\right\} = \exp\left(D_{H3}\frac{\Delta t}{2}\right)\left\{r_{i,\alpha}^{(6)}, p_{i,\alpha}'^{(6)}, s^{(6)}, p_s^{(6)}\right\}$$

$$\begin{Bmatrix} r_{i,\alpha}^{(7)} \\ p_{i,\alpha}'^{(7)} \\ s^{(7)} \\ p_s^{(7)} \end{Bmatrix} = \begin{Bmatrix} r_{i,\alpha}^{(6)} \\ p_{i,\alpha}'^{(6)} + \frac{\Delta t}{2} s^{(6)} \left(\left(1 - \frac{1}{s^{(6)2}}\right) \sum_{\beta=1}^{3} m_i' u_\beta\left(r_i^{(6)}, t\right) \frac{\partial u_\beta\left(r_i^{(6)}, t\right)}{\partial r_{i,\alpha}'} - \frac{1}{M'}\left(1 - \frac{1}{s^{(6)2}}\right) \sum_{\beta=1}^{3}\left(\sum_{j=1}^{N} m_j' u_\beta\left(r_j^{(6)}, t\right)\right) m_i' \frac{\partial u_\beta\left(r_i^{(6)}, t\right)}{\partial r_{i,\alpha}'} \right) \\ s^{(6)} \\ p_s^{(6)} + \frac{\Delta t}{2}\left(\frac{1}{2}\left(1 + \frac{1}{s^{(6)2}}\right) \sum_{j=1}^{N}\sum_{\alpha=1}^{3} m_j' \left(u_\alpha\left(r_j^{(6)}, t\right)\right)^2 - \frac{1}{2M}\left(1 + \frac{1}{s^{(6)2}}\right) \sum_{\alpha=1}^{3}\left(\sum_{j=1}^{N} m_j' u_\alpha\left(r_j^{(6)}, t\right)\right)^2 \right) \end{Bmatrix}$$

(4.56)

The eighth operator acts on the positions and the thermostat momentum,

$$\begin{aligned} \left\{r_{i,\alpha}^{(8)}, p_{i,\alpha}'^{(8)}, s^{(8)}, p_s^{(8)}\right\} &= \exp\left(D_{H4}\frac{\Delta t}{2}\right)\left\{r_{i,\alpha}^{(7)}, p_{i,\alpha}'^{(7)}, s^{(7)}, p_s^{(7)}\right\} \\ &= \left\{r_{i,\alpha}^{(7)} + \frac{\Delta t}{2}\left(F_{i,\alpha}'\left(r_j^{(7)}\right)\right) s^{(7)}, p_{i,\alpha}'^{(7)}, s^{(7)}, p_s^{(7)} - \frac{\Delta t}{2} U\left(r_j^{(7)}\right)\right\} \end{aligned} \tag{4.57}$$

The ninth operator acts on the thermostat variables,

$$\left\{r_{i,\alpha}^{(9)}, p_{i,\alpha}'^{(9)}, s^{(9)}, p_s^{(9)}\right\} = \exp\left(D_{H5}\frac{\Delta t}{2}\right)\left\{r_{i,\alpha}^{(8)}, p_{i,\alpha}'^{(8)}, s^{(8)}, p_s^{(8)}\right\}$$

$$= \left\{ r_{i,\alpha}^{(8)}, p_{i,\alpha}'^{(8)}, s^{(8)}\left(1 + \frac{\Delta t}{2}\frac{p_s^{(8)}}{2Q_s}\right)^2, \frac{p_s^{(8)}}{1 + \frac{\Delta t}{2}\left(\frac{p_s^{(8)}}{2Q_s}\right)} \right\}$$

(4.58)

4.6. Results and discussion

In this section, we present the results obtained by simulating a system of N=500 particles at a reduced temperature of 1.0 and at a reduced number density of $n=N/V$=0.95. We use the equipartition theorem to identify the temperature from the simulation. We use a simple Weeks-Chandler-Andersen (WCA) [28] fluid, modeled with the interaction potential

$$\phi(r)=\begin{cases} 4\varepsilon\left(\left(\frac{\sigma}{r}\right)^{12}-\left(\frac{\sigma}{r}\right)^{6}\right)+\varepsilon, & r\le 2^{1/6}\sigma \\ 0, & r>2^{1/6}\sigma \end{cases} \tag{3.45}$$

Here, ε is the well depth of the pair potential and σ is the particle exclusion diameter. This is the Lennard-Jones potential, shifted upwards by ε and truncated at the LJ potential minimum of $2^{1/6}\sigma$.

The initial configurations were obtained from an equilibrated EMD simulation performed at the same reduced temperature and number density. The equations of motion were integrated using the symplectic integration scheme following Nosé [16]. The controller frequency was set at τ = 0.05 (reduced units). All simulations were performed in the absence of any external field, although the equations of motion are capable of simulating systems in the presence of external fields.

The conservation of the Hamiltonian is a proper diagnostic check to determine if simple coding errors exist in the program. Due to the fact that we use a numerical algorithm to solve for the equations of motion, we get approximate solutions. Hence, we

do not conserve the Hamiltonian exactly. However, there are ways to check for conservation of the Hamiltonian. The Hamiltonian is said to be conserved if the standard deviation of the Hamiltonian is at least two orders of magnitude lesser than the standard deviation of kinetic, potential or the thermostat energy of the system, whichever is the least:

$$\frac{\sigma_{KE}}{\sigma_H} \text{ or } \frac{\sigma_{PE}}{\sigma_H} \text{ or } \frac{\sigma_{TsE}}{\sigma_H} \geq 100 \tag{3.46}$$

where σ_H is the standard deviation of the Hamiltonian, σ_{KE} standard deviation of kinetic energy, σ_{KE} standard deviation of potential energy, and σ_{TsE} standard deviation of thermostat energy. Table 3 shows the average and standard deviations of all the energies in the system.

Since we use a second-order integrator, the errors are of the order Δt^2. Consequently, the standard deviation of the Hamiltonian evaluated at a particular time

Table 3. The average and standard deviation values for the Hamiltonian, kinetic energy, potential energy and the thermostat energy of the system (using NoséPoincaré formulation).

Energy	Time average	Standard deviation
H_{np}	7.6053E-02	1.0791E-02
$\frac{1}{2}\sum_{i=1}^{N}\sum_{\alpha=1}^{3}\frac{(\pi_{i,\alpha})^2}{m_i}$	7.4852E+02	1.1038E+01
Potential energy	1.5020E+01	7.0587E+01
Thermostat energy	1.5107E+03	7.6507E+02

step should be two orders of magnitude greater that the standard deviation of the Hamiltonian evaluated at one-tenth of that time step. Table 4 shows the standard deviation of the Hamiltonian evaluated at two different time steps (2.5 ns and 0.25 ns).

The Lees-Edwards Boundary Conditions (LEBCs) are not applied in the y dimension. In other words, we allow the particles to float away in the y dimension. Once we apply the LEBCs, the Hamiltonian is no longer a conserved quantity, since some of the kinetic energy terms are dependent on the y position, and application of LEBCs will introduce a sudden change in them. Figure 10 shows the time evolutions of the various energies of the system under the application of the LEBCs. In Figure 10.d, the potential energy decreases as the particles move farther away from each other.

The simulation was performed at a reduced shear rate of 0.1 and a time step of 2.5 ns. All energies reported are in reduced units. Obviously, since the particles float away, the potential energy decreases. Also, the kinetic energies $\frac{1}{2}\sum_{i=1}^{N}\sum_{\alpha=1}^{3} m_i u_\alpha^2 (r_i, t)$ and

Table 4. The average and standard deviation values of the Hamiltonian (Nosé-Poincaré) evaluated at two different time steps.

Time scale (ns)	$\langle H \rangle$	σ_H
2.5	7.6053E-02	1.0791E-02
0.25	4.5361E-04	2.4327E-04

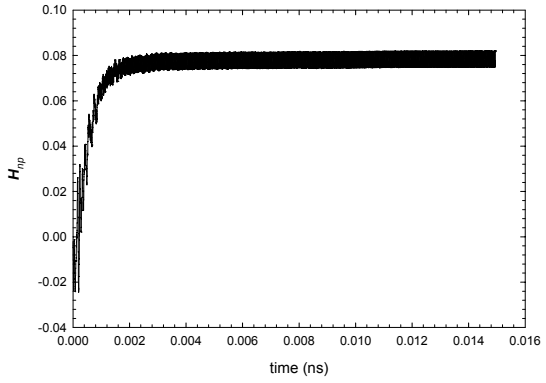

a)

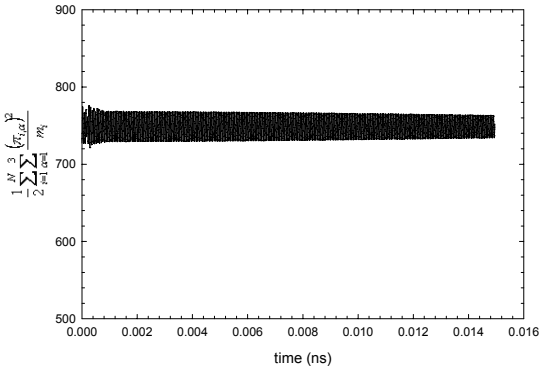

b)

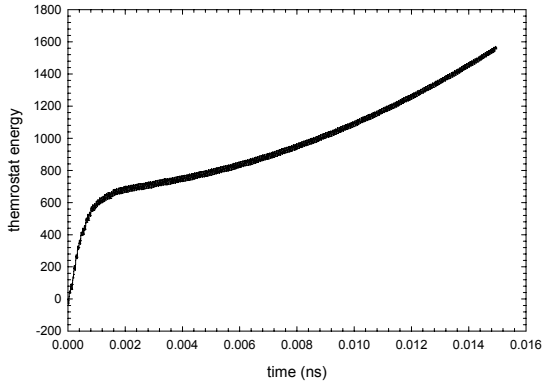

c)

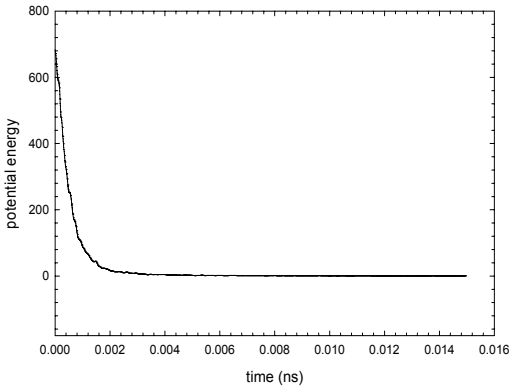

d)

Figure 10. The time evolution of the Hamiltonian (Nosé-Poincaré, conserved): a)the Hamiltonian as a function of time, b) $\sum_{i=1}^{N}\sum_{\alpha=1}^{3}\frac{\pi_{i,\alpha}{}^{2}}{2m_i}$ as a function of time, c) thermostat energy as a function of time, and d) potential energy as a function of time.

$\sum_{i=1}^{N}\sum_{\alpha=1}^{3}(\eta_T \pi_{i,\alpha})u_\alpha(r_i,t)$ continue to increase in magnitude due to the removal of the y periodic conditions (i.e., the LEBCs).

However, as one energy term increases another decreases, compensating for this increase. Thus, the Hamiltonian is conserved. For example, the decrease in potential energy is compensated by the increase in the thermostat energy. From the equations of motion, especially equations (4.3.d) or (4.8.f), it is clear that the thermostat momentum variable depends not only on the instantaneous peculiar kinetic energy, but also on the time evolution of the Hamiltonian. A drift in the Hamiltonian due to round-off errors would mean that the temperature would also show a corresponding drift because the Hamiltonian is coupled with the thermostat momentum variable

Based on this fact, we chose the symplectic integrator [16] over the r-RESPA [13, 24] integrator since the Hamiltonian drift due to round-off errors was suppressed in the former case. Figure 11 shows the drift of the Hamiltonian for equilibrium molecular dynamics simulation using the symplectic [16] and r-RESPA [13, 24] integrators. In Figure 11, we plot the Hamiltonian as a function of time for two EMD simulations evaluated at reduced temperatures of 1.0 and 6.0. The drift of the Hamiltonian is suppressed when we use the symplectic integrator [16], unlike the r-RESPA [13, 24]. As known, if a particle leaves the simulation volume then a new particle is re-introduced into the simulation box by the LEBCs (in the case of shear flow). This re-introduction of the particle alters the Hamiltonian, which in turn disturbs the thermostat momentum variable, eventually resulting in poor temperature control.

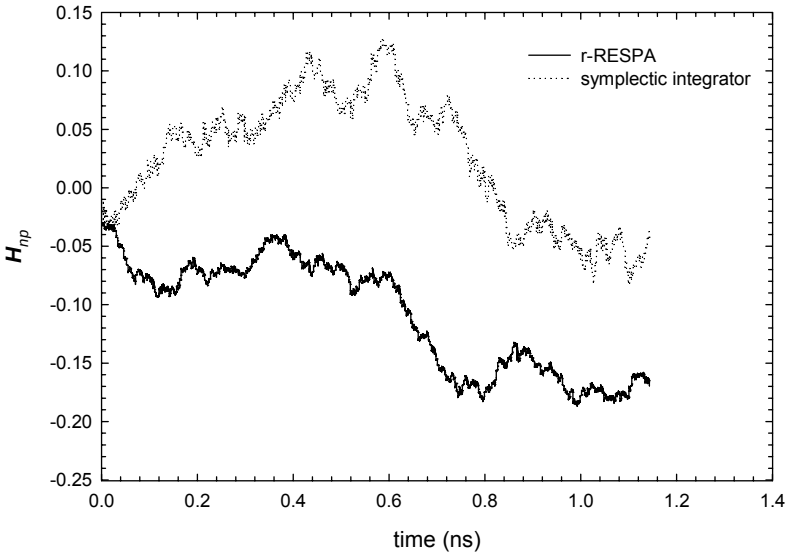

a)

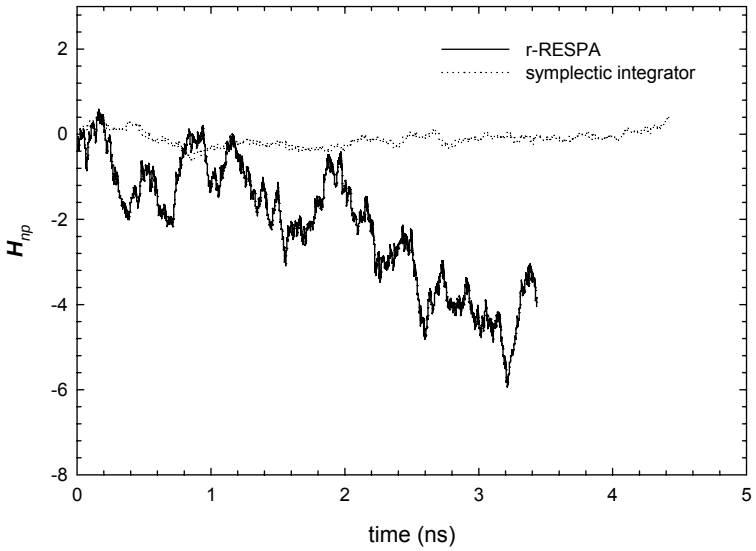

b)

Figure 11. Comparison of the Hamiltonian (Nosé-Poincaré) for EMD simulations using the r-RESPA integration scheme and Symplectic integrator scheme for two temperatures; a) T* =1.0 and b) T* = 6.0.

Therefore, we performed five simulations to identify the most rigorous method to overcome the disturbance caused by the LEBCs. Basically, we conducted three simulations: 1) No re-evaluation of the Hamiltonian after the LEBCs are applied, 2) re-evaluate *H(0)* to the Hamiltonian obtained after the LEBCs are applied, *H(0)=H(after LEBC)*, and 3) evaluating the change in the Hamiltonian before and after the LEBCs are applied and adding it to *H(0),* i.e., $H(0)= H(0)+\Delta H_{LEBCs}$. Two more simulations that were performed were similar to cases two and three with the only difference being that the velocities were scaled to the temperature of the system, as evaluated before the LEBCs were applied. In all the cases, the momentum of the particle that leaves the box and re-enters has been changed according to

$$p_{i,\alpha}^{after\ \ LEBCs} = p_{i,\alpha}^{before\ \ LEBCs} - m_i\left(q_{i,\alpha}^{after\ \ LEBCs} - q_{i,\alpha}^{before\ \ LEBCs}\right) \tag{3.47}$$

Figure 12 shows the drift in the Hamiltonian and the corresponding drift of the temperature for the simulation where the Hamiltonian was left unchanged after the LEBCs. We plot *H(t)-H(0),* which is nothing but the Nosé-Poincaré Hamiltonian without the time dilation variable ($H_{NP}=s\ (H(t)-H(0))$).

In the second case, when we replace *H(0)* with the Hamiltonian evaluated after every LEBC, the Hamiltonian drift due to the LEBCs is eliminated and we have good temperature control.

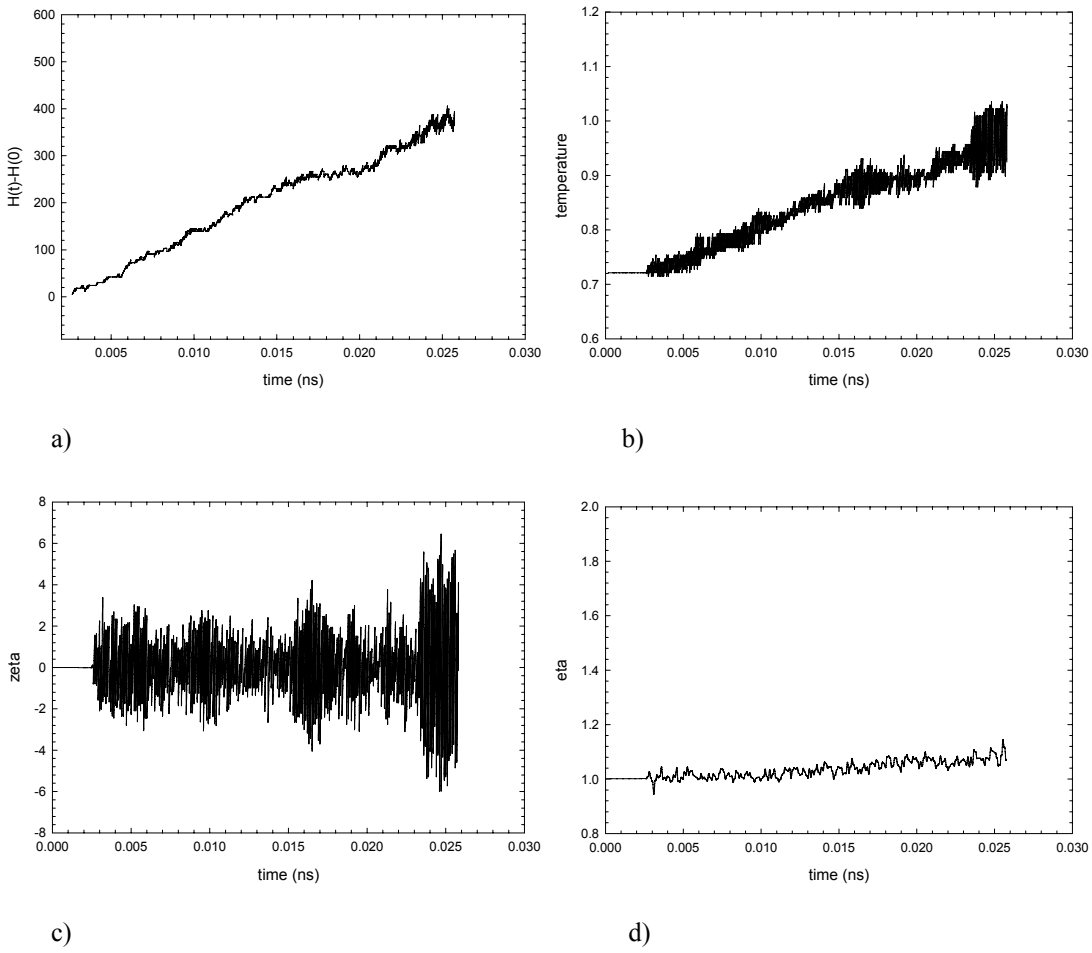

Figure 12. The Hamiltonian *H(t)-H(0)*, temperature, and the thermostat variables as functions of time (when the Hamiltonian is left unchanged after the LEBCs). a) The Hamiltonian as a function of time, b) temperature as a function of time, c) thermostat momentum (ζ_T) as a function of time, and d) time dilation variable (η_T) as a function of time.

The time dilation variable seems to increase, causing instability in the algorithm. Figure 13 shows the Hamiltonian, temperature, and the thermostat variables as functions of time. In the third case, when we add just the change in the Hamiltonian across the LEBCs to *H(0)* (i.e., $H(0)= H(0)+\Delta H_{LEBCs}$), the Hamiltonian drift was not suppressed and there was a corresponding temperature drift. There was no apparent steady state for the variables, and the simulation inevitably crashed due to instability. Figure 14 shows the drift of the Hamiltonian *H(t)-H(0)*, temperature, and the thermostat variables as functions of time

The last two simulations were repeated with only one difference. The velocities were scaled after the LEBCs were applied to the temperature that existed before the LEBCs were applied. It should be noted that since we change the momentum of the particle that re-enters the box due to the LEBCs, the temperature will change across the LEBCs. Figure 15 shows the Hamiltonian *H(t)-H(0)*, temperature, and the thermostat variables as functions of time (when the Hamiltonian *H(0)* is re-evaluated as *H(0)=H(after LEBC)*) and the velocities were scaled after the LEBCs. These plots show that the problem of the time dilation variable not reaching a steady state still exists, and that velocity scaling has no effect. We tried scaling the velocities after the LEBCs are applied for the third case, (i.e., $H(0)= H(0)+\Delta H_{LEBCs}$). Figure 16 shows the Hamiltonian *H(t)-H(0)*, temperature, and the thermostat variables as functions of time (when the Hamiltonian *H(0)* is re-evaluated as $H(0) = H(0) + \Delta H_{LEBCs}$) and the velocities were scaled after the LEBCs. In this plot, we find that the Hamiltonian is still drifting, and also that the time dilation variable has not reached a steady. Interestingly, the time dilation variable tends to decrease, unlike the other case where it was increasing

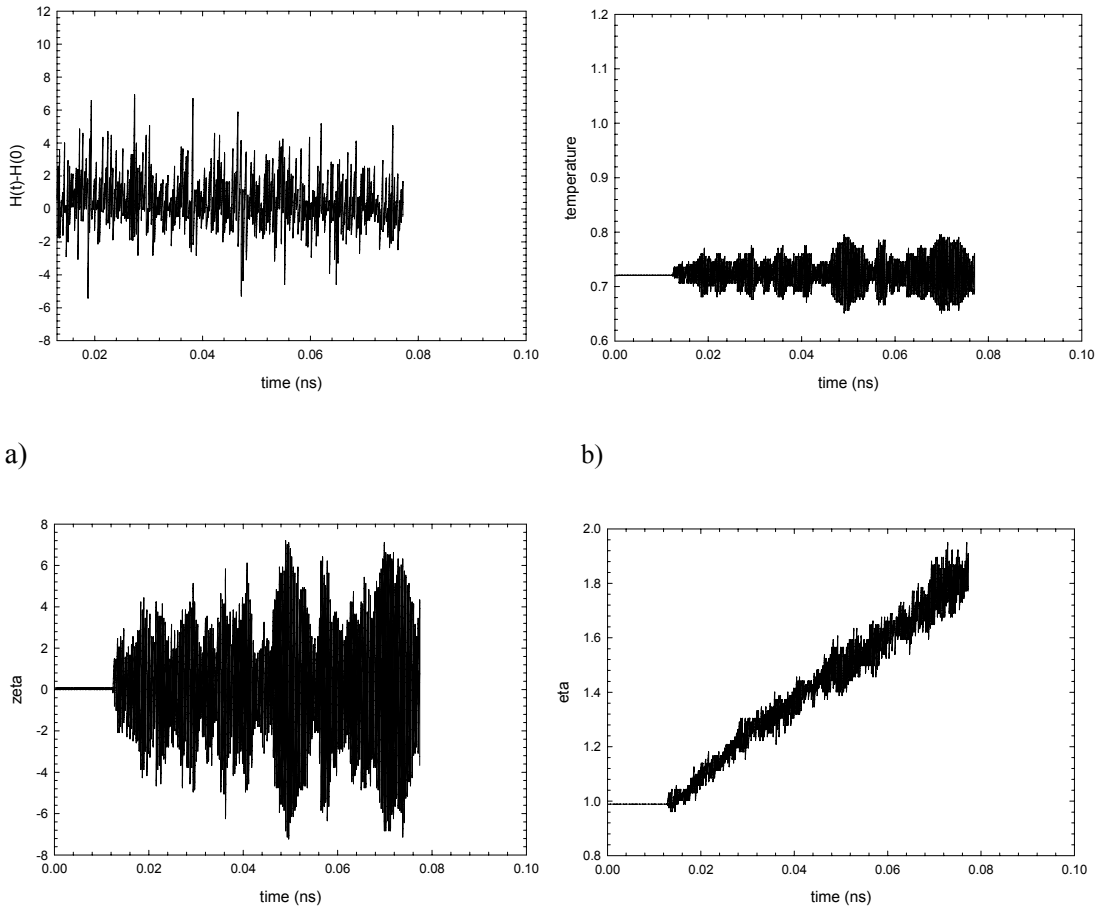

a) b)

c) d)

Figure 13. The Hamiltonian *H(t)-H(0)*, temperature, and the thermostat variables as functions of time (when the Hamiltonian *H(0)* is re-evaluated as *H(0)=H(after LEBC)*): a) The Hamiltonian as a function of time, b) temperature as a function of time, c) thermostat momentum (ζ_T) as a function of time, and d) time dilation variable (η_T) as a function of time.

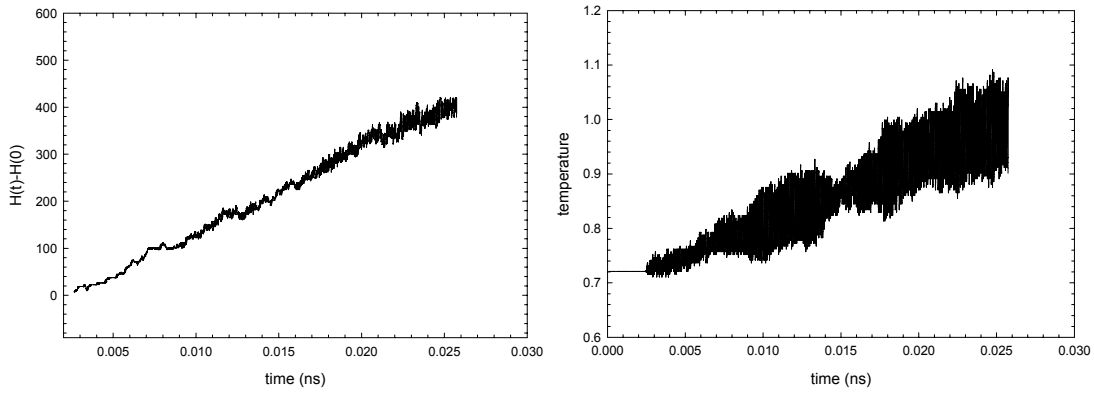

a) b)

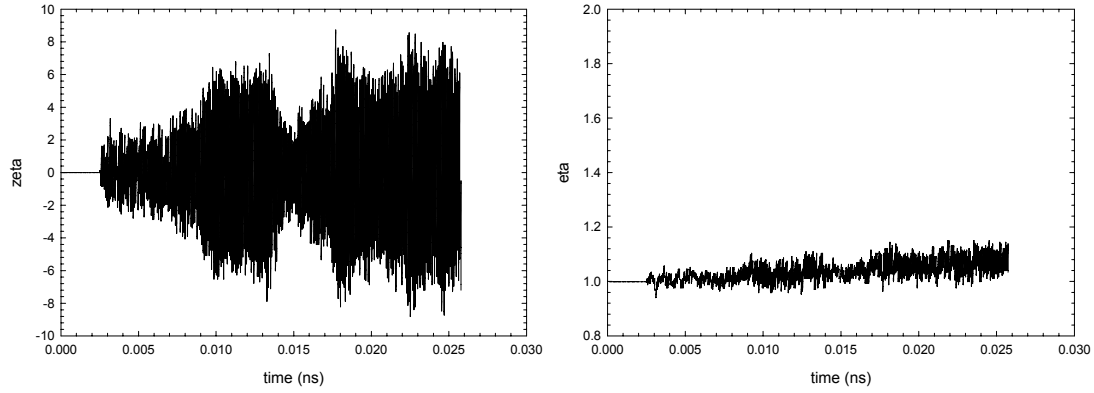

c) d)

Figure 14. The Hamiltonian *H(t)-H(0)*, temperature, and the thermostat variables as functions of time (when the Hamiltonian *H(0)* is re-evaluated to be $H(0)= H(0)+\Delta H_{LEBCs}$): a) The Hamiltonian as a function of time, b) temperature as a function of time, c) thermostat momentum (ζ_T) as a function of time, and d) time dilation variable (η_T) as a function of time.

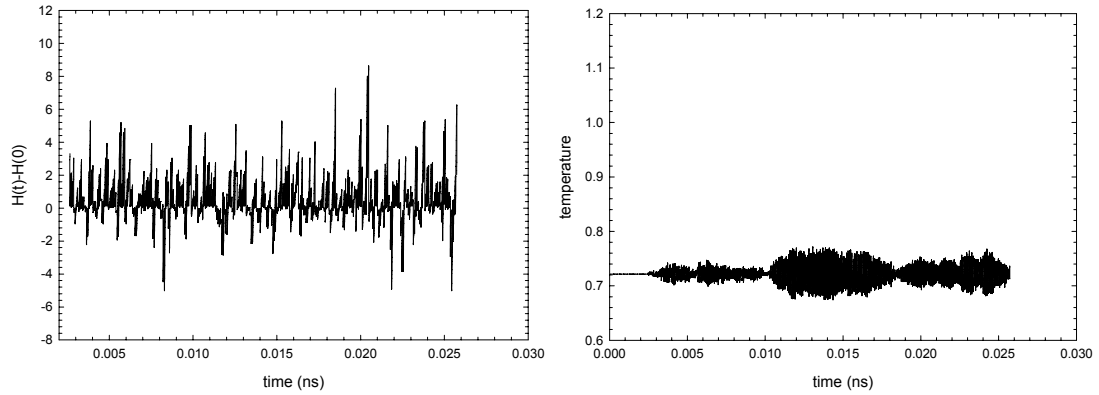

a) b)

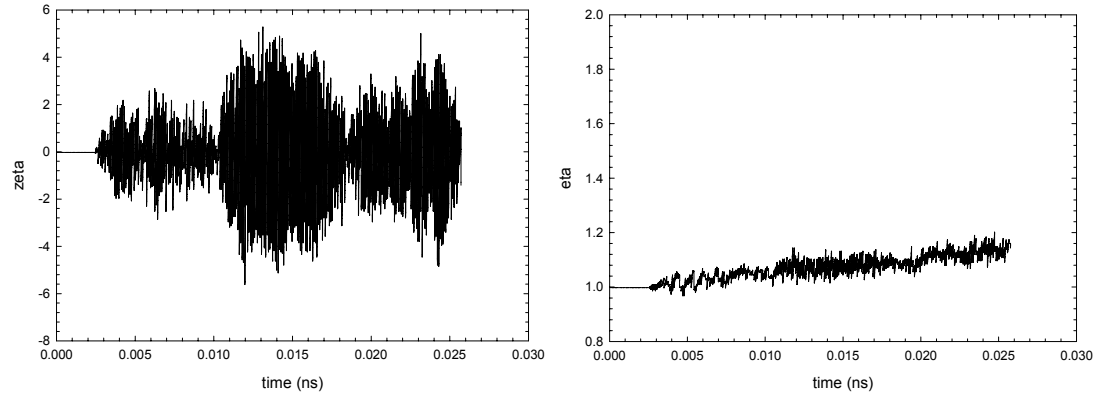

c) d)

Figure 15. The Hamiltonian *H(t)-H(0)*, temperature, and the thermostat variables as functions of time (when the Hamiltonian *H(0)* is re-evaluated as *H(0)=H(after LEBC)*) and the velocities were scaled after the LEBCs): a) The Hamiltonian as a function of time, b) temperature as a function of time, c) thermostat momentum (ζ_T) as a function of time, and d) time dilation variable (η_T) as a function of time.

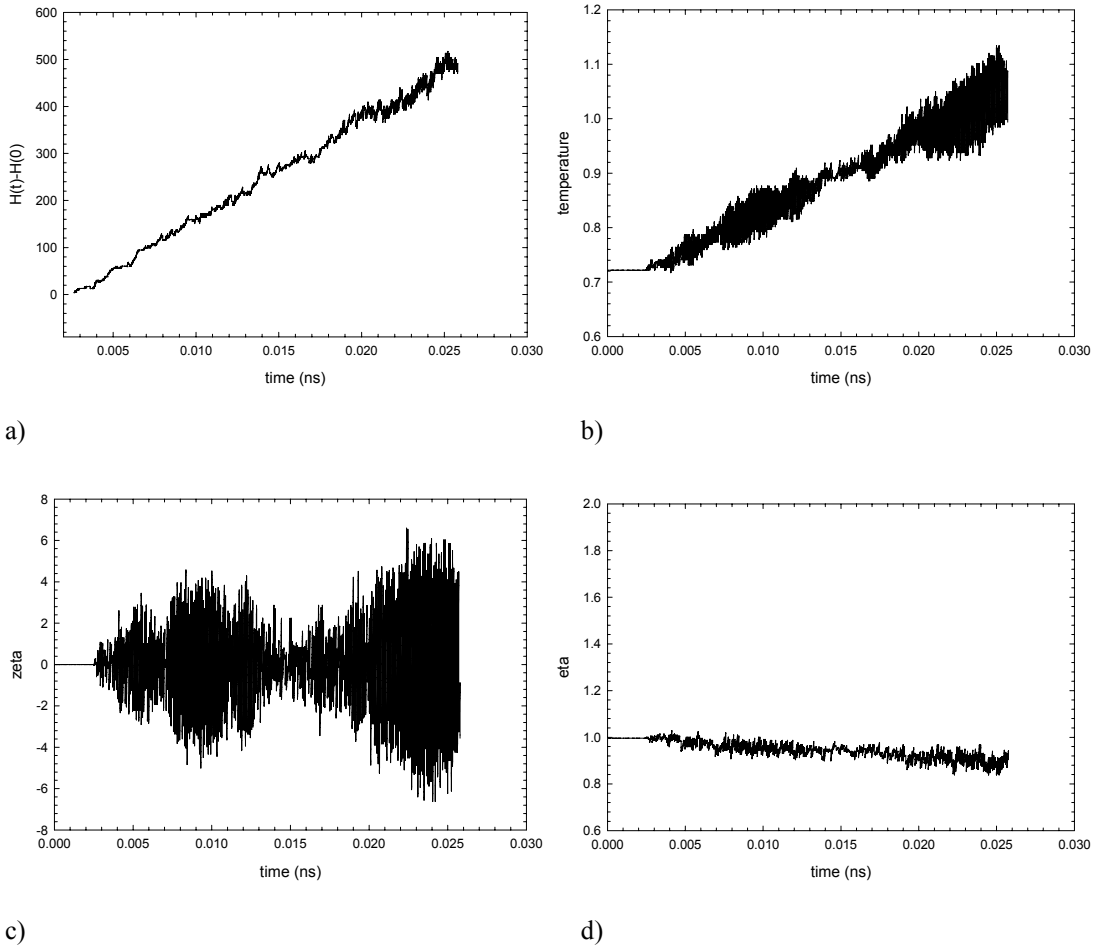

Figure 16. The Hamiltonian *H(t)-H(0)*, temperature, and the thermostat variables as functions of time (when the Hamiltonian *H(0)* is re-evaluated to be $H(0)= H(0)+\Delta H_{LEBCs}$ and velocities were scaled after the LEBCs): a) The Hamiltonian as a function of time, b) temperature as a function of time, c) thermostat momentum (ζ_T) as a function of time, and d) time dilation variable (η_T) as a function of time.

. In spite of all the methods used to reduce the fluctuations, the thermostat variable never seemed to reach a steady-state value. Once we apply the LEBCs, the algorithm becomes unstable and long time simulations were not possible. The underlying reason for this behavior is that once we switch on the LEBCs, we introduce flow into the system, which in turn will increase the kinetic energy of the system. The thermostat tries to control this increase in the kinetic energy by absorbing this energy and consequently increases the time dilation variable. The time dilation variable increases exponentially, resulting in an unstable algorithm. Further analysis of the effect of the boundary conditions and the thermostat on the equations of motions had to be done to understand this behavior thoroughly.

4.7. Conclusions

A Hamiltonian-based, rigorous algorithm for NEMD simulations in the NVT ensemble using a reformulated Nosé-Poincaré thermostat was derived. The p-SLLOD transformation was used to identify the variable transformation from the mathematical frame of reference to the physical frame of reference. An eight step methodical procedure was followed to obtain the equations of motion in terms of the peculiar coordinates in the physical frame of reference. The derived equations of motion 1) follow Hamiltonian dynamics, 2) are valid in the presence of an external field, and 3) rigorously thermostat the nonequilibrium temperature. The resulting equations of motion were found to conserve the Hamiltonian in the absence of the LEBCs in the y dimension. The symplectic [16] integrator was preferred over r-RESPA [13, 30] as it suppressed the drift

of the Hamiltonian due to round-off errors. In the presence of the LEBCs, the equations of motion did not conserve the Hamiltonian as some of the kinetic energy terms were dependent on the y position of the particle, and the application of the LEBCs were found to alter the values of these energy terms. The thermostat momentum variable is coupled with the time evolution of the Hamiltonian, and hence a Hamiltonian drift would affect the temperature control of the system. Five methods were tested to avoid the drift of the Hamiltonian due to the LEBCs to control the drift. All the methods were unsuccessful in controlling the drift and the algorithm became unstable. The reason could be the fact that the LEBCs drive the flow, causing the kinetic energy to increase and this increase is absorbed by thermostat. Consequently, the time dilation variable was found to increase exponentially, causing instability in the algorithm. The effects of the boundary conditions and the thermostat on the equations of motion have to be analyzed to gain a more thorough understanding.

Chapter V

Validation of the p-SLLOD Philosophy through Simulations

Stress tensor values obtained from the simulation could answer the question as to whether the equations of motion or the boundary conditions are responsible for driving the flow. In this chapter, we compare the values of the stress tensor (xy component) generated in the presence/absence of the boundary conditions and thermostat. As known, if the stress tensor (xy component) is zero, then the particles are not subjected to flow. However, a non-zero stress tensor could indicate that the particles are subjected to flow. Based on this, it is possible to identify the factor which drives the flow.

Four simulations were performed using the SLLOD algorithm [3, 5]. As known, the SLLOD [3, 5] algorithm is equivalent to the p-SLLOD [8, 9] algorithm in the case of shear flow. The first simulation was carried out in the absence of a thermostat. In the y dimension, we replaced the conventional Lees-Edwards boundary conditions with smooth repulsive walls. The second simulation was carried out in the presence of Lees-Edwards Boundary Conditions (LEBCs) and in the absence of the thermostat. The third simulation was carried out in the presence of the thermostat and smooth repulsive walls in the y dimension. The final simulation was the full shear flow simulation using the SLLOD algorithm [3, 5] with both the Nosé-Hoover thermostat and the Lees-Edwards boundary conditions [11, 12].

The stress tensor (xy component) is given by,

$$p_{xy} = \frac{1}{V}\sum_{i=1}^{N} p_{i,x} p_{i,y} + \sum_{i=1}^{N} r_{i,x} F_{i,y} \tag{5.1}$$

where $p_{i,x}$ and $p_{i,y}$ are the momentum of particle i in the x and y dimensions respectively. $r_{i,x}$ is the x position and $F_{i,y}$ is the force acting on the particle i in the y dimension.

We used an equilibrated set of positions and momenta corresponding to a reduced temperature of 0.722 and a reduced density of 0.844. The time step was 2.5 fs, and the reduced shear rate was 1.0. Table 5 shows the temperatures as a function of shear rate (NVE with smooth repulsive walls in the y dimension). The table shows that nonequilibrium kinetic temperature T_{kin}^{NE}, and the configurational temperature T_{conf} are equivalent at all shear rates. Table 6 shows that the value of the stress tensor corresponds to that of shear flow only in the presence of the thermostat and LEBCs.

Table 5. Temperature as a function of shear rate (reduced units) (NVE with smooth repulsive walls). The table shows the average (time average) and the standard deviation of the temperature as a function of shear rate.

Shear rate	T_{kin}^{EQ}	T_{kin}^{NE}	T_{conf}	$\sigma_{T_{kin}^{EQ}}$	$\sigma_{T_{kin}^{NE}}$	$\sigma_{T_{conf}}$
0.1	0.7651	0.7450	0.7463	0.0066	0.0033	0.0083
0.5	1.5263	1.0435	1.0447	0.0363	0.0122	0.0296
1	3.9436	2.0013	2.0031	0.0877	0.0066	0.0196
2	13.8390	6.1147	6.1261	0.3464	0.0451	0.1643
3	30.7789	13.4193	13.4615	0.7258	0.0252	0.1139
10	351.8914	162.3723	161.0399	9.7285	0.4086	3.2579

Table 6. Stress Tensor for NVE and NVT simulations with LEBCs/repulsive wall (xy component). a) Stress tensor obtained in the absence of thermostat and LEBCs, b) Stress tensor obtained in the absence of thermostat, c) Stress tensor obtained in the absence of thermostat and LEBCs, and d) Stress tensor obtained for NVT shear flow using SLLOD algorithm.

	π_{xy}	π_{xy}^{kin}	π_{xy}^{pot}
Average	-0.0014	0.0027	-0.0041
Standard deviation	0.0356	0.0096	0.0357

a)

	π_{xy}	π_{xy}^{kin}	π_{xy}^{pot}
Average	-0.2470	-0.0461	-0.2009
Standard deviation	0.1626	0.0576	0.1296

b)

	π_{xy}	π_{xy}^{kin}	π_{xy}^{pot}
Average	-0.8320	-0.0349	-0.7970
Standard deviation	0.0492	0.0063	0.0446

c)

	π_{xy}	π_{xy}^{kin}	π_{xy}^{pot}
Average	-1.8200	-0.0869	-1.7300
Standard deviation	0.0572	0.0073	0.0565

d)

In the absence of LEBCs and the thermostat, the value of the stress tensor fluctuates around zero, which proves that the equations of motion do not drive the flow. Once the LEBCS are applied, the kinetic energy tends to increase indefinitely (without the thermostat). Since the simulation never reaches steady-state, no meaningful data could be obtained from this simulation. (If it never reached steady state, how did you calculate an average value for it?) In the presence of the thermostat and smooth repulsive walls, a non-zero stress tensor was obtained. However, the stress tensor value does not correspond to the stress tensor value reported for shear flow simulations. (This might be because the thermostat is applied to the equilibrium temperature. I think now that this is not correct. However, this is probably good enough for the thesis, but I think we should figure it out for the paper. I think I know what to do.) Hence, it is clear that thermostat is not responsible for driving the flow. In the presence of the LEBCs and the Nosé-Hoover thermostat [11, 12], the stress tensor corresponds to the value reported for shear flow. It is obvious from this result that it is the boundary conditions (LEBCs) that drive the flow.

Thus, the philosophy of the p-SLLOD algorithm that the boundary conditions drive the flow and the effect of the boundary conditions are felt by the particles through interparticle force interactions stands proven.

Chapter VI

Conclusions

We derived a generalized Hamiltonian-based rigorous NEMD algorithm using a reformalized Nosé-Hoover thermostat and using a Nosé-Poincaré thermostat. The p-SLLOD algorithm was used to identify the variable transformation from the mathematical frame of reference to the physical frame of reference. An eight step methodical procedure was followed to obtain the equations of motion in terms of the peculiar coordinates in the physical frame of reference. In the p-SLLOD algorithm [8], the boundary conditions are used to drive the flow, just as in actual experiments, and all the effects of these boundary conditions are then felt on each particle through the interparticle force applied to it. We developed a new NEMD algorithm that is rigorous, Hamiltonian-based, identifies the correct temperature in nonequilibrium states, thermostats this temperature rigorously, and is valid in the presence or absence of an external field.

In the second chapter, we identified the correct nonequilibrium temperature in the microcanonical ensemble (NVE) using the p-SLLOD transformation [8]. In the special case of planar Couette flow, the SLLOD [5] and the p-SLLOD algorithm are equivalent. The simulations were performed in the NVE ensemble to avoid artifacts caused by the thermostat. The y boundaries were replaced with smooth repulsive boundaries to study the behavior of the simulations in the absence of the Lees-Edwards Boundary Conditions

(LEBCs). The velocity distribution evaluated from the simulation did not fit a Maxwell-Boltzmann distribution, either locally or globally. The transformed momenta (using the p-SLLOD transformation) were found to fit a Maxwell-Boltzmann distribution both locally and globally. The nonequilibrium temperature defined by this transformation was found to be equivalent to the configurational temperature. This suggests the equivalence of the kinetic and configurational temperature in nonequilibrium states.

In the third chapter, we developed a new NEMD algorithm that is rigorous, Hamiltonian-based, identifies the correct temperature in nonequilibrium states, thermostats this temperature rigorously, uses a reformulated Nosé-Hoover thermostat [11, 12], and is valid in the presence of the external field. The eight step procedure was used to obtain the equations of motion in the peculiar coordinates in the physical frame of reference. In the absence of the LEBCs, the Hamiltonian was found to be conserved. The equations of motion were solved using the r-RESPA [13, 14] integration scheme. The Lees-Edwards Boundary Conditions were removed in the y dimension. In other words, the particles were allowed to float away in the y dimension. The LEBCs destroyed the conservation of the Hamiltonian, as they caused a sudden change in the some of the kinetic energy terms that were y position dependent. The algorithm becomes unstable as the time dilation variable increases exponentially. The Nosé-Poincaré thermostat was used to eliminate this instability.

The Nosé-Poincaré thermostat would provide a stable algorithm in EMD even under large fluctuations of temperature and thermostat variables. The methodical procedure to obtain the equations of motion based on the reformulated Nosé-Poincaré

thermostat was derived in the fourth chapter. The eight step procedure described in the third chapter was used to arrive at the equations of motion. The equations of motion were integrated using the symplectic integrator, which suppresses the Hamiltonian drift, unlike the r-RESPA [13, 14] integration scheme. We observed a change in the Hamiltonian once we applied the LEBCs (i.e., the Hamiltonian was not conserved under the application of the periodic boundary conditions). The Nosé-Poincaré thermostat variables were formulated in such a way that they were dependent on the Hamiltonian. Hence, a change in the Hamiltonian due to the LEBCs would affect their evolution. We tried three different methods to overcome this effect of the LEBCs on the thermostat variables. However, the time dilation variable never reached steady-state in all three cases, causing the algorithm to be unstable.

This led us to look at the stress tensor of the particles with and without the thermostat and LEBCs. The y boundaries were replaced with smooth repulsive boundaries. In the canonical ensemble, (in the presence of the repulsive y boundaries), the average stress tensor (xy dimension) was found to be zero. This indicates the equations of motion do not drive the flow. Once we apply the LEBCs, the kinetic energy is driven towards infinity, a clear sign that the LEBCs (i.e., periodic boundary conditions) drive the flow. In the microcanonical ensemble, the stress tensor did not correspond to a shear flow (in the absence of LEBCs). However, in the presence of the LEBCs, the stress tensor (xy component) corresponded to shear flow. We also looked at the behavior of the NEMD simulations in the canonical ensemble (described in chapter two), and found the equivalence of the kinetic and configurational temperatures in nonequilibrium states.

Thus, the philosophy of the p-SLLOD algorithm that the boundary conditions drive the flow and the effect of the boundary conditions are felt by the particles through interparticle force interaction stands proven. Further work has to be done to identify and rigorously prove the nonequilibrium temperature. The nonequilibrium temperature should be homogeneous throughout the system, and the corresponding momenta should fit to a Maxwell-Boltzmann distribution, both locally and globally.

List of References

List of References

1. Edwards, B.J., C. Baig, and D.J. Keffer, *A validation of the p-SLLOD equations of motion for homogeneous steady-state flows.* J. Chem. Phys., 2006. **124**: p. 194104.
2. Allen, M.P. and D.J. Tildesley, *Computer Simulation of Liquids*. 1987, Oxford: Oxford Science Publications.
3. Evans, D.J. and G.P. Morriss, *Statistical Mechanics of Nonequilibrium Liquids*. Theoretical Chemistry Monograph Series. 1990, London: Academic Press.
4. Hoover, W.G., et al., Phys. Rev. A, 1980. **22**: p. 1690.
5. Evans, D.J. and G.P. Morriss, *Nonlinear response theory for steady planar Couette flow.* Phys. Rev. A, 1984. **30**(3): p. 1528-1530.
6. Todd, B.D. and P.J. Daivis, J. Chem. Phys., 2000. **112**: p. 40.
7. Edwards, B.J., C. Baig, and D.J. Keffer, *An examination of the validity of nonequilibrium molecular-dynamics simulation algorithms for arbitrary steady-state flows.* J. Chem. Phys., 2005. **123**: p. 114106.
8. Edwards, B.J. and M. Dressler, *A reversible problem in non-equilibrium thermodynamics: Hamiltonian evolution equations for non-equilibrium molecular dynamics simulations.* J. Non-Newtonian Fluid Mech., 2001. **96**: p. 163-175.
9. Baig, C., et al., *A proper approach for nonequilibrium molecular dynamics simulations of planar elongational flow.* J. Chem. Phys., 2005. **122**: p. 114103.
10. Baig, C., et al., *Rheological and structural studies of liquid decane, hexadecane, and tetracosane under planar elongational flow using nonequilibrium molecular dynamics simulations.* J. Chem. Phys., 2005. **122**: p. 184906.
11. Hoover, W.G., *Canonical dynamics: Equilibrium phase-space distributions.* Phys. Rev. A, 1985. **31**(3): p. 1695-1697.
12. Nosé, S., *A molecular dynamics method for simulations in the canonical ensemble.* Mol. Phys., 1984. **52**(2): p. 255-268.
13. Tuckerman, M., B.J. Berne, and G.J. Martyna, *Reversible multiple time scale molecular-dynamics.* J. Chem. Phys., 1992. **97**: p. 1990-2001.
14. Cui, S.T., P.T. Cummings, and H.D. Cochran, *Multiple time step nonequilibrium molecular dynamics simulation of the rheological properties of liquid n-decane.* Journal Of Chemical Physics, 1996. **104**(1): p. 255-262.
15. Bond, S.D., B.J. Leimkuhler, and B.B. Laird, *The Nose-Poincare method for constant temperature molecular dynamics.* Journal Of Computational Physics, 1999. **151**(1): p. 114-134.
16. Nose, S., *An improved symplectic integrator for Nose-Poincare thermostat.* Journal Of The Physical Society Of Japan, 2001. **70**(1): p. 75-77.
17. Rugh, H.H., *Dynamical approach to temperature.* Physical Review Letters, 1997. **78**(5): p. 772-774.
18. Butler, B.D., et al., *Configurational temperature: Verification of Monte Carlo simulations.* Journal Of Chemical Physics, 1998. **109**(16): p. 6519-6522.
19. Jepps, O.G., G. Ayton, and D.J. Evans, *Microscopic expressions for the thermodynamic temperature.* Physical Review E, 2000. **62**(4): p. 4757-4763.
20. Edwards, B.J., C. Baig, and D.J. Keffer, *Nonlinear response theory for arbitrary steady-state flows.* J. Chem. Phys., 2005. **123**: p. 114106.
21. Edwards, B.J., C. Baig, and D.J. Keffer, *A validation of the p-SLLOD equations of motion for homogeneous steady-state flows.* J. Chem. Phys., 2006. **124**: p. 194104.

22. Daivis, P.J. and B.J. Todd, *A simple, direct derivation and proof of the validity of the SLLOD equations of motion for generalized homogeneous flows.* J. Chem. Phys., 2006. **124**: p. 194103.
23. Tuckerman, M.E., et al., *Modified nonequilibrium molecular dynamics for fluid flows with energy conservation.* J. Chem. Phys., 1997. **106**(13): p. 5615-5621.
24. Cui, S.T., P.T. Cummings, and H.D. Cochran, *Multiple time step nonequilibrium molecular dynamics simulation of the rheological properties of liquid n-Decane.* J. Chem. Phys., 1996. **104**: p. 255-262.
25. Keffer, D.J., et al. *A Hamiltonian-Based Algorithm for Rigorous Molecular Dynamics Simulation in the NVE, NVT, NpT, and NpH Ensembles*. in *AIChE Annual Meeting*. 2005. Cincinnati, OH.
26. Keffer, D.J., et al., *A generalized Hamiltonian-based algorithm for rigorous equilibrium molecular dynamics simulation in the canonical ensemble.* J. Chem. Phys., 2005. **submitted**.
27. Keffer, D.J., et al., *A generalized Hamiltonian-based algorithm for rigorous equilibrium molecular dynamics simulation in the isobaric-isothermal ensemble.* Mol. Sim., 2006. **accepted**.
28. Andersen, H.C., J.D. Weeks, and D. Chandler, *Relationship between hard-sphere fluid and fluids with realistic repulsive forces.* Physical Review A-General Physics, 1971. **4**(4): p. 1597-+.
29. Nosé, S., *An improved symplectic integrator for Nosé-Poincaré thermostat.* Journal of the Physical Society of Japan, 2001. **70**(1): p. 75-77.
30. Cui, S.T., et al., *Molecular dynamics simulations of the rheology of normal Decane, Hexadecane, and Tetracosane.* J. Chem. Phys. Rev., 1996. **105**: p. 1214-1220.

APPENDIX

Appendix A

In this appendix, we derive the equations of motion for the NVT ensemble in terms of the peculiar and COM coordinates in the physical frame of reference. Using equation (3.15a), one can write the time derivative of property q in terms of our transformed time as

$$\frac{dq}{dt} = \frac{dq}{dt'}\frac{dt'}{dt} = s\frac{dq}{dt'} \tag{A.1}$$

Equations (3.11.c) through equation (3.11.h) are differentiated with respect to the new time,

$$\frac{d\rho_{i,\alpha}}{dt} = \frac{d\rho'_{i,\alpha}}{dt'}\frac{dt'}{dt} = s\frac{d\rho'_{i,\alpha}}{dt'} \tag{A.2.a}$$

$$\begin{aligned}\frac{d\pi_{i,\alpha}}{dt} = \frac{d\pi_{i,\alpha}}{dt'}\frac{dt'}{dt} = s\frac{d\pi_{i,\alpha}}{dt'} = &-\frac{\pi'_{i,\alpha} - m'_i u_\alpha(r_i,t) + \frac{m'_i}{M'}\sum_{j=1}^{N} m'_j u_\alpha(r_j,t)}{s}\frac{ds}{dt'} \\ &+ \frac{d(\pi'_{i,\alpha})}{dt'} - m'_i\frac{d(u_\alpha(r_i,t))}{dt'} + \frac{m'_i}{M'}\left(\sum_{j=1}^{N} m'_j\frac{du_\alpha(r_j,t)}{dt'}\right)\end{aligned} \tag{A.2.b}$$

$$\frac{dR_\alpha}{dt} = \frac{dR'_\alpha}{dt} = \frac{dR'_\alpha}{dt'}\frac{dt'}{dt} = s\frac{dR'_\alpha}{dt'} \tag{A.2.c}$$

$$\frac{1}{M}\frac{dP_\alpha}{dt} = \frac{s}{M'}\frac{dP'_\alpha}{dt'} - \frac{s}{M'}\sum_{j=1}^{N} m'_j\frac{du_\alpha(\mathbf{r}_j,t)}{dt'} \tag{A.2.d}$$

$$\frac{d\eta_T}{dt} = \frac{ds}{dt'}\frac{dt'}{dt} = s\frac{ds}{dt'} \tag{A.2.e}$$

$$\frac{d\zeta_T}{dt} = \frac{1}{Q_s}\frac{dp_s}{dt'}\frac{dt'}{dt} = \frac{s}{Q_s}\frac{dp_s}{dt'} \tag{A.2.f}$$

Equations (3.1) and (3.2) are differentiated with respect to the old time *t'*,

$$\frac{d\rho'_{i,\alpha}}{dt'} \equiv \frac{dr'_{i,\alpha}}{dt'} - \frac{dR'^{'}_{\alpha}}{dt'} \tag{A.3.a}$$

$$\frac{1}{m'_i}\frac{d\pi'_{i,\alpha}}{dt'} \equiv \frac{1}{m'_i}\frac{dp'^{'}_{i,\alpha}}{dt'} - \frac{1}{M'_i}\frac{dP'_{\alpha}}{dt'} \tag{A.3.b}$$

$$\frac{dP'_{\alpha}}{dt'} \equiv \sum_{i=1}^{N}\frac{dp'_{i,\alpha}}{dt'} \tag{A.3.c}$$

$$\frac{dR'_{\alpha}}{dt'} \equiv \frac{1}{M'}\sum_{i=1}^{N} m'_i \frac{dr'^{'}_{i,\alpha}}{dt'} \tag{A.3.d}$$

Equations (3.10) and (A.3) are substituted in equations (A.2),

$$\frac{d\rho_{i,\alpha}}{dt} = \frac{\pi_{i,\alpha}}{m_i} + \eta_T u_\alpha(r_i,t) - \frac{\eta_T}{M}\sum_{i=1}^{N}\left(m_i u_\alpha(r_i,t)\right) \tag{A.4.a}$$

$$\begin{aligned}\frac{d\pi_{i,\alpha}}{dt} = &-\left(1-\frac{1}{\eta_T{}^2}\right)\sum_{\gamma=1}^{3}\left(\eta_T\pi_{i,\gamma}\right)\frac{\partial u_\gamma(r_i,t)}{\partial r_{i,\alpha}} \\ &+ F^{\text{int}}_{i,\alpha} + F^{ext,pec}_{i,\alpha} - \frac{m_i}{M'}\sum_{j=1}^{N}F^{ext,pec}_{j,\alpha} \\ &+ \frac{m_i}{M}\left(1-\frac{1}{\eta_T{}^2}\right)\sum_{i=1}^{N}\sum_{\gamma=1}^{3}\left(\eta_T\pi_{i,\gamma}\right)\frac{\partial u_\gamma(r_i,t)}{\partial r_{i,\alpha}} \\ &- m_i\frac{du_\alpha(r_i,t)}{dt'} + \frac{m_i}{M}\sum_{j=1}^{N}m_j\frac{du_\alpha(r_j,t)}{dt'} \\ &- \pi_{i,\alpha}\zeta_T\end{aligned} \tag{A.4.b}$$

$$\frac{dR_\alpha}{dt} = \frac{dR'_\alpha}{dt} = \frac{\eta_T P'_\alpha}{M'} = \frac{\eta_T}{M}\left(P_\alpha + \sum_{j=1}^{N} m_j u_\alpha(\mathbf{r}_j, t) \right) \tag{A.4.c}$$

$$\begin{aligned} \frac{dP_\alpha}{dt} = & -\eta_T{}^2 \left(1 - \frac{1}{\eta_T{}^2} \right) \sum_{i=1}^{N} \sum_{\gamma=1}^{3} (\pi_{i,\gamma}) \frac{\partial u_\gamma(r_i, t)}{\partial r_{i,\alpha}} \\ & + \eta_T F_\alpha^{ext,COM} - \eta_T \sum_{j=1}^{N} m_j \frac{du_\alpha(\mathbf{r}_j, t)}{dt'} \end{aligned} \tag{A.4.d}$$

$$\frac{d\eta_T}{dt} = \eta_T \zeta_T \tag{A.4.e}$$

$$\frac{d\zeta_T}{dt} = \frac{f k_B T_{set}}{Q_s} \left(\sum_{i=1}^{N} \sum_{\alpha=1}^{3} \frac{(\pi_{i,\alpha})^2}{m_i f k_B T_{set}} - 1 \right) \tag{A.4.f}$$

where

$$\begin{aligned} \frac{du_\alpha(\mathbf{r}_i, t)}{dt'} &= \frac{\partial u_\alpha(\mathbf{r}_i, t)}{\partial t'} + \sum_{\beta=1}^{3} \frac{\partial u_\alpha(\mathbf{r}_i, t)}{\partial r'_{i,\beta}} \frac{dr'_{i,\beta}}{dt'} \\ &= \frac{\partial t}{\partial t'} \frac{\partial u_\alpha(\mathbf{r}_i, t)}{\partial t} + \sum_{\beta=1}^{3} \frac{\partial u_\beta(\mathbf{r}_i, t)}{\partial r_{i,\beta}} \frac{\partial r_{i,\beta}}{\partial r'_{i,\beta}} \frac{dr'_{i,\beta}}{dt'} = \frac{1}{s} \frac{\partial u_\alpha(\mathbf{r}_i, t)}{\partial t} + \sum_{\gamma=1}^{3} \frac{\partial u_\beta(\mathbf{r}_i, t)}{\partial r_{i,\gamma}} \frac{dr'_{i,\gamma}}{dt'} \\ &= \frac{1}{\eta_T} \frac{\partial u_\alpha(\mathbf{r}_i, t)}{\partial t} + \sum_{\gamma=1}^{3} \frac{\partial u_\beta(\mathbf{r}_i, t)}{\partial r_{i,\gamma}} \left(\frac{\pi_{i,\gamma}}{m_i \eta_T} + \frac{P_\gamma}{M} + u_\gamma(r_i, t) \right) \end{aligned} \tag{A.5}$$

Now equation (A.5) is substituted in equations (A.4),

$$\frac{d\rho_{i,\alpha}}{dt} = \frac{\pi_{i,\alpha}}{m_i} + \eta_T u_\alpha(r_i, t) - \frac{\eta_T}{M} \sum_{i=1}^{N} (m_i u_\alpha(r_i, t)) \tag{A.6.a}$$

$$\begin{aligned}\frac{d\pi_{i,\alpha}}{dt} = &-\left(1-\frac{1}{\eta_T{}^2}\right)\sum_{\gamma=1}^{3}\left(\eta_T\pi_{i,\gamma}\right)\frac{\partial u_\gamma\left(r_i,t\right)}{\partial r_{i,\alpha}} \\ &+ F_{i,\alpha}^{\text{int}} + F_{i,\alpha}^{ext,pec} - \frac{m_i}{M'}\sum_{j=1}^{N}F_{j,\alpha}^{ext,pec} \\ &+ \frac{m_i}{M}\left(1-\frac{1}{\eta_T{}^2}\right)\sum_{i=1}^{N}\sum_{\gamma=1}^{3}\left(\eta_T\pi_{i,\gamma}\right)\frac{\partial u_\gamma\left(r_i,t\right)}{\partial r_{i,\alpha}} \\ &- m_i\left(\frac{1}{\eta_T}\frac{\partial u_\alpha\left(\mathbf{r}_i,t\right)}{\partial t} + \sum_{\gamma=1}^{3}\frac{\partial u_\alpha\left(\mathbf{r}_i,t\right)}{\partial r_{i,\gamma}}\left(\frac{\pi_{i,\gamma}}{m_i\eta_T} + \frac{P_\gamma}{M} + u_\gamma\left(r_i,t\right)\right)\right) \\ &+ \frac{m_i}{M}\sum_{j=1}^{N}m_j\left(\frac{1}{\eta_T}\frac{\partial u_\alpha\left(\mathbf{r}_j,t\right)}{\partial t} + \sum_{\gamma=1}^{3}\frac{\partial u_\alpha\left(\mathbf{r}_j,t\right)}{\partial r_{i,\gamma}}\left(\frac{\pi_{j,\gamma}}{m_j\eta_T} + \frac{P_\gamma}{M} + u_\gamma\left(r_j,t\right)\right)\right) \\ &- \pi_{i,\alpha}\zeta_T\end{aligned} \tag{A.6.b}$$

$$\begin{aligned}\frac{dP_\alpha}{dt} = &-\eta_T{}^2\left(1-\frac{1}{\eta_T{}^2}\right)\sum_{i=1}^{N}\sum_{\gamma=1}^{3}\left(\pi_{i,\gamma}\right)\frac{\partial u_\gamma\left(r_i,t\right)}{\partial r_{i,\alpha}} + \eta_T F_\alpha^{ext,COM} \\ &- \eta_T\sum_{j=1}^{N}m_j\left(\frac{1}{\eta_T}\frac{\partial u_\alpha\left(\mathbf{r}_j,t\right)}{\partial t} + \sum_{\gamma=1}^{3}\frac{\partial u_\alpha\left(\mathbf{r}_j,t\right)}{\partial r_{i,\gamma}}\left(\frac{\pi_{j,\gamma}}{m_j\eta_T} + \frac{P_\gamma}{M} + u_\gamma\left(r_j,t\right)\right)\right)\end{aligned} \tag{A.6.c}$$

$$\frac{dR_\alpha}{dt} = \frac{dR'_\alpha}{dt} = \frac{sP'_\beta}{M'} = \frac{\eta_T}{M}\left(P_\alpha + \sum_{j=1}^{N}m_j u_\alpha\left(\mathbf{r}_j,t\right)\right) \tag{A.6.d}$$

$$\frac{d\eta_T}{dt} = \eta_T\zeta_T \tag{A.6.e}$$

$$\frac{d\zeta_T}{dt} = \vartheta^2\left(\frac{T(t)}{T_{set}} - 1\right) \tag{A.6.f}$$

Appendix B

In the appendix, we will show how the potential energy is split into the external and the internal component.

The total potential energy, U, is split into two contributions,

$$U = U_{int}\left(\rho'_{i,\alpha} - \rho'_{j,\alpha}\right) + U_{ext}\left(\rho'_{i,\alpha}, R'_{\alpha}\right) \tag{B.1}$$

The first term represents, the intermolecular and intramolecular interactions of dynamic particles, U_{int}, and is a function only of the distance between peculiar positions of particles. The second potential energy term U_{ext} represents any externally imposed potential, which is a function of the peculiar and COM positions.

We take the partial differential of the potential energy with respect to the laboratory position.

$$-\frac{\partial U}{\partial r'_{i,\alpha}} = -\frac{\partial U_{int}\left(\rho'_{i,\alpha} - \rho'_{j,\alpha}\right)}{\partial r'_{i,\alpha}} - \frac{\partial U_{ext}\left(\rho'_{i,\alpha}, R'_{\alpha}\right)}{\partial r'_{i,\alpha}} \tag{B.2}$$

We use chain rule to differentiate the potential energy,

$$\begin{aligned} -\frac{\partial U}{\partial r'_{i,\alpha}} = & -\sum_{\substack{j=1 \\ j\neq i}}^{N} \frac{\partial U_{int}\left(\rho'_{i,\alpha} - \rho'_{j,\alpha}\right)}{\partial\left(\rho'_{i,\alpha} - \rho'_{j,\alpha}\right)} \frac{\partial\left(\rho'_{i,\alpha} - \rho'_{j,\alpha}\right)}{\partial r'_{i,\alpha}} \\ & -\sum_{j=1}^{N} \frac{\partial U_{ext}\left(\rho'_{j,\alpha}, R'_{\alpha}\right)}{\partial \rho'_{j,\alpha}} \frac{\partial \rho'_{j,\alpha}}{\partial r'_{i,\alpha}} - \frac{\partial U_{ext}\left(\rho'_{i,\alpha}, R'_{\alpha}\right)}{\partial R'_{\alpha}} \frac{\partial R'_{\alpha}}{\partial r'_{i,\alpha}} \end{aligned} \tag{B.3}$$

The peculiar and COM positions are functions of all of the laboratory positions,

$$\frac{\partial \rho'_{i,\alpha}}{\partial r'_{j,\beta}} = \delta_{ij}\delta_{\alpha\beta} - \frac{m'_j}{M'}\delta_{\alpha\beta} \tag{B.4.a}$$

$$\frac{\partial R'_{\alpha}}{\partial r'_{i,\beta}} = \frac{m'_i}{M'}\delta_{\alpha\beta} \tag{B.4.b}$$

and

$$\frac{\partial\left(\rho'_{i,\alpha} - \rho'_{j,\alpha}\right)}{\partial r'_{k,\beta}} = \delta_{ik}\delta_{\alpha\beta} - \frac{m'_k}{M'}\delta_{\alpha\beta} - \delta_{jk}\delta_{\alpha\beta} + \frac{m'_k}{M'}\delta_{\alpha\beta} = \left(\delta_{ik} - \delta_{jk}\right)\delta_{\alpha\beta} \tag{B.4.b}$$

To simplify notation, the forces are defined as

$$F^{int}_{i,\alpha} = -\sum_{\substack{j=1 \\ j\neq i}}^{N} \frac{\partial U_{int}\left(\rho'_{i,\alpha} - \rho'_{j,\alpha}\right)}{\partial\left(\rho'_{i,\alpha} - \rho'_{j,\alpha}\right)} \tag{B.5.a}$$

$$F^{ext,pec}_{i,\alpha} = -\frac{\partial U_{ext}\left(\rho'_{i,\alpha}, R'_{\alpha}\right)}{\partial \rho'_{i,\alpha}} \tag{B.5.b}$$

$$F^{ext,com}_{\alpha} = -\frac{\partial U_{ext}\left(\rho'_{i,\alpha}, R'_{\alpha}\right)}{\partial R'_{\alpha}} \tag{B.5.c}$$

Now equation (B.3) can be written as

$$-\frac{\partial U}{\partial r'_{i,\alpha}} = F^{int}_{i,\alpha} + F^{ext,pec}_{i,\alpha} - \frac{m'_i}{M'}\sum_{j=1}^{N} F^{ext,pec}_{j,\alpha} + F^{ext,COM}_{\alpha}\,\frac{m'_i}{M'} \tag{B.6}$$

Appendix C

In this appendix, we derive the equations of motion for the NVT ensemble in terms of the peculiar and COM coordinates in the physical frame of reference. The time derivative of property q in terms of our transformed time is given in appendix A in equation (A.1):

$$\frac{dq}{dt} = \frac{dq}{dt'}\frac{dt'}{dt} = s\frac{dq}{dt'} \tag{A.1}$$

Equations (3.11.c) through equation (3.11.h) are differentiated with respect to the new time,

$$\frac{d\rho_{i,\alpha}}{dt} = \frac{d\rho'_{i,\alpha}}{dt'}\frac{dt'}{dt} = s\frac{d\rho'_{i,\alpha}}{dt'} \tag{A.2.a}$$

$$\begin{aligned}\frac{d\pi_{i,\alpha}}{dt} = \frac{d\pi_{i,\alpha}}{dt'}\frac{dt'}{dt} = s\frac{d\pi_{i,\alpha}}{dt'} = &-\frac{\pi'_{i,\alpha} - m'_i u_\alpha(r_i,t) + \frac{m'_i}{M'}\sum_{j=1}^{N} m'_j u_\alpha(r_j,t)}{s}\frac{ds}{dt'} \\ &+ \frac{d(\pi'_{i,\alpha})}{dt'} - m'_i\frac{d(u_\alpha(r_i,t))}{dt'} + \frac{m'_i}{M'}\left(\sum_{j=1}^{N} m'_j\frac{du_\alpha(r_j,t)}{dt'}\right)\end{aligned} \tag{A.2.b}$$

$$\frac{dR_\alpha}{dt} = \frac{dR'_\alpha}{dt} = \frac{dR'_\alpha}{dt'}\frac{dt'}{dt} = s\frac{dR'_\alpha}{dt'} \tag{A.2.c}$$

$$\frac{1}{M}\frac{dP_\alpha}{dt} = \frac{s}{M'}\frac{dP'_\alpha}{dt'} - \frac{s}{M'}\sum_{j=1}^{N} m'_j\frac{du_\alpha(\mathbf{r}_j,t)}{dt'} \tag{A.2.d}$$

$$\frac{d\eta_T}{dt} = \frac{ds}{dt'}\frac{dt'}{dt} = s\frac{ds}{dt'} \tag{A.2.e}$$

$$\frac{d\zeta_T}{dt} = \frac{1}{Q_s}\frac{dp_s}{dt'}\frac{dt'}{dt} = \frac{s}{Q_s}\frac{dp_s}{dt'} \tag{A.2.f}$$

Equations (3.1) and (3.2) are differentiated with respect to the old time *t'*,

$$\frac{d\rho'_{i,\alpha}}{dt'} \equiv \frac{dr'_{i,\alpha}}{dt'} - \frac{dR'^{'}_{\alpha}}{dt'} \tag{A.3.a}$$

$$\frac{1}{m'_i}\frac{d\pi'_{i,\alpha}}{dt'} \equiv \frac{1}{m'_i}\frac{dp'_{i,\alpha}}{dt'} - \frac{1}{M'_i}\frac{dP'_{\alpha}}{dt'} \tag{A.3.b}$$

$$\frac{dP'_{\alpha}}{dt'} \equiv \sum_{i=1}^{N}\frac{dp'_{i,\alpha}}{dt'} \tag{A.3.c}$$

$$\frac{dR'_{\alpha}}{dt'} \equiv \frac{1}{M'}\sum_{i=1}^{N} m'_i \frac{dr'_{i,\alpha}}{dt'} \tag{A.3.d}$$

Equations (4.3) and (A.3) are substituted in equations (A.2), yielding

$$\frac{d\rho_{i,\alpha}}{dt} = \eta_T\left(\frac{\pi_{i,\alpha}}{m_i} + \eta_T u_\alpha(r_i,t) - \frac{\eta_T}{M}\sum_{i=1}^{N}\left(m_i u_\alpha(r_i,t)\right)\right) \tag{C.1.a}$$

$$\frac{d\pi_{i,\alpha}}{dt} = \eta_T\left(\begin{array}{l} -\left(1-\frac{1}{{\eta_T}^2}\right)\sum_{\gamma=1}^{3}\left(\eta_T\pi_{i,\gamma}\right)\frac{\partial u_\gamma(r_i,t)}{\partial r_{i,\alpha}} + F^{\text{int}}_{i,\alpha} + F^{ext,pec}_{i,\alpha} - \frac{m_i}{M'}\sum_{j=1}^{N}F^{ext,pec}_{j,\alpha} \\ +\frac{m_i}{M}\left(1-\frac{1}{{\eta_T}^2}\right)\sum_{i=1}^{N}\sum_{\gamma=1}^{3}\left(\eta_T\pi_{i,\gamma}\right)\frac{\partial u_\gamma(r_i,t)}{\partial r_{i,\alpha}} - m_i\frac{du_\alpha(r_i,t)}{dt'} \\ +\frac{m_i}{M}\sum_{j=1}^{N}m_j\frac{du_\alpha(r_j,t)}{dt'} - \pi_{i,\alpha}\zeta_T \end{array}\right) \tag{C.2.b}$$

$$\frac{dR_{\alpha}}{dt} = \frac{{\eta_T}^2}{M}\left(P_\alpha + \sum_{j=1}^{N} m_j u_\alpha(\mathbf{r}_j,t)\right) \tag{C.2.c}$$

$$\frac{dP_\alpha}{dt} = \eta_T \left(-{\eta_T}^2 \left(1 - \frac{1}{{\eta_T}^2} \right) \sum_{i=1}^{N} \sum_{\gamma=1}^{3} \left(\pi_{i,\gamma} \right) \frac{\partial u_\gamma \left(r_i, t \right)}{\partial r_{i,\alpha}} + \eta_T F_\alpha^{ext,COM} - \eta_T \sum_{j=1}^{N} m_j \frac{du_\alpha \left(\mathbf{r}_j, t \right)}{dt'} \right) \tag{C.2.d}$$

$$\frac{d\eta_T}{dt} = {\eta_T}^2 \zeta_T \tag{C.2.e}$$

$$\frac{d\zeta_T}{dt} = \eta_T \frac{fk_B T_{set}}{Q_s} \left(\sum_{i=1}^{N} \sum_{\alpha=1}^{3} \frac{\left(\pi_{i,\alpha} \right)^2}{m_i fk_B T_{set}} - 1 - \frac{\Delta H_f}{fk_B T_{set}} \right) \tag{C.2.f}$$

where

$$\Delta H_f = H(t) - H(0) \tag{C.3}$$

$$\begin{aligned} \frac{du_\alpha \left(\mathbf{r}_i, t \right)}{dt'} &= \frac{\partial u_\alpha \left(\mathbf{r}_i, t \right)}{\partial t'} + \sum_{\beta=1}^{3} \frac{\partial u_\alpha \left(\mathbf{r}_i, t \right)}{\partial r'_{i,\beta}} \frac{dr'_{i,\beta}}{dt'} \\ &= \frac{\partial t}{\partial t'} \frac{\partial u_\alpha \left(\mathbf{r}_i, t \right)}{\partial t} + \sum_{\beta=1}^{3} \frac{\partial u_\beta \left(\mathbf{r}_i, t \right)}{\partial r_{i,\beta}} \frac{\partial r_{i,\beta}}{\partial r'_{i,\beta}} \frac{dr'_{i,\beta}}{dt'} = \frac{1}{s} \frac{\partial u_\alpha \left(\mathbf{r}_i, t \right)}{\partial t} + \sum_{\gamma=1}^{3} \frac{\partial u_\beta \left(\mathbf{r}_i, t \right)}{\partial r_{i,\gamma}} \frac{dr'_{i,\gamma}}{dt'} \\ &= \frac{1}{\eta_T} \frac{\partial u_\alpha \left(\mathbf{r}_i, t \right)}{\partial t} + \sum_{\gamma=1}^{3} \frac{\partial u_\beta \left(\mathbf{r}_i, t \right)}{\partial r_{i,\gamma}} \left(\frac{\pi_{i,\gamma}}{m_i \eta_T} + \frac{P_\gamma}{M} + u_\gamma \left(r_i, t \right) \right) \end{aligned} \tag{C.4}$$

We substitute equation (C.4) in equation (C.2.f), obtaining

$$\frac{d\rho_{i,\alpha}}{dt} = \eta_T \left(\frac{\pi_{i,\alpha}}{m_i} + \eta_T u_\alpha \left(r_i, t \right) - \frac{\eta_T}{M} \sum_{i=1}^{N} \left(m_i u_\alpha \left(r_i, t \right) \right) \right) \tag{C.5.a}$$

$$\frac{d\pi_{i,\alpha}}{dt} = \eta_T \left(\begin{array}{l} -\left(1-\frac{1}{{\eta_T}^2}\right)\sum_{\gamma=1}^{3}\left(\eta_T \pi_{i,\gamma}\right)\frac{\partial u_\gamma(r_i,t)}{\partial r_{i,\alpha}} + F_{i,\alpha}^{\text{int}} + F_{i,\alpha}^{ext,pec} - \frac{m_i}{M'}\sum_{j=1}^{N} F_{j,\alpha}^{ext,pec} \\ +\frac{m_i}{M}\left(1-\frac{1}{{\eta_T}^2}\right)\sum_{i=1}^{N}\sum_{\gamma=1}^{3}\left(\eta_T \pi_{i,\gamma}\right)\frac{\partial u_\gamma(r_i,t)}{\partial r_{i,\alpha}} \\ -m_i\left(\frac{1}{\eta_T}\frac{\partial u_\alpha(\mathbf{r}_i,t)}{\partial t} + \sum_{\gamma=1}^{3}\frac{\partial u_\alpha(\mathbf{r}_i,t)}{\partial r_{i,\gamma}}\left(\frac{\pi_{i,\gamma}}{m_i\eta_T} + \frac{P_\gamma}{M} + u_\gamma(r_i,t)\right)\right) \\ +\frac{m_i}{M}\sum_{j=1}^{N} m_j\left(\frac{1}{\eta_T}\frac{\partial u_\alpha(\mathbf{r}_j,t)}{\partial t} + \sum_{\gamma=1}^{3}\frac{\partial u_\alpha(\mathbf{r}_j,t)}{\partial r_{i,\gamma}}\left(\frac{\pi_{j,\gamma}}{m_j\eta_T} + \frac{P_\gamma}{M} + u_\gamma(r_j,t)\right)\right) \\ -\pi_{i,\alpha}\zeta_T \end{array} \right) \tag{C.5.b}$$

$$\frac{dP_\alpha}{dt} = \eta_T \left(\begin{array}{l} -{\eta_T}^2\left(1-\frac{1}{{\eta_T}^2}\right)\sum_{i=1}^{N}\sum_{\gamma=1}^{3}\left(\pi_{i,\gamma}\right)\frac{\partial u_\gamma(r_i,t)}{\partial r_{i,\alpha}} + \eta_T F_\alpha^{ext,COM} \\ -\eta_T\sum_{j=1}^{N} m_j\left(\frac{1}{\eta_T}\frac{\partial u_\alpha(\mathbf{r}_j,t)}{\partial t} + \sum_{\gamma=1}^{3}\frac{\partial u_\alpha(\mathbf{r}_j,t)}{\partial r_{i,\gamma}}\left(\frac{\pi_{j,\gamma}}{m_j\eta_T} + \frac{P_\gamma}{M} + u_\gamma(r_j,t)\right)\right) \end{array} \right) \tag{C.5.c}$$

$$\frac{dR_\alpha}{dt} = \frac{{\eta_T}^2}{M}\left(P_\alpha + \sum_{j=1}^{N} m_j u_\alpha(\mathbf{r}_j,t)\right) \tag{C.5.d}$$

$$\frac{d\eta_T}{dt} = {\eta_T}^2\zeta_T \tag{C.5.e}$$

$$\frac{d\zeta_T}{dt} = \eta_T\,\frac{fk_BT_{set}}{Q_s}\left(\sum_{i=1}^{N}\sum_{\alpha=1}^{3}\frac{\left(\pi_{i,\alpha}\right)^2}{m_i fk_BT_{set}} - 1 - \frac{\Delta H_f}{fk_BT_{set}}\right) \tag{C.5.f}$$

Vita

Joseph Gerald Leo Rajkumar was born in Thanjavur, India, on December 17, 1983. He was raised in Chennai, India. He graduated from Union Christian School in 2001. From there he went to Sri Venkateswara College of Engineering and received a B.Tech. in Chemical Engineering in 2005. From there he went to the University of Tennessee, Knoxville and received a M.S. in Chemical Engineering in 2007.

Rajkumar is currently working at the Computational Materials Research Group at the University of Tennessee, Knoxville.